Evaluation of two pathogen-derived resistance strategies for *Grapevine leafroll-associated virus 3*

by

Faira Suidgeest

Dissertation presented for the Degree of Master of Sciences

at

Stellenbosch University

Department of Genetics

Natural Sciences

Supervisor: Professor JT Burger

Co-supervisor: Dr HJ Maree

March 2015

Declaration

By submitting this thesis electronically, I declare that the entirety of the work contained therein is my own original work, that I am the authorship owner thereof (unless to the extent explicitly otherwise stated) and that I have not previously in its entirety or in part submitted it for obtaining any qualification.

Signature:

Date:

Abstract

Grapevine leafroll disease (GLD), caused by the members of the family *Closteroviridae*, is one of the most economic important viral diseases affecting grapevine. *Grapevine leafroll associated virus 3* (GLRaV-3), of the genus *Ampelovirus,* is the most widespread member of the leafroll associated virus family. To prevent the spread of GLD, management strategies such as rogueing and insect vector control are required to limit crop losses. Alternative control strategies based on genetic modification of the grapevine genome, such as pathogen-derived resistance (PDR), is proven to be effective in conferring resistance to several viruses. Therefore, the focus of this study was to evaluate pathogen-derived resistance strategies for GLRaV-3 using the following two approaches; 1) evaluation of transgenic plants expressing a dysfunctional GLRaV-3 heat shock protein 70 homolog (HSP70h) in order to confer resistance against GLRaV-3, and 2) the construction of artificial microRNAs (amiRNAs) to use as a tool for silencing specific sequences of GLRaV-3 in the grapevine host and the development of an amiRNA-mediated silencing validation system.

In the first part of this study, six transgenic plant lines (plant lines #1, #3, #9, #14, #15 and #17) as well as a non-modified plant line, were inoculated with GLRaV-3 by grafting buds of each onto GLRaV-3 infected plant material. After approximately five months, GLRaV-3 virus titres of all grafted plants were quantified relative to two reference genes using RT-qPCR. Results were evaluated by comparing the relative virus titre of each transgenic plant line to that of the non-modified control plant line. Results showed that resistance levels of plant line #3 was significantly enhanced (>99%) and remarkably, plant line #14, showed to be more susceptible to the virus.

The second part of the study was the construction and validation of amiRNAs targeting GLRaV-3 sequences. Two 21 nt regions of GLRaV-3 were successfully incorporated into miRNA backbone vvi167b of grapevine. Moreover, target constructs were developed by incorporating corresponding GLRaV-3 target sequences into the 3' UTR of a green fluorescence protein (GFP) gene. Subsequently, the target constructs were co-infiltrated with the constructed amiRNA in *Nicotiana benthamiana* and GFP expression levels were quantified to determine the silencing efficiency of the amiRNAs. Results showed that the amiRNAs were successful in silencing the GFP target construct, however, they were not specific in silencing exclusively their corresponding target. These amiRNA constructs are

ideal for further viral studies to determine the efficiency of silencing GLRaV-3 in GLD infected grapevines.

Opsomming

Wingerd rolblaar siekte (GLD), wat veroorsaak word deur die lede van die familie *Closteroviridae*, is een van die ekonomies mees belangrike virus siektes van wingerd. *Grapevine leafroll-associated virus 3* (GLRaV-3), van die genus *Ampelovirus*, is die mees wydverspreide lid van die rolblaar geassosieerde virus familie. Om die verspreiding van GLD te voorkom, is bestuur strategieë, soos die verwydering van geïnfekteerde plante en insekvektor beheer, ’n vereiste om oes verliese te beperk. Alternatiewe beheer strategieë gebaseer op genetiese modifikasie van die wingerdgenoom, soos patogeen-afgeleide weerstand (PDR), is bewys om effektief te wees in die verlening van weerstand teen verskeie virusse. Daarom was die fokus van hierdie studie om patogeen-afgeleide weerstand strategieë vir GLRaV-3 te evalueer met behulp van die volgende twee benaderings; 1) die evaluering van transgeniese plante wat 'n disfunksionele GLRaV-3 hitte-skok proteïen 70 homoloog (HSP70h) uitdruk, ten einde weerstand te verleen teen GLRaV-3, en 2) die konstruksie van kunsmatige mikroRNAs (amiRNAs) om te gebruik as 'n instrument vir die ondrukking van spesifieke genoomvolgordes van GLRaV-3 in die wingerd gasheer en die ontwikkeling van ’n stelsel om amiRNA-bemiddelde onderdrukking te bevestig.

In die eerste deel van hierdie studie, is ses transgeniese plant lyne (plant lyne # 1, # 3, # 9, # 14, # 15 en # 17) sowel as 'n nie-gemodifiseerde gesonde plant lyn, geïnokuleer met GLRaV-3 deur enting van ogies van elk op GLRaV-3 besmette plantmateriaal. Na ongeveer vyf maande, is GLRaV-3 virus konsentrasies van alle ingeënte plante gekwantifiseer relatief tot twee verwysing gene deur gebruik te maak van tru-transkripsie kwantitatiewe PCR (RT-qPCR). Resultate is geëvalueer deur die relatiewe virus konsentrasie van elke transgeniese plant lyn te vergelyk met dié van die nie-gemodifiseerde kontrole lyn. Resultate het getoon dat weerstand vlakke van plant lyn # 3 beduidend verbeter is (> 99%) en merkwaardig is plant lyn # 14 bewys om meer vatbaar vir die virus te wees.

Die tweede deel van die studie was die konstruksie en bevestiging van kunsmatige mikroRNAs (amiRNAs) wat GLRaV-3 genoomvolgordes teiken. Twee 21 nt streke van GLRaV-3 is suksesvol geïnkorporeer in die ruggraat van wingerd mikroRNA vvi167b. Verder is teiken konstrukte ontwikkel deur die inkorporering van ooreenstemmende GLRaV-3 teiken genoomvolgordes in die 3'UTR (3’ ongetransleerde area) van 'n groen fluoressensie proteïen (GFP) geen. Daarna is die teiken konstrukte gesamentlik geïnfiltreer met die gekonstrueerde

amiRNA in *Nicotiana benthamiana* en GFP uitdrukkingsvlakke is gekwantifiseer deur die onderdrukkingsdoeltreffendheid van die amiRNAs te bepaal. Resultate het getoon dat die amiRNAs suksesvol was in die onderdrukking van die GFP teiken konstruk, maar hulle was egter nie-spesifiek in die eksklusiewe onderdrukking van die ooreenstemmende teiken. Hierdie amiRNA konstrukte is ideaal vir verdere virus studies om die doeltreffendheid van GLRaV-3 onderdrukking in GLD besmette wingerdstokke te bepaal.

Acknowledgements

I would like to sincerely thank the following individuals:

My supervisors, Professor JT Burger and Dr. HJ Maree, for their guidance, great supervision and patients throughout this study, especially during the writing part of this thesis.

Dr. T. Pepler for his help with the statistical analyses.

All the members of the Vitis lab and my special friends in South Africa for their support, help and all the great moments we had together.

THRIP, Winetech and Stellenbosch University for financial support.

My parents for being so awesome. I could not have done this study without their support, love, encouragement and skyping sessions.

Table of Contents

List of Figures

List of Tables

List of Abbreviations

µg	microgram(s)
µl	microlitre(s)
3'UTR	3' untranslated region
5'UTR	5' untranslated region
aa	*amino acid*
AGO	argonaute
AlMV	*Alfalfa mosaic virus*
amiRNA	*artificial microRNA*
Amp	ampicillin
AWSV	*Alligatorweed stunting virus*
bp	*base pair*
BPMV	*Bean pod mottle virus*
BPyV	*Bovine polyomavirus*
BYSV	*Beet yellow stunt virus*
BYV	*Beet yellows virus*
BYVaV	*Blackbarry yellow vein associated virus*
cDNA	complementary DNA
CHS	chalcone synthase
CoV-1	*Cordyline virus 1*
CP	coat protein
CPMR	coat protein-mediated resistance
Ct	threshold cycle
CTV	*Citrus tristeza virus*
cv	cultivar
CYLV	*Carrot yellow leaf virus*
DAS	double antibody sandwich
DCL	dicer-like
dCP	divergent coat protein
dH_2O	deionised water
DNA	deoxyribonucleic acid
dNTP	deoxynucleotide triphosphate
dsRNA	double-stranded RNA

ssRNA	single-stranded RNA
ELISA	enzyme-linked immunosorbent assay
GAPDH	glyceraldehyde 3-phosphate dehydrogenase
GCMV	*Grapevine chrome mosaic nepovirus*
GDP	gross domestic product
GFLV	*Grapevine fanleaf virus*
GFP	green fluorescence protein
GLD	Grapevine leafroll disease
GLRaV-1	*Grapevine leafroll-associated virus 1*
GLRaV-2	*Grapevine leafroll-associated virus 2*
GLRaV-3	*Grapevine leafroll-associated virus 3*
GLRaV-4	*Grapevine leafroll-associated virus 4*
GLRaV-5	*Grapevine leafroll-associated virus 5*
GLRaV-6	*Grapevine leafroll-associated virus 6*
GLRaV-7	*Grapevine leafroll-associated virus 7*
GLRaV-8	*Grapevine leafroll-associated virus 8*
GLRaV-9	*Grapevine leafroll-associated virus 9*
GLRaV-Pr	*Grapevine leafroll-associated virus Pr*
GLRaV-De	*Grapevine leafroll-associated virus De*
GLRaV-Car	*Grapevine leafroll-associated virus Car*
gRNA	genomic RNA
GUS	β-Glucuronidase
GVA	*Grapevine virus A*
HSP70h	heat shock protein 70-homolog
HSP-Mut	heat shock protein mutated plant lines
IPTG	isopropyl-β-D-thiogalactoside
IR	inverted-repeat
kb	kilobase
kDa	kilodalton
LB	Luria Bertani broth
LChV-2	*Little cherry virus 2*
LIYV	*Lettuce infectious yellows virus*
M	molar
MegMV	*Megakepasma mosaic virus*

miRNA	microRNA
mM	millimolar
MP	movement protein
MPMR	movement protein-mediated resistance
Mr	molecular weight
mRNA	messenger RNA
MVBV	*Mint vein banding virus*
ng	nanograms
NGS	next generation sequencing
nt	nucleotide
NVT	normalized virus titre
OD600	absorpsion value at 600 nm
ORF	open reading frame
PBNSPaV	*Plum bark necrosis stem pitting associated virus*
PCR	polymerase chain reaction
PDR	pathogen-derived resistance
PMWaV-1	*Pineapple mealybug wilt associated virus 1*
PMWaV-2	*Pineapple mealybug wilt associated virus 2*
PMWaV-3	*Pineapple mealybug wilt associated virus 3*
PTGS	post-transcriptional gene silencing
PVY	*Potato virus Y*
OLYaV	*Olive leaf yellowing-associated virus*
qPCR	quantitative polymerase chain reaction
REST	Relative Expression Software Tool
RISC	RNA-induced silencing complexes
RNA	ribonucleic acid
RNAi	RNA interfering
RMVR	RNA-mediated virus resistance
RT-PCR	reverse transcriptase polymerase chain reaction
RT-qPCR	reverse transcriptase quantitative polymerase chain reaction
SAWIS	South African Wine Industry Statistics
sgRNA	sub-genomic RNA
siRNA	small interfering RNA
SMV	*Soybean mosaic virus*

sncRNA	small non-coding RNA
SNP	single-nucleotide polymorphisms
SPCSV	*Sweet potato chlorotic stunt virus*
TEV	*Tabacco etch virus*
Taq	*Thermus aquaticus* DNA polymerase
TMV	*Tobacco mosaic virus*
TuMV	*Turnip mosaic virus*
TYMV	*Turnip yellow mosaic virus*
U	units
UTR	untranslated region
V	volt
v/v	volume per volume
w/v	weight per volume
β-ME	β-mercaptoethanol

Chapter 1 Introduction

1.1 General introduction

Grapevine is an important crop grown worldwide for consumption as fresh fruit or the production of wine, raisins, jam and juice. According to the latest studies of the South African Wine Industry Statistics (SAWIS), a total of 99 680 hectares were used to grow grapevines for the wine industry by December 2013. The domestic sales for 2013-2014 accounted for over R332 million and another R481 million in sales were exported the same year. More than 27 billion gross litres of wine were sold in 2012. South Africa ranks number eight in the production of wine globally.

A macro-economic impact study in 2009 revealed that the total turnover of the wine industry in South Africa in 2008 amounted to approximately 20 billion Rands, this amounts to 2.2% of the total gross domestic product (GDP) (http://www.sawis.co.za). Of the R26.2 billion GDP, about R14.2 billion (approximately 54%) is derived from the Western Cape only. The same macro-economic impact study showed that the wine industry generates 17% of the household income which supports over 275 000 employment opportunities in South Africa (http://www.sawis.co.za).

Grapevine leafroll disease (GLD), caused by the members of the family *Closteroviridae,* is considered to be one of the most important viral diseases affecting grapevine (Rayapati *et al*., 2008). A study in 2012 conducted by Atallah *et al.,* revealed that 27% of grapevine yield losses are a result of GLD. Consequently, the collective financial losses caused by viral diseases in grapevine are claimed to be over a million dollars annually (Burger and Maree, unpublished data). The focus of this study is to evaluate control strategies against the most widespread member of the leafroll-associated family *Closteroviridae* which is *Grapevine leafroll-associated virus* 3 (GLRaV-3) in the genus *Ampelovirus*.

1.2 Previous studies

This study is a continuation of earlier projects by Micheal-John Freeborough (2003) and Stefanie Malan (2009). The Freeborough-study developed transgenic grapevines (rootstock cultivar Richter 110) expressing a dysfunctional GLRaV-3 heat shock protein 70-homolog

(HSP70h) in order to confer resistance against GLRaV-3. The dysfunctional HSP70h was created by incorporating four point mutations using site-directed mutagenesis to alter four conserved amino acids in the ATPase domain of this protein. A previous study with *Beet Yellows Virus* (BYV), which is also a member of the family *Closteroviridae*, suggested that the HSP70h functions as a movement protein (Peremyslov *et al.,* 1999).

Stefanie Malan (2009) evaluated the copy number and expression levels of the dysfunctional HSP70h of 20 HSP-Mut transgenic plant lines. Of the original 20 transgenic HSP-Mut grapevine lines, six lines were available for this study. These are #1, #3, #9, #14, #15 and #17, all of which are growing in a standard GMO greenhouse facility at the Welgevallen experimental farm in Stellenbosch.

Another potential management strategy to control GLRaV-3 in grapevine is the use of artificial microRNAs (amiRNAs), targeting specific sequences of the virus. The second part of this study focuses on the construction and validation of such amiRNAs. The pre-miRNA of *Vitis vinifera* 167b was shown to be an effective backbone in a previously conducted project, and therefore used as a backbone for the construction of two amiRNAs in this study (Pers. Comm. M. Snyman). In addition, a validation system was designed to evaluate the efficiency of amiRNAs.

1.3 Aim of this study

The aim of this study was to evaluate pathogen-derived resistance strategies for GLRaV-3 using the following two approaches; 1) evaluation of transgenic plants expressing a dysfunctional GLRaV-3 HSP70h in order to confer resistance against GLRaV-3, and 2) the construction of amiRNAs to use as a tool for silencing specific sequences of GLRaV-3 in the grapevine host and the development of an artificial microRNA-mediated silencing validation system.

1.4 Objectives

1.4.1 Objectives for the evaluation of HSP-Mut plants

- To optimise an RT-qPCR protocol for relative quantitation of GLRaV-3 virus titres.

- To construct standard correlation curves for the GLRaV-3 ORF1a gene and reference genes using RT-qPCR.
- To evaluate the efficiency in conferring resistance to GLRaV-3 infection in transgenic plants expressing a dysfunctional form of the HSP70h by determining the relative titres of GLRaV-3 in the HSP-Mut plants

1.4.2 Objectives for the construction and validation of amiRNAs

- To construct amiRNAs targeting GLRaV-3 to use as a tool for silencing specific sequences of GLRaV-3.
- To construct a target vector for the validation of amiRNAs by incorporating the target sequences of the specific amiRNA in the 3' UTR of a green fluorescence protein (GFP) gene.
- To validate the silencing efficiency of the amiRNA by quantifying the expression levels of GFP using the IVIS Living Image System.

1.5 Breakdown of chapters

Chapter 1: Introduction

This chapter describes the wine industry and the motivation of this study including the aims, objectives and a brief description of every chapter.

Chapter 2: Literature review

All the relevant literature related to this study is reviewed in this chapter including leafroll disease, *grapevine leafroll-associated virus 3*, virus detection and management strategies.

Chapter 3: Evaluation of transgenic HSP mutated grapevines

This chapter describes the evaluation of transgenic grapevines, containing a mutated HSP70h, in conferring resistance to GLRaV-3. Six HSP-Mut plant lines were inoculated with the virus through graft transmission and quantities of the virus titre were determined for analyses.

Chapter 4: Development and validation of artificial microRNA constructs to silence specific GLRaV-3 sequences in *Nicotiana* benthamia

This research chapter describes the construction and validation of amiRNAs targeting specific sequences of GLRaV3. The amiRNA-mediated silencing system is a general validation method using a GFP gene to visualise the silencing efficiency of amiRNAs.

Chapter 5: Conclusion

This chapter describes the final conclusion of this thesis including future prospects.

1.6 References

Atallah, S. S., Gómez, M. I., Fuchs, M. F., and Martinson, T. E. 2012. Economic impact of Grapevine leafroll disease on *Vitis vinifera* cv. Cabernet franc in Finger Lakes vineyards of New York. *American Journal for Enology and Viticulture* 63, 73–79.

Burger, J.T.B. and Maree, H.J. 2014. Metagenomic next-generation sequencing of viruses infecting grapevines. *Unpublished data*.

Freeborough, M-J. 2003. A pathogen-derived resistance strategy for the broad-spectrum control of Grapevine leafroll-associated virus infection. *Thesis University of Stellenbosch*

Malan, S. 2009. Real Time PCR as a versatile tool for virus detection and transgenic plant analysis. MSc thesis, Stellenbosch University.

Peremyslov, V.V., Hagiwara, Y. and Dolia, V.V. 1999. HSP70 homolog functions in cell-to-cell movement of a plant virus. *PNAS*. 96(26): 14771 – 14776

Rayapati, N., O'Neal, S. and Walsh, D. 2008. Grapevine leafroll disease. *Washington State University Extension.*

Sawis, 2013. Wine Export Analysis 200812 – 1 March 2013. Available at: http://www.sawis.co.za/info/download/Wine_Exports_Analysis_200812_-_1_March_2013.pdf. Accessed 8 March 2013

Chapter 2 Literature review

2.1 Introduction

It is believed that the first wine was produced in Persia around 6000 BC. Over the years, winemaking spread to other countries in Southern-Europe and North-Africa (http://www.wosa.co.za/sa/history_beginning.php). Today, wine is produced all over the globe in tropical and mild climate regions and grapevines are considered to be one of the most economically important crops. South Africa ranks number eight in the top wine-producing countries worldwide, which contributed to over 26 billion Rands to the South African economy in 2008 (SAWIS).

2.2 Grapevine leafroll disease

2.2.1 Introduction

Numerous factors can influence the efficiency and health of grapevines. Abiotic elements such as nutritional deficiencies, climate conditions and air contamination can have detrimental effects on the crop. Other negative effects can be explained by infections caused by pathogens and pests including insects, bacteria, fungi and viruses (Martelli 2014). Plant viruses are the most damaging and widespread of the diseases infecting grapevine. They are known to cause crop losses and limit the productive lifespan of grapevines (Martelli and Boudon-Padieu, 2006; Martelli 2014). A single grapevine can be infected by multiple virus species (Coetzee *et al*., 2010; Prosser *et al.,* 2007). Up to date, over 70 infectious agents (viruses, viroids and phytoplasmas) have been documented from grapevines (Martelli 2014). However, there are only four major virus diseases known in grapevines; grapevine leafroll disease, rugose wood complex, grapevine fanleaf infectious degeneration and grapevine fleck complex (Martelli 2008). Grapevine leafroll disease (GLD), caused by the members of the family *Closteroviridae,* is considered to be one of the most important economically diseases (Rayapati *et al*., 2008).

The most widespread member of the leafroll-associated is *Grapevine leafroll-associated virus* 3 (GLRaV-3) of the genus *Ampelovirus* in the family *Closteroviridae*. GLRaV-3 is considered to be the most destructive agent for GLD since it has consistently been associated with GLD. In addition to this, the study of Engelbrecht and Kasdorf in 1990 revealed that GLRaV-3 is

also associated with other grapevine diseases such as Shiraz disease and grapevine corky-bark.

2.2.2 Symptomology of GLD

In most red fruit varieties of *Vitis vinifera,* GLD symptoms start in late spring or summer and are characterized by red patches in the interveinal areas. These patches expand until most of the leaf surface becomes reddish except for the primary and secondary veins as indicated in figure 2.1. In severe cases, the colour becomes deep purple without green veins. Additionally, the leaf becomes brittle, thick and the margins roll downwards. In white-berry grapevines, the symptoms are comparable but the leaves become chlorotic instead of red. Chardonnay show noticeable down-rolling of the leaf, while other cultivars like Sauvignon blanc and Thompson Seedless rarely show leaf-rolling. Most rootstocks and certain white varieties infected with GLD can be completely symptomless. However, GLD symptoms are generally dependent on environmental conditions, grape cultivar and the season of the year (Martelli and Boudon-Padieu 2006).

Figure 2.1 Grapevine leaf showing GLD symptoms, the leaf surface is reddish except for the primary and secondary veins (Hansen 2011).

2.2.3 Physiological effects of GLD

Several studies proved the harmful effects of GLRaV-3 infection in grapevines; it decreases the sugar content, lowers the pH, modifies aromatic profiles, and reduces yield (Cabaleiro *et al.,* 1999; Komar *et al.,* 2007; Mannini *et al.*, 2012). More specifically, the virus infection affects grapevine by degeneration of the phloem in stems, leaves petioles and fruit. Starch collects in degenerated chloroplasts, subsequently shutting down the photosynthetic activity and increasing leaf thickness and brittleness. Additionally, other physiological factors, such as depletion of the protein content and potassium reduction in leaves have been documented in GLD infected plants (Martelli and Boudon-Padieu 2006).

2.2.4 Viruses associated with GLD

In the mid-1990s it was discovered that GLD is caused by numerous serologically distinct viruses. Consequently, six grapevine leafroll-associated viruses (GLRaVs 1 - 6) were documented at that time (Boscia *et al.,* 1995). To date, the number of reported distinct viruses associated with GLD has doubled. An additional six GLRaVs have been described, namely: GLRaV-7, GLRaV-8, GLRaV-9, GLRaV-Pr, GLRaV-De and GLRaV-Car. The family *Closteroviridae* is classified into four genera based on their biological and molecular characteristics: *Closterovirus* (GLRaV-2), *Ampelovirus* (GLRaV-1, -3, -4, -5, -6, -9, -Pr, -De and –Car), *Crinivirus* and *Velarivirus* (GLRaV-7) (Martelli 2012). However, in 2009 Bertsch *et al*. showed that the sequence of GLRaV-8 was not of viral origin and in fact is part of the grapevine genome. Furthermore, the study of Ghanem-Sabanadzovic *et al.* (2012) suggested that GLRaV-4, -5, -6 (and its –De variant), -9 and -Pr form a sub-cluster instead of distinct species. Martelli *et al*. (2012) suggested to group these variants to GLRaV-4 like viruses.

Additional studies of the GLRaVs in the genus *Ampelovirus* suggest that these viruses can be divided into two subgroups according to their molecular and biological characteristics as shown in Figure 2.2: subgroup I includes GLRaV-1, GLRaV-3, *Little cherry virus 2* (LChV-2) and *Pineapple mealybug wilt associated virus 2* (PMWaV-2). Subgroup II includes GLRaV-4, *Plum bark necrosis stem pitting associated virus* (PBNSPaV), PMWaV-1 and PMWaV-3 (Martelli *et al.,* 2012).

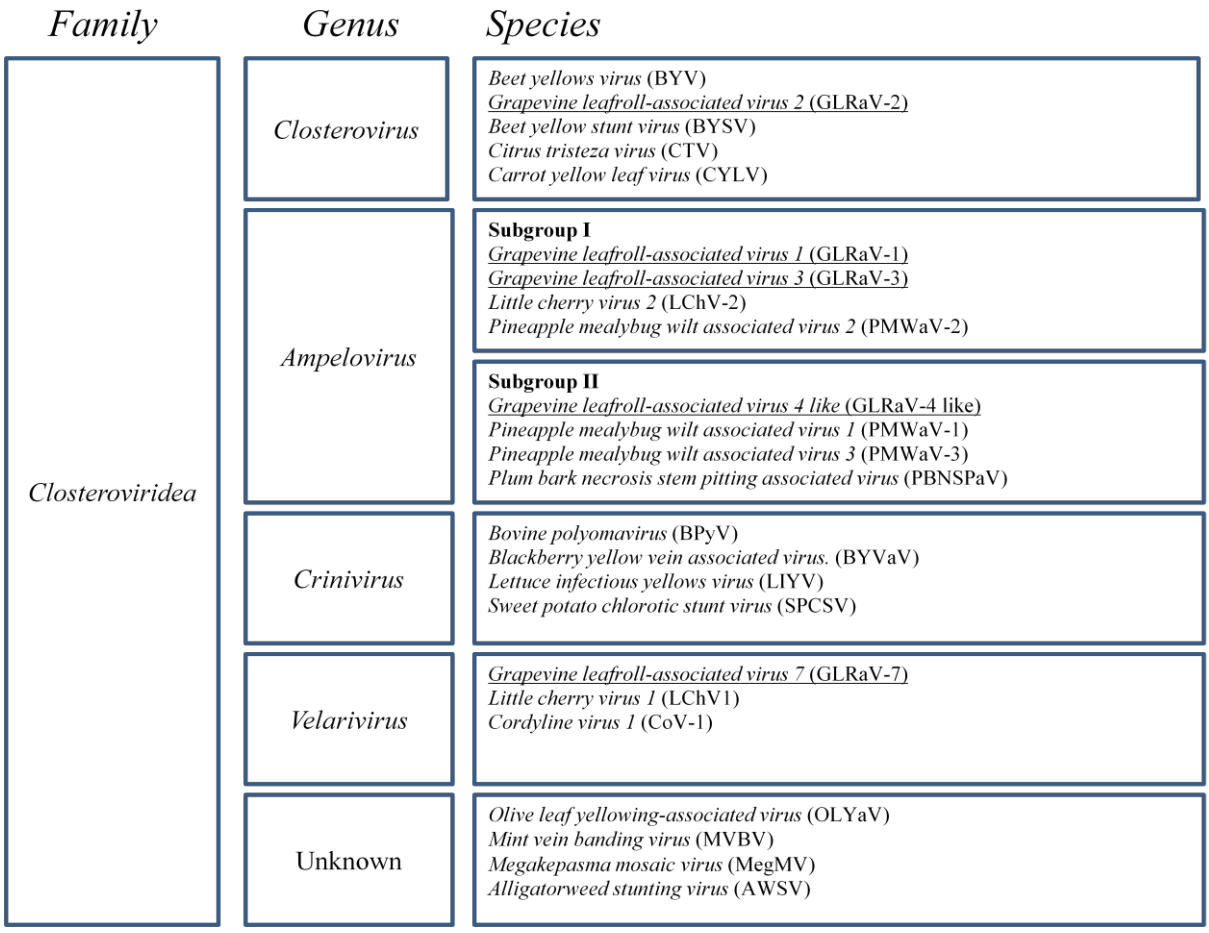

Figure 2.2 Diagram of virus classification based on their molecular and biological characteristics in the family *Closteroviridea* (Maree et al., 2013; Martelli *et al.,* 2012). Viruses associated with GLD are underlined.

2.2.5 **Transmission of GLD**

Up until the 1980s it was assumed that the distribution of GLD only occurred through infected plant material. Although this is still the major cause of the spread of GLRaVs, in 1983 Rosciglione *et al.* discovered that some insects, more specifically mealybugs (*Planococcus spp.*), are vectors of GLRaVs. Subsequently, more studies confirmed the role of mealybugs and soft scales (*Coccidae*) as vectors of grapevine leafroll associated viruses (Engelbrecht and Kasdorf 1990; Krake *et al*., 1999; Tsai *et al.,* 2010). Several species of mealybugs, more specifically *Planococcus ficus* and *Pseudococcus longispinus*, and a few species of soft scales have been described to be vectors of GLRaVs (Tsai *et al.,* 2010; Douglas and Krüger, 2008). In 2008, Douglas and Krüger showed virus transmission by single nymphs to be up to 70% efficient. Furthermore, they are able to transmit the virus throughout the whole growing season and do not need vines with high virus titres to establish a successful infection in the next plant (Petersen and Charles, 1997; Kingston, 2002). The first instar stage is believed to be a more efficient vector than older nymphs or adults (Petersen and Charles, 1997; Kingston,

2002; Habili *et al.,* 1995). This might due to the immobility of the adults since small instars can be easily dispersed by wind (Barrass *et al.,* 1994).

Figure 2.3 Elongate-oval shaped mealybug. (Hodges and Hodges, 2006)

The body size of mealybugs are small, first instars are approximately 0.6 mm in length, female adults are 3-5 mm and males are about 1.5 mm in size (reviewed in Daane *et al.* 2012). Mealybugs are flat and elongate-oval shaped as shown in Figure 2.3.

GLRaV-3 is graft transmissible and infected grafted vines often contribute to disease spread. Pathirana and McKenzie (2005), used a modified green-grafting protocol to index grapevine viruses. Ninety percent of the grafts showed symptoms after 12 weeks, confirming that grafting is an efficient transmission method.

2.3 Grapevine leafroll associated virus-3

2.3.1 Physical properties

GLRaV-3 consists of a filamentous and flexuous virion of 1800 - 1900 nm in length (Zee *et al*., 1987). The exact molecular weight of the coat protein is unclear. According to a study by Hu *et al,* (1990) the virion contains a 43 kDa coat protein, while Ling *et al* (1997) described a coat protein of 41 kDa. The predicted calculated coat protein molecular weight is however 35 kDa. The GLRaV-3 genome is approximately 18,500 nt in length, depending on the genetic variant, and contains a linear positive-sense single stranded RNA which is divided into 13 open reading frames (ORFs); ORF 1a and 1b, as well as ORFs 2-12 as shown in Figure 2.4. (Ling *et al.,* 1998; Ling *et al.,* 2004; Maree *et al.,* 2008).

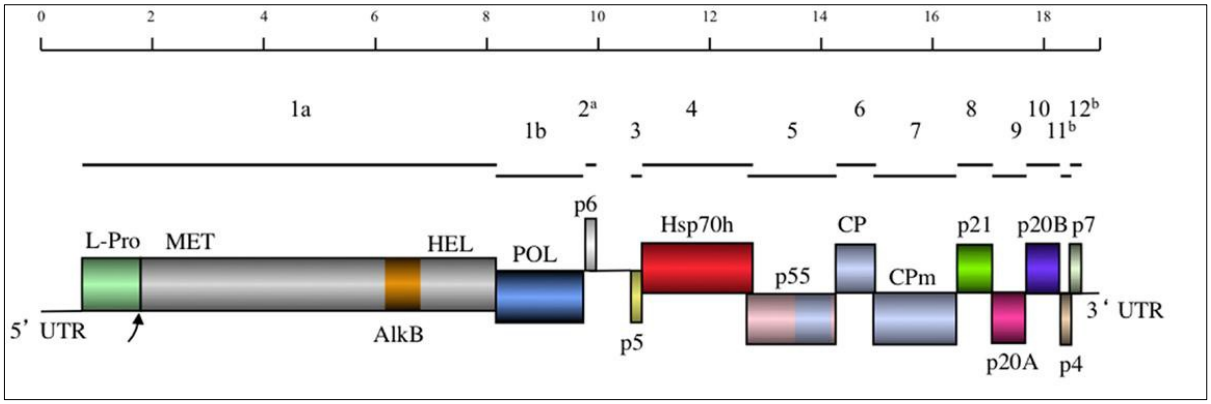

Figure 2.4 GLRaV-3 genome organisation. L-Pro, leader protease; MET, methyltransferase domain; HEL, RNA helicase domain; RdRp, RNA-dependent RNA polymerase; HSP70h, heat shock protein 70 homolog; CP, coat protein; CPm, minor coat protein (Rwahnih et al., 2012)

2.3.2 GLRaV-3 genome replication

In the 1990's, a number of studies suggested the production of several sub-genomic RNAs (sgRNAs) (Hu *et al.,* 1990; Saldarelli *et al.,* 1994; Rezaian *et al.,* 1991; Ling *et al.,* 1997). These sgRNAs express ORFs located on the 3' half of the genome. SgRNA products, like movement proteins or structural proteins, are known to function during intermediate and late stages of infection. It is suggested that the sgRNAs are transcribed from genomic RNA (gRNA) by a viral replicase (Miller and Koev, 2000), however, the precise mechanism is more complex than was previously expected (Ayllón *et al.,* 2004). Only recently, sgRNAs of two GLRaV-3 isolates have been characterized and studied in detail (Maree *et al.,* 2010; Jagugula *et al.,* 2010). According to the study conducted by Jarugula *et al.*, (2010) ORF 6 (CP), 8 (p21), 9 (p20A) and 10 (p20B) are abundantly expressed in the viral GLRaV-3 infection by their corresponding sgRNAs, whereas ORF 10 was found to accumulate to the highest levels, followed by ORFs 8, 9 and 6. This shows that there are differences in the expression and/or accumulation of the sgRNAs, which possibly could be the result of temporal and quantitative regulation of the sgRNA transcription during the infection cycle.

2.3.3 Genetic variants of GLRaV-3

Due to the high mutation rates and large population sizes of RNA viruses, the genetic variations in viral populations are high (Holmes, 2009). In 2004, Ling *et al.* reported a 5' untranslated region (UTR) of 158 nt but through further investigation of this region, Maree *et al.* (2008) discovered a significantly larger 5' UTR of 737 nt. This extended UTR was subsequently confirmed in all isolates of GLRaV-3. Furthermore, an overlap of 82 nt between

ORF 1a and ORF1b in the sequence of isolate GP18 was identified (Maree *et al.,* 2008). Through single strand conformation polymorphism (SSCP) profiles, three variants were discovered in South Africa (Jooste and Goszczynski, 2005; Jooste *et al.,* 2010; Maree *et al.,* 2008). These include variants 621 (Group I, GQ352631), 623 (Group II, GQ352632) and PL-20 (Group III, GQ352633). To date, 13 GLRaV-3 complete genomes were described globally, which represent four major groups of genetic variants (Maree *et al.,* 2013; Ling *et al.,* 2004; Engel *et al.,* 2008; Maree *et al.,* 2008; Jarugula *et al*., 2010; Jooste *et al.,* 2010; Bester *et al.,* 2012; Maree *et al.,* unpublished). Remarkably, isolates of group VI do not contain ORF 2. Furthermore, no complete genomes are available for groups IV, V and putative group VII (Bester *et al.,* 2012; Maree *et al.,* 2013). Figure 2.5 represents a phylogenetic tree containing all the known GLRaV-3 variants divided in 6 groups based on their nucleotide similarities.

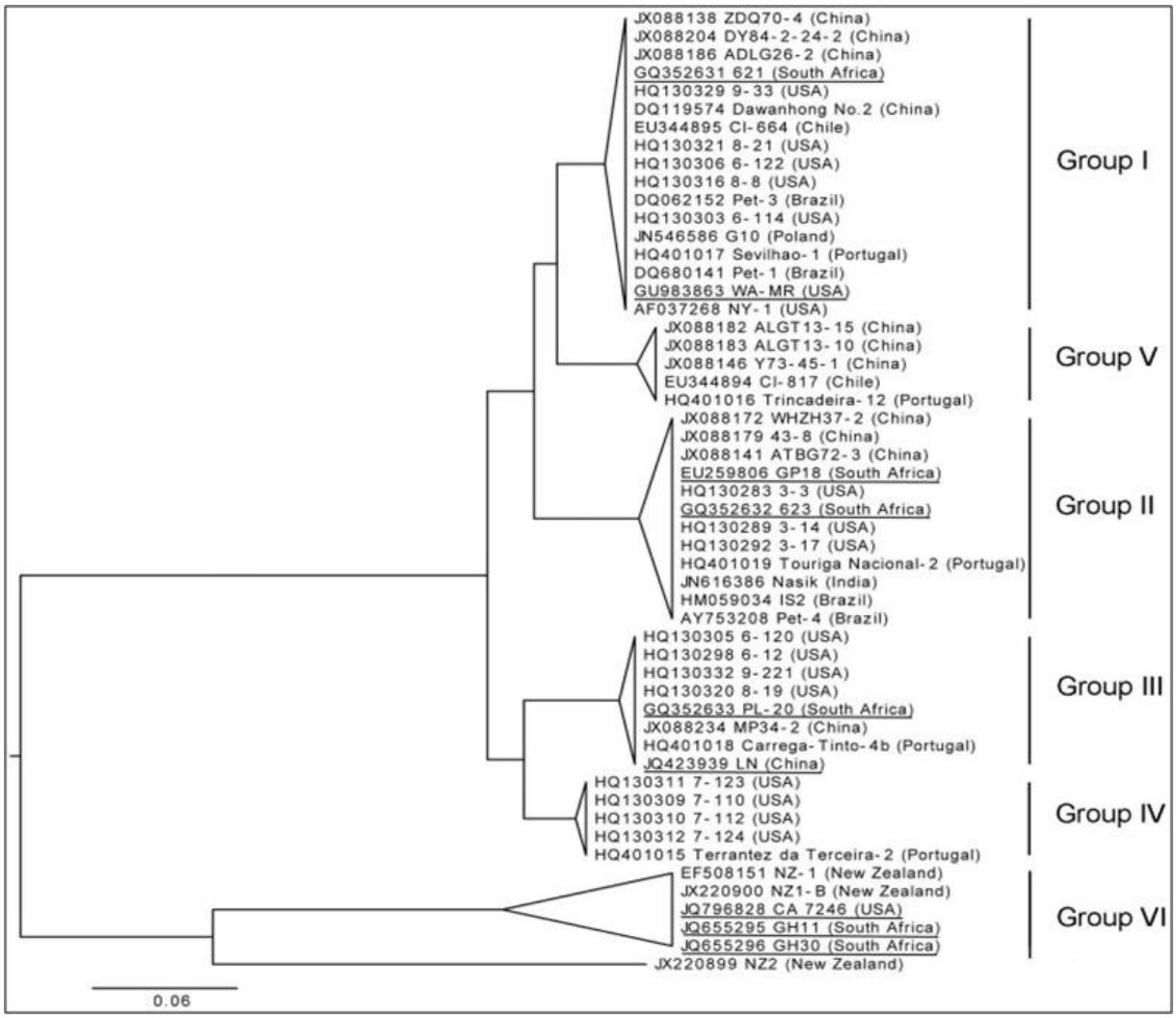

Figure 2.5 Phylogenetic tree of GLRaV3 variants. Roman numerals show variant groups. Isolates contain accession number, isolate name, and country where samples were collected. Full-length sequenced genomes are underlined (Maree *et al.,* 2013).

2.4 Virus detection

2.4.1 Introduction

Visual detection of GLD can be complicated by a number of factors; unrelated viruses can cause symptoms similar to those of GLD, while, conversely, some grapevine varieties remain symptomless, which makes visual detection challenging. Furthermore, new infections often contain a lower virus titre. Therefore, several techniques have been developed to identify viruses associated with GLD in grapevines, including biological indexing, serological methods, PCR-based methods and next generation sequencing (NGS).

2.4.2 Biological indexing

Before laboratory tests were available for viral diseases, biological indexing was the only reliable technique available to test for GLD. A bud of the candidate vine is grafted onto an indicator grapevine cultivar and studied for at least two years for the development of GLD symptoms (Rowhani and Golino, 1995; Weber *et al.,* 2002). However, this technique lacks specificity, is labor intensive, depends on the success rate of the virus inoculation and is time-consuming (Weber *et al.,* 2002). Furthermore, a skilled virologist is required for the confirmation of visual observations.

2.4.3 Serological methods

One of the most commonly used serological detection methods is enzyme-linked immunosorbent assay (ELISA). The first ELISA was developed by Clark and Adams in 1976 and the principle of this technique is based on the interaction of antibodies and viral antigens. Various types of ELISA are available, including competitive ELISA, direct ELISA, indirect ELISA and the most frequently used variant; double-antibody sandwich enzyme-linked immunosorbent assay (DAS-ELISA).

2.4.4 PCR-based methods

PCR-based methods, such as reverse transcription PCR (RT-PCR), have been shown to be more sensitive and capable to detect low viral titres when compared to ELISA (Charles et al., 2006). RT-PCR converts template RNA into complementary DNA (cDNA) followed by PCR amplification with primers specific for the gene of interest. This technique has since become the technique of choice because of its higher accuracy, sensitivity and reliability (López-Fabuel et al., 2013).

Viral RNA titre can be determined by reverse transcription quantitative PCR (RT-qPCR) using virus-specific primers. Quantitative PCR, also known as Real-Time PCR, is used to measure the initial amounts of RNA, DNA and cDNA targets. The principle of qPCR detection techniques is the recognition of a fluorescent signal, which increases proportional to the amount of PCR product in the sample. With each new cycle, the signal intensity accumulates due to the increased PCR product. There are two chemistries which can be used for the detection of PCR products, target-specific fluorescently labelled probes such as TaqMan, and target non-specific fluorescence dyes such as SYBR Green.

Fluorescent dyes, such as SYBR Green and Syto9, exhibit little fluorescence when unbound in solution; however, when bound to dsDNA they generate a highly fluorescent signal. The main advantages are the low cost and the ability to analyse many different targets without having to synthesize fluorescently labelled sequence-specific probes. However, fluorescent dyes cannot distinguish between different dsDNA fragments. Therefore, the formation of primer-dimers and non-specific targets must be prevented by PCR optimisation and correct primer design.

The use of fluorescence dyes allows for the post-PCR evaluation of PCR products using melting curve analysis. Melting curve analysis has the ability to characterize double-stranded DNA fragment through heat. When the temperature raises, the DNA starts to dissociate resulting in a decrease in fluorescence. The melting point can then be used to infer the presence of different PCR products and even identify single-nucleotide polymorphisms (SNP) in PCR products.

Fluorescently labelled probes provide a highly accurate and sensitive method for the detection of PCR product, as only a sequence specific region is targeted. Probes are oligonucleotides labelled with a quencher and reporter molecule that can bind specifically to the PCR product of interest. Several probe-based chemistries have been developed such as TaqMan®, hybridization (FRET), molecular beacon, and Eclipse® probes. For example, during the PCR extension step, a Taqman probe is partially displaced and the reporter molecule (fluorophore) is cleaved by Taq DNA polymerase to generate a fluorescence signal. Probe-based chemistry allows the user to perform multiplex reactions using different fluorophores. However, fluorescence probes are more expensive when compared to DNA-binding dyes and the design

can be complex.

For both fluorescence dye and probe-based chemistries, the target products can be quantified using either relative or absolute quantitation. Relative quantitation determines the proportion between the quantity of product and an endogenous reference molecule, usually a stably expressed reference gene, whereas absolute quantitation determines the absolute amount of target by comparing it to a standard DNA sample (expressed as concentration or copy number).

2.4.5 Next generation sequencing

Although PCR-based methods are reliable and accurate, they do require prior knowledge of the target virus sequence. In addition, grapevines are often infected by multiple viruses, which makes the establishment of the total viral complement of one sample, challenging (Prosser *et al.,* 2007). The use of Next Generation Sequencing (NGS) has overcome these limitations by using universal adapters and the sequencing of millions of short fragments in parallel, rather than the use of chain termination chemistry as in Sanger sequencing. Several NGS platforms are available including Roche 454, Applied Biosystems SOLiD and Illumina.

2.5 Management of grapevine leafroll disease

2.5.1 Current management practices

No natural resistance to viral disease has been detected in grapevine and therefore other management practices or resistance strategies are required. The most successful method of virus control relies on the production and retention of healthy plants. Rogueing, the removal of infected plants, and replanting virus-free plants is currently the best approach to control the impact and spread of GLD. It reduces the disease impact six- to seven-fold depending on the cultivar (Atallah *et al.,* 2011). However, the virus can survive for at least another 12 months in remnants of the roots, which allows for the possibility of re-infection in newly replanted vines (Bell *et al.,* 2009). Other techniques, such as thermotherapy, meristem culture and mealybug control are also used to control GLD (Wang *et al.,* 2003; Walton *et al.,* 2009).

In South Africa, mealybug control is one of the most common methods for management and control of GLRaV-3 infections. These include chemical control through pesticides, biological control using natural enemies of the mealybug such as lady beetle and crab spiders,

monitoring programs and the removal of weeds (Charles *et al*., 2006). However, the control of viral infections in grapevine remains inadequate, requires reliable, accurate and sensitive detection methods and is unlikely to eliminate all viruses from grapevine. Furthermore, the latent phase of new virus infections and some of the symptomless cultivars make diagnostics of virus diseases challenging.

2.5.2 Pathogen-derived resistance

An alternative strategy to manage virus spread can be through the genetic modifications of grapevines. One such approach is known as pathogen-derived resistance, which is based on the expression of the genes derived from the pathogen itself. The virus infection is repressed and the pathogenicity is reduced when genes derived from the virus are expressed in a dysfunctional form, inappropriate concentration or at an incorrect time in the infection cycle. The first transgenic plants based on this concept were constructed in 1985 by Stanford and Johnston. Since then, several transgenic plants have been successfully created using this approach, which resulted in several virus resistant crops (Beachy, 1993; Wilson, 1993; Baulcombe, 1994; Lommonossoff, 1995). There are several forms of pathogen-derived resistance; coat protein-mediated resistance (CPMR), movement protein-mediated resistance (MPMR) and RNA mediated resistance are the most well known.

2.5.2.1 Coat protein-mediated protection

The first successful study using CPMR was conducted by Powell-Abel *et al.* in 1986, transgenic tobacco plants, expressing high levels of the wild type coat protein (CP) gene of *Tobacco mosaic virus* (TMV), were created. Furthermore, transgenic plants expressing a mutant recombinant form of the TMV CP also conferred resistance to the virus (Clark *et al.,* 1995). Since the CP is involved in several biological aspects including virus replication, encapsulation, cell-to-cell or systemic movement, symptom development and vector transmission, it was assumed that the mutant CP interacts with the virus' own CP to inhibit virion disassembly. Graft experiments in 1990 by Wisniewski *et al.* have showed a correlation between the inhibited TMV movement through the vascular system of the plant and the influence of CPMR. To date, the use of CPMR has been documented for over 35 viruses from 15 different taxonomic groups (reviewed by Glavez *et al.,* 2014).

The first CPMR transgenic grapevine, in which the CP of *Grapevine chrome mosaic nepovirus* (GCMV) was expressed in high levels, was generated in 1994 by Le Gal *et al.* However, it is unknown if those plants were ever evaluated in conferring resistance to

GCMV. Since then, several studies have introduced the CP in different varieties to achieve resistance in grapevines (Valet *et al.,* 2006; Krastanova, *et al.,* 1995; Xue *et al.,* 1999; Spielmann *et al.,* 2000). Although the CP is the most common used gene in PDR, other viral genes including the movement protein (MP) have also been used to limit the virus spread.

2.5.2.2 Movement protein-mediated resistance

The first successful study using MPMR was reported in tobacco plants expressing a dysfunctional MP, which was proposed to compete with the virus' endogenous MP for the binding sites in the plasmodesmata. Remarkably, the transgenic tobacco plants also limited the spread of a broad spectrum of unrelated and distantly related viruses including caulimo-, astobra- and the nepo-viruses (Lapidot *et al.,* 1993).

In plant viruses, cell-to-cell movement is one of the most essential phases of the life cycle. In order for a virus to infect the plant, it must move towards the vascular tissue by cell-to-cell movement. From there, the virus will translocate to other tissues to establish the disease. The first movement protein, from *Tobacco mosaic virus* (TMV), was discovered in 1987 by Deom *et al.* Since then, several MPs have been classified.

The family *Closteroviridae* does not encode proteins closely related to MPs. It was therefore suggested that the HSP70h protein has a function in the cell-to-cell movement for these viruses. In 1999, this theory was proven by Peremyslov *et al.* with a study on *Beet Yellow Virus* (BYV), another member of the family *Closteroviridae.* It is therefore assumed that the HSP70h of GLRaV-3 has a similar function to that of BYV, however no scientific proof is available.

2.5.2.3 RNA mediated resistance

RNA mediated resistance, also known as RNA silencing, has become an important tool for therapeutics, gene function analysis and bio-engineering in conferring resistance against plant pathogens. The observation that RNA silencing was involved in PDR goes back to 1990 when Lawson *et al.* discovered that the accumulation of the transgene did not correlate with the level of resistance in the transgenic plant. Furthermore, several studies showed that transgenic plants expressing untranslatable viral RNAs also conferred resistance against the particular virus (De Haan, *et al.,* 1992; Lindbo and Dougherty, 1992; Van der Vlugt *et al.,* 1992). The resistance mechanism behind these findings was associated with post-transcriptional

suppression of the transgene, which led to discovery of RNA silencing, also known as RNA interferance (RNAi) (Lindbo *et al.,* 1993; Ingelbrecht *et al.,* 1994).

RNAi is triggered by the presence of double stranded RNA (dsRNA) molecules homologous to its target messenger transcript or viral sequence. By the action of a Dicer-like (DCL) protein, the dsRNAs are sliced into small 20-26 nt dsRNA fragments. Subsequently, the guide strand of the small dsRNA will be incorporated into RNA-induced silencing complexes (RISCs). The main component of the RISC complex is a member of the Argonaute (AGO) protein family, which plays a catalytic role to guide the small RNA to the target position of the mRNA. This is followed by cleavage which results in degradation of the targeted mRNA transcript as shown in Figure 2.6.

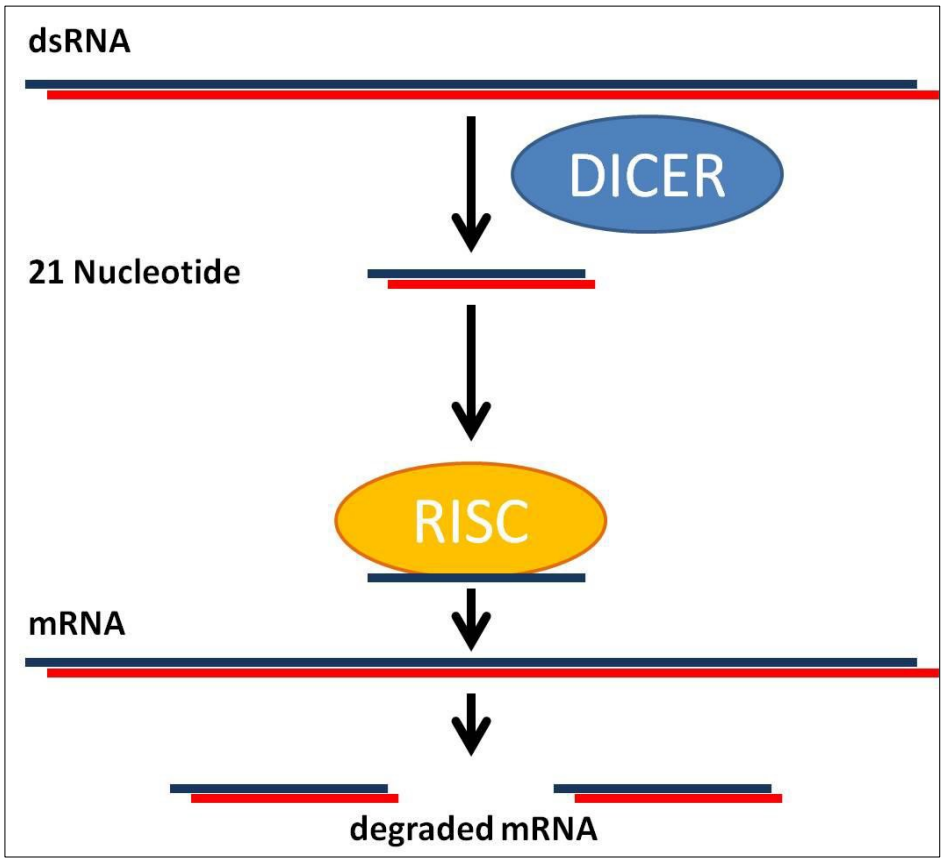

Figure 2.6 the mechanism of RNAi. Double stranded RNA is cleaved by Dicer, loaded into RISC, which then cleave mRNA in a sequence-specific manner.

RNA silencing is also part of a plant's own defence mechanism. In virus-infected plants, RNAi can be triggered by the accumulation of certain viral ssRNAs that have high secondary structures. By spreading silencing signals, the plant may confer sequence-specific resistance to uninfected adjoining cells before viral movement (Vionnet *et al.,* 2000; Yaegashi *et al.,* 2008). Local silencing can spread from the originally silenced cell to adjacent cells by plasmodesmata whereas long distance silencing is spread via the phloem (Palauqui *et al.,* 1997; Yaegashi *et al.,* 2008).

2.5.2.3.1 sncRNAs involved in RNAi

There are several small RNAs that can be involved in RNAi. The first silencing mechanism discovered, was silencing through sense RNA, or co-suppression. Overexpressed single stranded RNAs (ssRNAs) of the transgene were converted to dsRNA molecules and consequently triggered the RNAi pathway. This phenomenon was first documented in 1990 by Rich Jorgensen *et al.,* they tried to overexpress the chalcone synthase (CHS) gene in order to deepen the purple colour of petunia flowers by inserting an additional copy of the gene. Surprisingly, many flowers became white and failed to express the transgene (Napoli *et al.,* 1990).

A variant of sense RNA silencing is through the production of anti-sense RNAs. Anti-sense RNAs inhibit gene expression by the hybridization of complementary RNAs with the endogenous mRNA, preventing the mRNA from translating the particular protein. Such an anti-sense construct was generated in 1998 by Waterhouse *et al.,* and was able to induce immunity against *Potato virus Y* (PVY) in potato plants.

Another high-efficiency resistance approach is silencing by inverted-repeat (IR) sequences, whereby a single transcript is designed, which contains multiple copies of the sense- and anti-sense sequences of the target gene. Transgenic plants generated through this IR approach showed up to 90% resistance efficiency, in contrast to the resistance frequency of 5-20% resulting from transgenic plants containing a single sense or anti-sense gene (Lapidot *et al.,* 1993; Lindho *et al.,* 1993). Subsequently, multiple virus resistance can be obtained through combining small RNA segments from different viruses in the same transcript, targeting several viruses at once. A recent study utilizing this multiple IR approach on three soybean viruses conferred strong resistance against *Alfalfa mosaic virus* (AlMV), *Bean pod mottle virus* (BPMV) and *Soybean mosaic virus* (SMV) (Zhang *et al.,* 2011).

Micro RNAs (miRNAs) are a different class of small RNAs. Unlike siRNAs, miRNAs derive from miRNA-genes and are transcribed by polymerase II into pre-miRNAs, which contain extensive fold-back structures, also called hairpin-like structures. The secondary miRNA structures are recognised by Dicer and further processed into the RISC as described previously. Moreover, miRNAs often contain one or more mismatches in the 5' region which enable them to target multiple mRNAs. The main mechanism of miRNAs is translational repression and target cleavage, however, they can also be involved in the control of DNA methylation. Since the miRNA and siRNA biogenesis pathways are fairly similar, table 2.1 present the most important differences of these small RNAs.

Table 2.1 Main differences between siRNAs and miRNAs including length of the small RNAs, origin, target recognition and mechanism involved.

	Length	**Derived**	**Target recognition**	**Mechanism**
siRNA	19-21 nt	Exogenous	Perfect match	mRNA cleavage
miRNA	19-25 nt	Endogenous	Imperfect match	Translation, repression, mRNA cleavage, direct DNA methylation

Modified microRNAs, also known as artificial miRNA (amiRNA) is another tool for conferring virus resistance. The first amiRNA was expressed in Arabidopsis, targeting the silencing suppressors P69 and HC-Pro of *Turnip mosaic virus* (TuMV) and *Turnip yellow mosaic virus* (TYMV) (Niu *et al.,* 2006). Since then, numerous amiRNA have been engineered to use as a tool for conferring resistance (Sablok *et al.,* 2011; Galvez *et al.,* 2014). The first amiRNAs reported in grapevine was in 2012; a natural pre-miR319a of *Arabidopsis thaliana* was modified by replacing the miR319a with two amiRNAs targeting the CP of *Grapevine fanleaf virus* (GFLV). The constructs were tested in grapevine somatic embryos and provided evidence for active processing of the pre-amiRNAs by the plant's machinery. Co-transformation assays with the pre-amiRNA constructs and a modified GUS- sensor construct, in which the target sequences of the amiRNAs were incorporated in the 3' terminus of the GUS gene, resulted in cleavage of the 21nt target sequence of GUS-sensors by the corresponding amiRNA (Jelly *et al.,* 2012). Another study on grapevine in 2012, conducted by Roumi *et al.,* engineered two amiRNA cassettes targeting *Grapevine virus A* (GVA) by replacing the 21 nt mature sequence of the pre-miRNA (vvi-miR166f) with a 21 nt sequence of the GVA genome. Validation of these amiRNAs in *N. benthamiana* showed different levels of resistance.

Several aspects need to be taken in consideration when designing and constructing amiRNAs. To resemble a natural amiRNA, the design requires three criteria including a 'U' for the first nt, an 'A' or a 'U' for the 10th nt, and the 5' end displays instability towards its amiRNA* (this is the complementary strand of the amiRNA) (Reynolds et al., 2004; Mallory et al., 2004). In order for a plant to process the amiRNA, the 21 nt mature amiRNA sequence needs to be incorporated into a plant's original miRNA precursor to maintain its secondary structure. Furthermore, it is not only the nature and structure of the amiRNA which influence the efficiency, also the target position is essential in order to effectively silence specific sequences. mRNAs contain local secondary structures which additionally influences the efficiency, some mRNA target sequences are therefore more accessible than others. (Duan, et al., 2008).

2.6 Conclusion

The great economic impact of GLD required various management strategies to limit crop losses. These strategies focus on the establishment and maintenance of clean material as well as prevention of spread through the control of the insect vector. The latest advances in molecular techniques offer alternatives such as pathogen derived resistance strategies (PDR). In this study, two PDR approaches have been investigated, namely; dysfunctional viral movement protein in stable transgenic lines and the use of artificial microRNAs in transient expression systems.

2.12 References

Alkowni, R., Rowhani, A., Daubert, S. and Golino, D. 2004. Partial characterization of a new ampelovirus associated with grapevine leafroll disease. *Journal of Plant Pathology*. 86 (2): 123-133

Agronovski, A.A., Boyko, V.P., Karasev, A.V., Koonin, E.V. and Doja, V.V. 1991. Putative 65 kDa protein of beet yellows closterovirus is a homologue of HSP70 heat shock proteins. *J.Mol.Biol.* 217: 603-610

Atallah, S.S., Gómez, M.I., Fuchs, M.F., Martinson, T.E., 2011. Economic impact of grapevine leafroll disease on *Vitis vinifera* cv. Cabernet franc in Finger Lakes Vineyards of New York. Am. J. Enol. Viticult. DOI: 10.5344/ajev.2011.11055

Ayllón, M.A., Gowda, S., Satyanarayana, T. and Dawson, W.O. 2004. Cis-acting elements at opposite ends of the Citrus tristeza virus genome differ in initiation and termination of subgenomic RNAs. *Virology*. 322: 41 – 50

Baulcombe, D.C.. 1995. Mechanisms of pathogen-derived resistance to viruses in HSP-Mut plants. *The Plant Cell*. 8: 1833-1844

Baulcombe, D.C. 1994. Novel strategies for engineering virus resistance in plants. *Curr. Opin. Biotechnol.* 5: 117-124

Beachy, R.N. 1993. Transgenic resistance to plant viruses. *Semin. Virol.* 4: 327-416

Bester, R., Maree, H.J. and Burger, J.T. 2012. Complete nucleotide sequence of a new strain of Grapevine leafroll-associated virus 3 in South Africa. *Archives of Virology*. 157(9): 1815-1819

Bester, R., Jooste, A.E.C., Maree, H.J. and Burger, J.T. 2012. Real-time RT-PCR high-resolution melting curve analysis and multiplex RT-PCR to detect and differentiate

Grapevine leafroll-associated virus 3 variant groups I, II, III and VI. *Virology Journal*. 9: 219-230

Bell, V.A., Bonfiglioli, R.G.E., Walker1, J.T.S., Lo1, P.L., Mackay, J.F. and McGregor, S.E. 2009. Grapevine leafroll-associated virus 3 persistence in *Vitis vinifera* remnant roots. J. Plant. Pathol. 91(3), 527-533.

Belli, G. 1995. Evidence that the closteroviruses GLRV-1 and GLRV-3 are causal agents of Grapevine leafroll disease. *Rivista di Patologia Vegetale*. 5: 95-98

Bonnet, E., Peer, Y. and Rouzé, P. 2005. The small RNA world of plants. *New Phytologist*. 171: 451-468

Boscia, D., Greif, C., Gugerli, P., Martelli, G.P., Walter, B. and Gonsalves, D. 1995.
Nomenclature of leafroll-associated putative closteroviruses. *Vitis*. 34:171-175

Bukau, B. and Horwich, A.L. 1998. The Hsp70 and Hsp60 chaperone machines. *Cell*. 92: 351-366

Cabaleiro, C. and Segura, A. 1997a. Some characteristics of the transmission of Grapevine leafroll-associated virus 3 by *Planococcus citri* Risso. *European Journal of Plant Pathology*. 103: 373-378

Cabaleiro, C. and Segura, A. 1997b. Field transmission of grapevine leafroll associated virus 3 (GLRaV-3) by the mealybug *Planococus citri. Plant disease*. 81:283-287

Cabaleiro, C., Segura, A. and Garcia-Berrios, J.J. 1999. Effects of grapevine leafroll associated virus 3 on the physiology and must of Vitis vinifera L. cv Albarino following contamination in the field. *Am. J. Enol. Vitic.* 50: 40-44

Carrington, J.C. and Amros, V. 2003. Role of MicroRNAs in Plant and Animal Development. *Science*. 301: 336-338

Charles, J.G., Cohen, D., Walker, J.T.S., Forgie, S.A., Bell, V.A. and Breen, K.C. 2005. A review of the ecology of grapevine leafroll associated virus type 3 (GLRaV-3). *New Zealand Plant Protection*. 59: 330-337

Charles, J. G., Cohen, D., Walker, J.T.S., Forgie, S.A., Bell, V.A. and Breen, K.C.2006. A review of Grapevine Leafroll associated Virus type 3 (GLRaV-3) for New Zealand wine industry. *Hort Research Client Report 18447*

Clark, M.F. and Adams, A.N. 1975. Characteristics of the microplate method of enzyme-linked immunosorbent assay for the detection of plant viruses. *Journal of General Virology*. 34:475-483

Clark, W.G., Fitchen, J.H. and Beachy, R.N. 1995. Studies of coat protein-mediated resistance to TMV. *Virology* 208: 485-491

Coetzee, B., Freeborough, M.J., Maree, H.J., Celton, J.M., Rees, D.J.G and Burger, J.T. 2010. Deep sequencing analysis of viruses infecting grapevines: Virome of a vineyard. *Virology*. 400(2): 157-163

De Haan, P., Gielen, J.J.L., Prins, M., Wijkamp, I.G., van Schepen, A., Petem, D., van Grinsven, M.Q.J.M. and Goldbach, R.W. 1992. Characterization of RNA-mediated resistance to tomato spotted wilt virus in transgenic tobacco plants. *Bio/technology*. 10: 1133-1137

Deluca-Flaherty, C., Flaherty, K.M., Mclntosh, L. J., Bahrami, B. and McKay, D.B. 1988. Crystals of an ATPase gragment of bovine clathrin uncoating ATPase. *Journal of Molecular Biology*. 200: 749-750

Deom, C.M., Oliver, M.J. and Beachy, R.N. 1987. The 30-Kilodalton gene product of Tobacco Mosaic Virus potentiates virus movement. *Science*. 237: 389 – 394

Dolja, V.V., Karasev, A.V. and Koonin, E.V. 1994. Molecular biology and evolution of closteroviruses: sophisticated build-up of large RNA genomes. *Annu. Rev. Phytopathol.* 32:261 – 285

Dolja, V.V., Kreuze, J.F. and Valkonen, J.P.T. 2006. Comparative and functional genomics of closteroviruses. *Virus Res.* 117: 38 – 51

Dorak, M.T. 2005. Real-Time PCR (Advanced Methods Series). http://www.dorak.info/genetics/realtime.html

Duan, C.G., Wang, C.H., Fang, R.X. and Guo, H.S. 2008. Artificial MicroRNAs highly accessible to targets confer efficient virus resistance in plants. *Journal of Virology*. 22(82): 11084- 11095

Engel, E.A., Escobar, P.F., Rojas, L.A., Rivera, P.A., Fiore, N. and Valenzuela, P.D.T. 2010. A diagnostic oligonucleotide microarray for simultaneous detection of grapevine viruses. *Journal of Virological Methods*. 163(2): 445-451

Engel, E.A., Girardi, C., Escobar, P.F., Arredondo, V., Dominguez, C., Pérez-Acle, T. and Valenzuela, P.D.T. 2008. Genome analysis and detection of a Chilean isolate of *Grapevine leafroll associated virus-3*. *Virus genes*. 37(1): 110-118

Engelbrecht, D.J. and Kasdorf, G.G.F. 1990. Field spread and corky bark, fleck, leafroll and Shiraz decline diseases and associated viruses in South African grapevines. *Phytophylactica*. 22(3): 347-354

Espinoza, C., Vega, A., Medina, C., Schlauch, K., Cramer, G. and Arce-Johnson, P. 2007. Gene expression associated with compatible viral disease in grapevine cultivars. *Functional & Integrative Genomics*. 7: 95-110

Farooq, A.B.U., Ma, Y., Wang, Z., Zhuo, N., Wenxing, X., Wang, G. and Hong, N. 2013. Genetic diversity analyses reveal novel recombination events in *Grapevine leafroll-associated virus 3* in China. *Virus Research.* 171 (1): 15-21

Ferri, M., Righetti, L. and Tassoni, A. 2011. Increasing sucrose concentrations promote phenylpropanoid biosynthesis in grapevine cell cultures. *Journal of Plant Physiology*.168(3): 189–195

Flaherty, K.M., Deluca-Flaherty, C. and McKay, D.B. 1990. Three dimensional structure of the ATPase fragment of a 70K heat shock cognate protein. *Nature*. 346: 623-628

Fortusini, A., Scattini, G., Prati, S., Cinquanta, S. and Belli, G. 1997. Transmission of grapevine leafroll virus 1 (GLRV-1) and grapevine virus A (GVA) by scale insects. *Extended abstracts of 12th meeting of ICVG, Lisbon 1997*, 121-122

Freeborough, M-J. 2003. A pathogen-derived resistance strategy for the broad-spectrum control of Grapevine leafroll-associated virus infection. *Thesis University of Stellenbosch*

Galvez, L.C., Banerjee, J., Pinar, H. and Mitra, A. 2014. Engineered plant virus resistance. *Plant Sciencei*. (In Press, Corrected Proof)

Ghanem-Sabanadzovic, N.A., Sabanadzovic, S., Gugerli, P. and Rowhani, A. 2012. Genome organization, serology and phylogeny of Grapevine leafroll-associated viruses 4 and 6: Taxonomic implications. *Virus Research*. 163: 120-128

Golino, D.A. 1993. Potential interactions between rootstocks and grapevine latent viruses. *Am. J. Enol, Vitic.* 44: 148-152

Golino, D.A., Sim, S.T. and Rowhani, A. 1995. Transmission studies of grapevine leafroll associated virus and grapevine corky bark associated virus by the obscure mealybug. *American Journal of Enology and Viticulture.* 46: 408

Hansen, M. 2011. Grape industry goes after viruses. *Good fruit grower*. http://www.goodfruit.com/Good-Fruit-Grower/December-2011/Grape-industry-goes-after-viruses/

Holmes, E.C. 2009. The evolution and emergence of RNA viruses. *Oxford Univerisity Press, New York*.

Hu, J.S., Gonsalces, D. and Teliz, D. 1990. Characterization of closterovirus-like particles associated with the grapevine leafroll disease. *Journal of Phytopathology*. 130: 1 -14

Ingelbrecht, I., Houdt, van, H., Montagu, van, M. and Depicker, A. 1994. Posttranscriptional silencing of reporter transgenes in tobacco correlates with DNA methylation. *Proc. Natl. Acad. Sci. USA*. 91: 10502-10506

Jarugula, S., Gowda, S., Dawson, W.O. and Naidu, R.A. 2010. 3' – coterminal subgenomic RNAs and putative cis-acting elements of Grapevine leafroll- associated virus 3 reveals ' unique' features of gene expression strategy in the genus Ampelovirus. *Virology Journal*. 7:180-194

Jelly, N.S., Schellenbaum, P., Walter, B. and Maillot, P. 2012. Transient expression of artificial microRNAs targeting Grapevine fanleaf virus and evidence for RNA silencing in grapevine somatic embryos. *Transgenic Research*. 21(6): 1319-1327

Jones, L. 2002. Revealing micro-RNAs in plants. *Trends in Plant Science.* 7(11): 473-475

Jooste, A.E.C. and Goszczynski, D.E. 2005. Sinle-strand conformation polymorphism (SSCP), cloning and sequencing reveal two major groups of divergent molecular variants of grapevine leafroll-associated virus-3 (GLRaV-3). *Vitis*. 44(1): 39-43

Jooste, A.E.C., Maree, H.J., Bellstedt, D., Goszczynski, D.E., Pietersen, G. and Burger, J.T. 2010. Three genetic grapevine leafroll-associated virus-3 variants identified from South African vineyards show high variability in their 5' UTR. *Archives of Virology*. 155(12):1997-2006

Jooste, A.E.C., Pietersen, G. and Burger, J.T. 2011. Distribution of grapevine leafroll associated virus-3 variants in South African vineyards. *Eur J Plant Pathol*. 131:137-381

Karasev, A.V. 2000. Genetic diversity and evolution of closteroviruses. *Annu. Rev. Phytopathol.* 38: 293-324

Katoh, H., Suzuki, S., Saitoh, T. and Takayanagi, T. 2009. Cloning and characterization of VIGG, a novel virus-induced grapevine protein, correlated with fruit quality. *Plant Physiology and Biochemistry*. 47(4): 291-299

Komar, V., Vigne, E., Demangeat, G. and Fuchs, M. 2007. Beneficial effect of selective virus elimination on the performance of *Vitis vinifera* cv. Chardonnay. *Am. J. Enol. Vitic.* 58: 202-210

Krake, L.R., Steele Scott, N., Rezaian, M.A. and Taylor, R.H. 1999. Graft-transmitted diseases of grapevines. CSIRO Publishing.

Krastanova, S., Perrin, M., Barbier, P., Demangeat, G., Cornuet, P., Bardonnet, N., Otten, L. and Walter, B. 1995. Transformation of grapevine rootstocks with coat protein gene of grapevine fanleaf nepovirus. *Plant Cell Rep.* 14: 550-554

Lapidot, M., Gafny, F., Ding, B., Wolf, S., Lucas, W.J., Beachy, R.N. A dysfunctional movement protein of tobacco mosaic virus that partially modifies the plasmodesmata and limits virus spread in transgenic plants. *Plant. J.* 4: 959-970

Lawson, C., Kaniewski, W.K., Haley, L., Rozman, R., Newell, C., Sanders, P. and Tumer, N.E. 1990. Engineering resistance to mixed virus infection in a commercial potato cultivar: Resistance to potato virus X and potato virus Y in transgenic Russet Burbank. *Biotechnology*. 8: 127-134

Le Gall, O., Torregrose, L., Danglot, Y., Candresse, T. and Bouquet, A. 1994. *Agrobacterium*-mediated genetic transformation of grapevine somatic embryos and regeneration of transgenic plants expressing the coat protein of grapevine chrome mosaic nepovirus (GCMV). *Plant Sci.* 102(2): 161-170

Lee, R.C., Feinbaum, R.L. and Ambros, V. 1993. The *C. elegans* heterochronic gene lin-4 encodes small RNAs with antisense complementarity to lin-14. *Cell*. 75: 843-854

Lindbo, J.A. and Dougherty, W.G. 1992. Untranslatable transcripts of the tobacco etch virus coat protein gene sequence can interfere with tobacco etch virus replication in transgenic plants and protoplasts. *Virology*. 189: 725-733

Lindbo, J.A., Silva-Rosales, L., Proebsting, W.M. and Dougherty, W.G. 1993. Induction of a highly specific antiviral state in transgenic plants: Implication for regulation of gene expression and virus resistance. *Plant Cell*. 5: 1749-1759

Ling, K.S., Zhu, H.Y., Alvizo, H, Hu, J.S., Drong, R.F., Slinghtom, J.L. and Gonsalves, D. 1997. The coat protein gene of grapevine leafroll associated closterovirus-3, cloning, nucleotide sequencing and expression in HSP-Mut plants. *Archives of Virology*. 142: 1101-1116

Ling, K.S., Zhu, H.Y., Drong, R.F., Slinghtom, J.L., McFerson, J.R. and Gonsalves, D. 1998. Nucleotide sequence of the 3«-terminal two-thirds of the grapevine leafroll-associated virus-3 genome reveals a typicalmonopartite closterovirus. *Journal of General Virology*. 79: 1299-1307

Ling, K.S., Zhu, H.Y. and Gonslaves, D. 2004. Complete nucleotide sequence and genome organization of Grapevine leafroll-associated virus 3, type member of the genus Ampelovirus. *J. Gen. Virol.* 85: 2009 – 2102

Lomonossoff, G.P. 1995. Pathogen-derived resistance to plant viruses. *Annu. Rev. Phytopahtol.* 33: 323-343

López-Fabuel, I., Wetzel, T., Bertolini, E., Bassler, A., Vidal, E., Torres, L.B., Yuste, A. and Olmos, A. 2013. Real-time multiplex RT-PCR for the simultaneous detection of the five main grapevine viruses. *Journal of Virological Methods*. 188(1-2): 21-24

Livak, K.J. and Schmittgen, T.D. 2001. Analysis of relative gene expression data using real-time quantitative PCR and the $2^{-\Delta\Delta Ct}$ method. *Methods*. 25: 402-208

Mackay, I.M., Arden, K.E. and Nitsche, A. 2002. Real-time PCR in virology. *Nucleotide Acids Research*. 30:1292-1305

Mannini, F., Mollo, A. and Credi, R. 2012. Field performance and wine quality modification in a clone of Vitis vinifera cv. Dolcetto after GLRaV-3 elimination. *Am. J. Enol. Vitic.* 63: 144-147

Maree, H.J., Almeida, R.P.P., Bester, R., Chooi, K.M., Coen, D., Dolja, V.V., Fuchs, M.F., Golino, D.A., Jooste, A.E.C., Martelli, G.P., Naidu, R.A., Rowhani, A., Saldarelli, P. and Burger, J.T. 2013. Review: Grapevine leafroll-associated virus 3. *Frontiers in Microbiology. 4, 82.*

Maree, H.J., Freeborough, M.-J. and Burger, J.T. 2008. Complete nucleotide sequence of a South African isolate of grapevine leafroll-associated virus 3 reveals a 5' UTR of 737 nucleotides. *Archives of Virology*. 153: 755-757

Maree, H.J., Pirie, M.D., Oosthuizen, K., Bester, R., Rees, D.J.G. and Burger, J.T. Phylogenomic analysis reveals deep divergence and recombination in an economically important grapevine virus. *Submitted*

Martelli, G.P., Agranovsky, A.A., Bar-Joseph, M., Boscia, D., Candresse, T., Coutts, R.H.A., Dolja, V.V., Falk, B.W., Gonsalves, D., Jelkmann, W., Karasev, A.V., Minafra, A., Namba, S., Vetten, H.J., Wisler, G.C., Yoshikawa, N. 2002. The family *Closteroviridae* revised. *Arch. Virol*. 147: 2039 – 2044

Martelli, G.P. 2012. Grapevine Virology Highlights: 2010-2012. *Proceeding of the 17th Congress of ICVG, Davis, California, USA October 7-14, 2012* (http://web.pppmb.cals.cornell.edu/fuchs/icvg/archive.htm)

Martelli, G.P. 2008. Plant Virus Diseases: Fruit Trees and Grapevine. *Encyclopedia of Virology*. 3: 201-207

Martelli, G.P. 1993. Graft transmissible diseases of grapevine: Handbook for detection and diagnosis, food and agriculture organization of the United Nations, Rome (1993)

Martelli, G.P. and Boudon-Padieu, E. 2006. Directory of Infectious Diseases of grapevines and viroses and virus-like diseases of the grapevine: Bibliographic report 1998-2004. *Optiones méditerranéennes.* Number B55

Martelli, G.P., Graniti, A. and Erolani, G.L. 1986. Nature and physiological effects of grapevine diseases. *Experientia*. 42: 933-942

Martelli, G.P., Abou Ghanem-Sabanadzovic, N., Agranovsky, A.A., Al Rwahnih, M., Doja, V.V., Dovas, C.I., Fuchs, M., Gugerli, P., Hu, J.S., Jelkmann, W., Katis, N.I., Maliogka, V.I., Melzer, M.J., Menzel, W., Minafra, A., Rott, M.E., Rowhani, A., Sabanadzovic, S. and Saldarelli, P. 2012. Taxonomic revision of the family closeroviridae with special reference to the grapevine leafroll-associated members of the genus ampelovirus and the putative species unassigned to the family. *Journal of Plant Pathology*. 94(1): 7-19

Martelli, G.P. 2014. Directory of virus and virus-like disease of the grapevine and their agents. *Journal of Plant Pathology*. 96(1S): 131-136

Miller, W.A. and Koev, G. 2000. Synthesis of subgenomic RNAs by positive-strand RNA viruses. *Virology* 273: 1 – 8

Niu, Q.W., Lin, S.S., Reyes, J.L., Chen, K.C., Wu, H.W., Yeh, S.D. and Chua, N.H. 2006. Expression of artificial microRNAs in transgenic *Arabidopsis thaliana* confers virus resistance. *Nat. Biotechnol.* 24: 1420-1428

Pacifico, D., Caciagli, P., Palmano, S., Mannini, F. and Marzachi, C. 2011. Quantitation of *Grapevine leafroll associated virus-1* and *-3*, *Grapevine virus A*, *Grapevine fanleaf virus* and *Grapevine fleck virus* in field-collected *Vitis vinifera* L. 'Nebbiolo' by real-time reverse transcription-PCR. *Journal of Virological Methods.* 172(1-2): 1-7

Palauqui, J-C., Elmayan, T., Pollien, J-M. and Vacheret, H. 1997. Systemic acquired silencing: transgene-specific post transcriptional silencing is transmitted by grafting from silenced stocks to non-silenced scions. *The EMBO Journal*. 16: 4738-4745

Peremyslov, V.V., Hagiwara, Y. and Dolia, V.V. 1999. HSP70 homolog functions in cell-to-cell movement of a plant virus. *PNAS*. 96(26): 14771 – 14776

Petersen, C.L. and Charles, J.G. 1997. Transmission of grapevine leafroll-associated closteroviruses by *Pseodococcus longispinus* and *P. calceolariae. Plant Pathology*. 26: 509-515

Pflaffl, M.W., Horgan, G.W. and Dempfle, L. 2002. Relative expression software tool (REST) for group-wise comparison and statistical analysis of relative expression results in real-time PCR. *Nucleic acid research*. 30: 1-10

Powell-Abel, P., Nelson, R.S., De, B., Hoffmann, N., Rogen, S.G., Fraley, R.T. and Beachy, R.N. 1986. Delay of disease development in transgenic plants that express the tobacco mosaic virus coat protein gene. *Science*. 232: 738-743

Prosser, S.W., Goszczynski, D.E. and Meng, B. 2007. Molecular analysis of double-stranded RNAs reveals complex infection of grapevines with multiple viruses. *Virus Research*. 124(1-2): 152-159

Rast, H.E., James, D., Habili, N. and Masri, S.A. 2012. Genome organisation and characterization of a novel variant of Grapevine leafroll-associated virus 3. *Proceedings of the 17th congress of ICVG, Davis, California, USA October 7-14, 2012*

Rayapati, N., O'Neal, S. and Walsh, D. 2008. Grapevine leafroll disease. *Washington State University Extension.*

Reid, K.E., Olsson, N., Schlosser, J., Peng, F. and Lund, S.T. 2005. An optimized grapevine RNA isolation procedure and statistical determination of reference genes for real-time RT-PCR during berry development. *BMC Plant Biology*. 6:27-38

Rezaian, M.A., Krake, L.R., Cunying, Q. and Hazzalin, C.A. 1991. Detection of virus-associated dsRNA from leafroll infected grapevines. *Journal of Virological Methods*. 31: 325-334

Rosciglione, B., Castellano, M.A., Martelli, G.P., Savino, V. and Cannizzaro, G. 1983. Mealybug transmission of grapevine virus A. *Vitis*. 22: 331-347

Roumi, V., Afsharifar, A., Saldarelli, P., Niazi, A., Martelli, G.P. and Izadpanah, K. 2012. Transient expression of artificial microRNAs confers resistance to Grapevine virus A in *Nicotiana benthamiana*. *Journal of Plant Pathology*. 94(3): 643-649

Rowhani, A. and Golino, D.A. 1995. ELISA test reveals new information about leafroll disease. *Cal. Agri.* 49: 26-29

Sablok, G., Pérez-Quintero, A.L., Hassan, M., Tatarinova, T.V. and López, C. 2011. Artificial microRNAs (amiRNAs) engineering – On how microRNA-based silencing methods have affected current silencing research. *Biochemical and Biophysical Research Communications*. 406(3): 315 – 319

Saldarelli, P, Minafra, A., Martelli, G.P., Prado, E. and Walter, B. 1994. Detection of grapevine leafroll-associated closterovirus III by molecular hybridization. *Plant Pathol*. 43: 91–96

Saldarelli, P., Cornuet, P., Vigne, E., Talas, F., Bronnenkant, I., Dridi, A.M., Andret-Link, P., Boscia, D., Gugerli, P., Fuchs, M. and Martelli, G.P. 2006. Partial characterization of two divergent variants of *grapevine leafroll-associated virus 4*. *J. Plant Pathol.* 88: 203–214

Sanfort, J.C. and Johnston, S.A. 1985. The concept of parasite-derived resistance – Deriving resistance genes from the parasite's own genome. *J. Theor. Biol.* 113: 395-405

Sawis, 2013. Wine Export Analysis 200812 – 1 March 2013. Available at: http://www.sawis.co.za/info/download/Wine_Exports_Analysis_200812_-_1_March_2013.pdf. Accessed 8 March 2013

Schena, L., Nigro, F., Ippolito, A. and Gallitelli, D. 2004. Real-time quantitative PCR: a new technology to detect and study phytopathogenic and antagonistic fungi. *European Journal of Plant Pathology*. 110:893-908

Seppänen, P., Puska, R., Honkanen, J., Tyulkina, L.G., Fedorkin, O., Morozov, S.Y. and Atabekove, J.G. 1997. Movement protein-derived resistance to triple gene block-containing plant viruses. *Journal of General Virology.* 78:1241-1246

Sforza, R., Komar, V. and Greif, C. 2000. New scale insect vectors of grapevine closteroviruses. *Extended abstract of the 13th ICVG meeting, Adelaide 2000.*

Spielmann, A., Krastanova, S., Douet-Orhant, V. and Gugerli, P. 2000. Analysis of transgenic grapevine and *Nicotiana benthamiana* plants expressing an *Arabis mosaic virus* coat protein gene. *Plant Sci.* 156: 235-244

Tanne, E., Nevah, L. and Sela, I. 1989. Serological and molecular evidence for the complexity of leafroll disease of grapevine. *Plant Pathology*. 38: 183-189

Tsai, C-W., Chau, J., Fernandez, L., Bosco, D., Daane, K. M. and Almeida, R.P.P. 2008. Transmission of Grapevine leafroll-associated virus 3 by the vine mealybug (Planococcus ficus). *Phytopathology*. 100: 830-834

Tsia, C-W., Rowhani, A., Golino, D.A., Daane, K.M. and Almeida, R.P.P. 2010. Mealybug transmission of grapevine leafroll viruses: an analysis of virus-vector specificity. *Virology.* 100(8): 830-834

Valet, L., Fuchs, M. and Burrus, M. 2006. Transgenic grapevine rootstock clones expressing the coat protein or movement protein genes of Grapevine fanleaf virus: Characterization and reaction to virus infection upon protoplast electroporation. *Plant Science.* 170: 739 - 747

Vionnet, O., Lederer, C. and Baulcombe, D. 2000. A viral movement protein prevents spread of the gene silencing signal in *Nicothiana benthamiana. Cell*. 103(1): 157-167

Vlugt, van der, R.A.A., Ruiter, R.K. and Goldbach, R.W. 1992. Evidence for sense RNA-mediated protection to PVY^N in tobacco plants transformed with the viral coat protein cistron. *Plant Mol. Biol.* 20:631-639

Wang, Q., Mawassi, M., Li, P., Gafny, R., Sela, I. and Tanne, E. 2003. Elimination of grapevine virus A (GVA) by cryopreservation of in vitro-grown shoot tips of *Vitis vinifera* L. *Plant Science*. 165(2): 321-327

Walton, V., Dreves, A., Skinkis, P., Kaiser, C., Buchanan, M., Hilton, R., Martin, B.R., Castagnoli, S. and Renquist, S. 2009. Grapevine Leafroll Virus and Mealybug Prevention and Management in Oregon Vineyards. *Oregon State University*

Waterhouse, P.M., Graham, M.W. and Wang, M.B. Virus resistance and gene silencing in plants can be induced by simultaneous expression of sense and anti-sense RNA. *Proc. Natl. Acad. Sci. U.S.A.* 95: 13959-13964

Weber, E., Golino, D. and Rowhani, A. 2002. Laboratory testing for grapevine diseases. *Practical winery and vineyard.* http://www.practicalwinery.com/janfeb02p13.htm

Wilson, T.M.A. 1993. Strategies protect crop plants against viruses: Pathogen-derived resistance blossoms. *Proc. Natl. Acad. Sci. USA*. 90: 3134 – 3141

Wisniewski, L.A., Powell, P.A., Nelson, R.S. and Beachy, R.N. 1990. Local and systemic spread of tobacco mosaic virus in transgenic tobacco. *Plant Cell*. 2: 559-567

Yaegashi, H., Tamura, A., Isogai, M. and Yoshikawa, N. 2008. Inhibition of long-distance movement of RNA silencing signals in *Nicotiana benthamiana* by Apple clorotic leaf spot virus 50 kDa. *Virology*. 382(2): 199-206

Xue, B., Ling, K.S., Reid, C.L., Krastanova, S., Sekiya, M., Momol, E.A., Sule, S., Mozsar, J., Gonsalves, D. and Burr, T. 1999. Transformation of five grape rootstocks with plant virus genes and a virE gene from *Agrobacterium tumefaciens*. *Cell Dev. Biol. Plant.* 35: 226-231

Zhang, X., Sato, S., Ye, X., Dorrance, A.E., Morris, T.J., Clemente, T.E., Qu, F. 2011. Robust RNAi-based resistance to mixed infection of three viruses in soybean plants expressing separate short hairpins from a single transgene. *Phytopathology*. 101: 1264-1269

Zhang, H., Lubberstedt, T. and Xu, M. 2013. The genetic and Molecular basis of plant resistance to pathogens. *Journal of Genetics and Genomics.* 40(1): 23-35

Zee, F., Gonsalves, D., Goheen, A., Kim, K.S., Pool, R. and Lee, R.F. 1987. Cytopathology of leafroll diseased grapevines and the purification and serology of associated closterovirus-like particles. *Phytopathology*. 77: 1427-1434

Chapter 3 Evaluation of transgenic HSP-Mut grapevines

3.1 General introduction

GLD is one of the most important viral diseases affecting grapevine causing a reduction in crop yield and quality and limiting the productive lifespan of the plant. Vector control and the production and retention of healthy plants are the most commonly used strategies to limit the impact of the disease. It was shown that transgenic control strategies based on pathogen-derived resistance (PDR) is effective in conferring resistance in several viruses (Stanford and Johnson, 1985; Galvez *et al.,* 2014). Genes derived from the pathogen that are expressed in a dysfunctional form, inappropriate concentration or at an incorrect time in the infection cycle, are able to repress the virus infection (Stanford and Johnson, 1985). PDR can either be based on the accumulation of RNAs that trigger the RNA silencing defence mechanism or by encoded proteins that interfere in the virus infection cycle (Grant, 1999).

3.1.1 **PDR in grapevine**

Since its invention in 1985, PDR has been extensively used to generate several virus resistant crops (Stanford and Johnson, 1985; Galvez *et al.,* 2014). In grapevine, only a small number of PDR studies have been reported. The first transgenic grapevine was generated in 1994 by Le Gall *et al.* in which they incorporated the coat protein (CP) of *Grapevine chrome mosaic nepovirus* (GCMV) into the *Vitis vinifera* genome. Since then, several other studies have been documented on transgenic grapevines, most of which integrated the CP of the target virus into the genome (Mauro *et al.,* 1995; Gölles *et al.,* 1998; Spielmann *et al.,* 2000). However, only a few reports show the efficiency of these transgenic grapevine lines in conferring resistance. In 2006, Valat *et al.* evaluated 42 transgenic grapevine lines for resistance to *Grapevine fanleaf virus* (GFLV), using a protoplast electroporation technique. This method is proposed to provide a rapid identification of GFLV resistance grapevines. However, to date, no transgenic grapevine targeting GLD have been described in literature.

3.1.2 Development of HSP-Mut transgenic grapevines

In an earlier project to introduce resistance against GLRaV-3, 20 transgenic grapevine lines were developed by expressing a dysfunctional form of the GLRaV-3 heat shock protein-homologue (HSP70h) in a rootstock cultivar of grapevine (Freeborough, 2003). A separate earlier study with Beet Yellows Virus (BYV), also a member of the family *Closteroviridae*, suggested that the HSP70h functions as a movement protein (Peremyslov *et al.,* 1999).

In order for the virus to establish a disease in the plant host, the virus must move from the initial infection side towards other organs by cell-to-cell movement and the vascular system. The involvement of movement proteins (MP) in the cell-to-cell movement have been determined in numerous plant viruses (Carrington *et al.,* 1996; Citovsky and Zambryski, 1991; van Lent *et al.,* 1990). In order to facilitate movement of the virus to adjacent plant cells, MPs modify the diameter of intercellular canals (plasmodesmata) that are important for the transport of water, nutrients and macromolecules between cells.

The HSP family is involved in multiple processes, such as transportation of receptors, protein folding, importation of proteins into mitochondria or endoplasmic reticulum, recovery from stress, etc. (Bukau and Horwich, 1998). The HSP70h is characterised by an N-terminal ATPase domain (Flaherty *et al.,* 1990; Zhu *et al.,* 1996). The active ATPase domain is a highly conserved region, which takes part in ATP hydrolysis (Deluca-Flaherty *et al.,* 1988; Flaherty *et al.,* 1990). It is believed that the ATPase activity of the HSP70h provides energy for the cell- to-cell movement (Peremyslov *et al.,* 1999). Figure 3.1 shows a peptide sequence alignment of the ATPase domain of various HSP70h proteins (Freeborough, 2003). This region is often used for phylogenetic analysis to study evolutionary relationships among associates of the family *Closteroviridae*, specifically among members of the genus *Ampelovirus* (Karasev, 2000; Martelli *et al.,* 2002; Dolja *et al.,* 2006; Saldarelli *et al.,* 2006).

Four amino acids were altered using site-directed mutagenesis to obtain a dysfunctional HSP70h; namely Asp^{6} > Asn, Thr^{9} > Pro, Glu^{174} > Gln and Asp^{197} > Asn (Freeborough, 2003) (Figure 3.1). The mutated amino acids Asp^{6} and Glu^{174} correspond to the amino acids Asp^{7} and Glu^{181} of BYV, which have been shown to be involved with the assembly and cell-to-cell movement of BYV (Peremyslov *et al.,* 1999; Freeborough, 2003). The dysfunctional GLRaV-3 HSP constructs were transformed at the Institute for Wine Biotechnology (IWBT)

(Stellenbosch University) using *Agrobacterium* transformation on pre-embryogenic callus tissue to generate 20 transgenic plant lines of the Richter 110 rootstock cultivar.

```
Bos taurus      1    MAKNMAIGIDLGTTYSCVGVFQHGKVEIIA    30
E coli DnaK     1    --MGKIIGIDLGTTNSCVAIMDGTTPRVLE    30
Homo sapiens    1    --KAAAIGIDLGTTYSCVGVFQHGKVEIIA    30
BYV             1    ---MVVFGLDFGTTFSSVCAYVGEELYLFK    30
GLRaV-3 NY1     1    ----MEVGIDFGTTFSTICFSPSGVSGCTP    30
GLRaV Stel      1    ----MEVGIDFGTTFSAICFSPSGCSGCTP    30

Bos taurus      163  GVIAGLNVLRIINEPTAAAIAYGLDRT       188
E coli DnaK     158  GRIAGLEVKRIINEPTAAALAYGLDKG       184
Homo sapiens    160  GVIAGLNVLRIINEPTAAAIAYGLDRT       186
BYV             167  VNLSGYPCVYMVNEPSAAA-LSACSRI       193
GLRaV-3 NY1     161  LKGLGIPVRGVVNEPTAAA-LYSLAKS       186
GLRaV Stel      161  LKGLGIPVRGVVNEPTAAA-LYSLAKS       186

Bos taurus      189  GKGERNVLIFDLGGGTFDVSILTIDDG       227
E coli DnaK     184  -TGNRTIAVYDLGGGTFDISIIEIDEV       209
Homo sapiens    187  GKGERNVLIFDLGGGTFDVSILTIDDG       213
BYV             194  KGATSPVLVYDFGGGTFDVSVISALNN       220
GLRaV-3 NY1     187  RVEDLLLAVFDFGGGTFDVSFVKKKGN       213
GLRaV Stel      187  RVEDLLLAVFDFGGGTFDVSFVKKKGN       213
```

Figure 3.1 HSP70 amino acid sequences of the ATPase domain (N-terminal) of Bos Taurus (GenBank AAA73914), E. coli DnaK (GenBank P04475), Homo sapiens (GenBank 1HJOA), BYV (GenBank CAA37551), GLRaV-3 NY-1(GenBank AAC40708) and GLRaV-3 Stel (M.-J. Freeborough, 2003). Amino acids that are essential for ATPase activity are highlighted in bold (M.-J. Freeborough, 2003).

A follow-up study on these transgenic plants determined the copy number and expression levels of the transgene (Malan, 2009). The copy number of the transgene was determined relatively to three *Vitis vinifera* reference genes, namely β-Tubulin, Cyclophilin and Glyceraldehyde 3-phosphate dehydrogenase (GAPDH) using RT-qPCR (Table 3.1). All reference genes were present as a single copy in the *Vitis vinifera* genome and were constitutively expressed. In addition, the expression levels of the transgene was quantified relatively to the reference gene GADPH using RT-qPCR.

Table 3.1 Copy number and expression level quantitation of twenty transgenic plant lines. The first column indicates the sample number of each transgenic grapevine, columns 2-4 show the copy number of the transgene relative to three reference genes determined by qPCR. Column 5 indicates the expression levels of the transgene relative to reference gene GAPDH, as determined by RT-qPCR (Malan, 2009).

	Copy number			**Expression level**
Sample	**B-tub**	**Cyclophilin**	**GADPH**	**GAPDH**
1	>4	>4	>4	3
2	1	1	1	1
3	1	1	2	1
4	1	1	2	7
5	1	1	1	4
6	0	0	0	0
7	0	0	0	0
8	4	4	4	1
9	2	2	2	>30
10	1	2	2	>30
11	>4	>4	>4	>30
12	0	0	0	0
13	>4	>4	>4	>30
14	1	1	1	>20
15	2	3	3	12
16	4	>4	2	0
17	0	0	0	0
18	2	2	2	>20
19	1	1	1	>50
20	2	2	2	1

In this study, six of these transgenic plant lines were evaluated for conferring resistance to GLRaV-3. The transgenic plant lines, as well as a non-modified control plant line, were inoculated with GLRaV-3 by grafting buds of each onto GLRaV-3 infected plant material. After approximately five months, GLRaV-3 virus titres of all grafted plants were quantified relative to two reference genes using RT-qPCR and results were evaluated by comparing the relative virus titre of each transgenic plant line to that of a non-modified control plant line. The experimental set-up and results are discussed in this chapter.

3.2 Materials and Methods

3.2.1 Sample collection

Of the original 20 transgenic HSP-Mut grapevine lines, six lines were available for this study. These were #1, #3, #9, #14, #15 and #17, all of which are growing in a standard GMO greenhouse facility at the Welgevallen experimental farm in Stellenbosch. Buds of these plants were grafted onto grapevines, cv. 'Cabernet Sauvignon' and 'Chardonnay', infected with GLRaV-3 variant GP18 [GenBank: EU259806.1]. Due to limited quantities of plant material, three batches of plants were created over time to allow for the plants to grow new material after each harvest.

In the field, grapevines are grafted in winter when the plants are in dormancy. It is believed that this phase is important for the bud to stimulate callus formation. Therefore, the harvested plants of batches 1 and 2 were stored at 4°C for one month before grafting to simulate the dormant phase. However, due to limited time, the plants from batch 3 were grafted immediately after harvesting.

The first batch was created in May 2013 and grafts were allowed to grow in water for 4 months. Due to poor growth conditions, grafts of batches 2 and 3 were transferred to soil after roots appeared, and subsequently watered daily. The water contained the following nutrient solution (164 g Sol-u-fert (Kynoch Fertilizers (Pty) Ltd, Milnerton, RSA), 2 g Microplex (Ocean Agriculture (Pty) Ltd, Muldersdrift, RSA), 77 ml calcium nitrate (180 g/l Ca, 125 g/l NO^3) in 100 l water). Batch 2 was created in September 2013 and batch 3 in January 2014.

In this study, plant line #17 was used as a negative control since this plant, as determined in a previous project, did not contain the transgene and no expression levels of the transgene was detected (Malan, 2009). The last batch (batch 3) also included a non-modified plant as an additional negative control.

3.2.2 Confirmation transgenic status

The transgenic status of the transgenic plant lines was confirmed in this study. PCR using Dys-HSP primers was performed on genomic DNA extracted from the transgenic plant lines. The DNA extraction was performed using the Nucleospin Plant II DNA extraction kit (Macherey-Nagel). The PCR amplification mixtures contained 50 ng of DNA, 2.5 µl of 10X KAPA Taq buffer A (+Mg), 0.4 mM forward primer, 0.4 mM reverse primer, 0.2 mM dNTPs, 2.5 µl of Cresol and 1.5 units of KAPA Taq DNA polymerase (KAPA Biosystems) in a total volume of 25 µl. A standard PCR amplification programme was used. DNA was initially denatured at 94°C for 5 minutes, followed by 35 cycles of 94°C for 30 seconds, 55°C for 30 seconds and 72°C for 30 seconds. A final extension step was performed for 10 minutes at 72°C.

3.2.3 Grafting

Grafting was performed as illustrated in Figure 3.2; a small horizontal incision with a slight angle was made just below the bud as shown in Figure 3.2.A. A second horizontal cut from above the bud downwards to the first cut was made to remove the bud from its cane (Figure 3.2.B.). Figures 3.2.C and 3.2.D present the same two incisions performed on the receiving cane (Cabernet Sauvignon or Chardonnay plant material infected with GLRaV-3 variant GP18). Subsequently, the bud was inserted into the gap of the receiving cane and grafting tape was used to seal the graft union (Figures 3.2.E and 3.2.F).

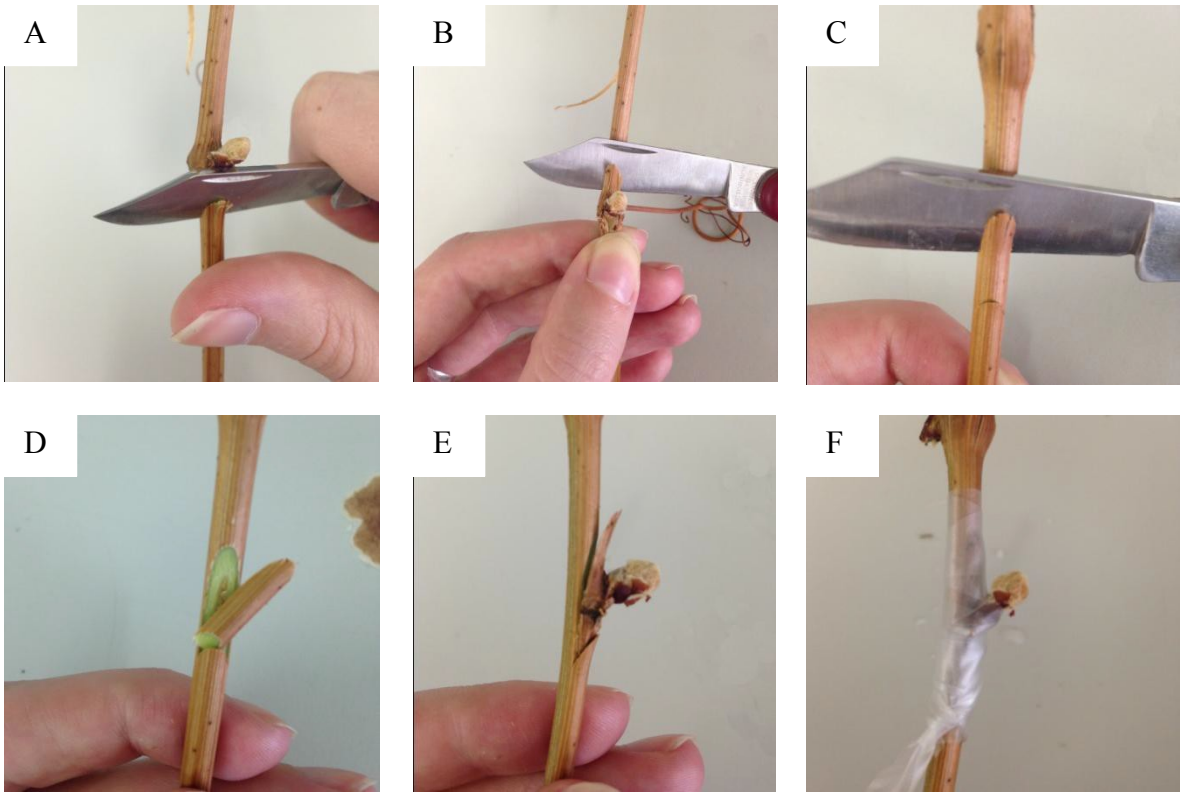

Figure 3.2 Grafting procedure. (A) Horizontal incision just below the bud of transgenic HSP-Mut plants. (B) A horizontal cut above the bud down to the first incision. (C) and (D) The same two cuts were made on the GLRaV-3 GP18 infected canes to match the bud. (E). Insertion of the bud in the cap of the receiving cane (F). The graft union was sealed with grafting tape.

A single grafted plant contained two graft samples, where even sample numbers represent shoot samples and uneven sample numbers refer to cane samples (Figure 3.3). The two sample types were processed separately. Phloem scrapings of each sample were collected, ground in liquid nitrogen and stored at -80°C. Shoots smaller than 10 cm were ground totality, whereas only the first 5 cm after the graft union was processed for shoots bigger than 10 cm.

Figure 3.3 Sampling procedure. A single grafted plant contained two samples. The shoot plant material was processed separately from the cane plant material.

3.2.4 Small-scale total RNA extraction and DNase treatment

Small-scale total RNA extractions were performed according to the modified CTAB method of White *et al.,* 2009. Approximately 0.2 grams of ground sample material was added to 1.8 ml of preheated (65°C) CTAB extraction buffer [2% CTAB, 2 M NaCl, 2.5% PVP-40, 100 mM Tris-HCl (pH 8), 25 mM EDTA (pH 8)] and 3% of 2-Mercaptoethanol (β-ME). Subsequently, the samples were vortexed and incubated in a waterbath for 30 minutes at 65°C. The samples were centrifuged for 10 minutes at 10000 rpm at 4°C. Supernatant was transferred into a new 2 ml tube containing an equal volume of chloroform:isoamyl alcohol (24:1). Subsequently, the samples were vortexed and centrifuged for 10 minutes at 4°C at 10000 rpm. The C:I (24:1) step was repeated once. The supernatant was transferred to a new 1.5 ml tube and LiCl was added to a final concentration of 2 M. Samples were mixed gently and stored overnight at 4°C. The following day, samples were centrifuged for 1 hour at 4°C at 10000 rpm. The supernatant was discarded and the pellet was washed with 70% EtOH. A centrifuge step followed for 10 minutes at 4°C at 10000 rpm and the EtOH was discarded. The pellet was air dried and dissolved in 30 µl of purified water.

Total RNA was visualized using agarose gel electrophoresis. Two microlitres of each sample were mixed with RNase-free loading dye (Fermentas) and loaded onto a 1% agarose gel [1X TEA buffer (40 mM Tris-acetate and 10 mM EDTA)] containing 0.01% v/v ethidium bromide (EtBr). Total RNA was electrophoresed at 100 Volts in 1X TAE buffer solution for 45 minutes and visualized using ultraviolet light in a Multi-Genius Bio-imaging system

(Syngene™). RNA quality was validated using spectrophotometric absorbance with a NanoDrop™ 1000 spectrophotometer (Thermo Fisher Scientific Inc.). Samples with A_{260}/A_{280} ratios between 1.8 and 2 and A_{260}/A_{230} ratios of approximately 2 were considered suitable for RT-qPCR experiments.

DNase treatment was performed on extracted RNA samples. Half a unit of RQ1 RNase-free DNase (Promega) together with 5 µl of RQ1 RNase-free DNase buffer (Promega) was added to each sample and made up to a final volume of 50 µl, and incubated at 37°C for 30 minutes. The mixture was purified using one phenol and several C:I (24:1) extraction steps, and the RNA finally precipitated using 100% EtOH and 0.3 M NaOAC (pH 5.2). RNA quality and purity was determined using agarose gel electrophoresis and spectrophotometer absorbance.

3.2.5 **RT-qPCR**

3.2.5.1 Primer design

Primers for amplification of GLRaV-3 variant GP18 were designed using Oligo Explorer 1.2 software. The following primer design parameters were adhered to: primer length (18-22 nt), primer melting temperature (52 – 58°C), primer annealing temperature (50 – 60°C), GC content (40 – 60%), amplicon length (small amplicons between 80 and 120 bp are considered suitable for RT-qPCR), product position (preferable conserved regions to target multiple variants), 3' end stability and primer secondary structures. The primers used to amplify GLRaV-3 are targeting ORF 1a, which encodes methyl transferase/helicase, and are called MTH in further descriptions. The MTH primers have a product size of 131 bp and a GC content of 46.6%. Primers used to amplify reference genes Ubiquitin C (UBC), elongation factor α and α-Tubulin were selected based on the study of Reid *et al.* in 2006. Malan (2009) designed primers for the dysfunctional HSP, which were used to confirm the presence of the transgene in the transgenic HSP-Mut plants. Table 3.2 shows all the primers used in this study.

Table 3.2 Primers used for RT-qPCR amplification in this study.

Primer	Forward primer (5' – 3')	Reverse primer (5' – 3')	Tm (°C)	Amplicon length (nt)	Designed
UBC	GAGGGTCGTCAGGATTTGGA	GCCCTGCACTTACCATCTTTAAG	55	75	Reid *et al.,* 2006
α-Tubulin	CAGCCAGATCTTCACGAGCTT	GTTCTCGCGCATTGACCATA	55	119	Reid *et al.,* 2006
Elongation factor α	GAACTGGGTGCTTGATAGGC	AACCAAAATATCCGGAGTAAAAGA	58	150	Reid *et al.,* 2006
GLRaV-3 MTH	CGTTTGCTACTTGTTGTCCT	CGTCATCAGTAGTTCCAAT	55	131	This study
Dys-HSP	GGGGGTCAAGTGCTCTAGTT	TGTCCCGGGTACCAGATATT	56	470	Malan, 2009
nptII	TCTCACCTTGCTCCTGCC	AGGCGATAGAAGGCGATGC	56	464	Maree, 2001

3.2.5.2 Complementary DNA synthesis

For complementary DNA (cDNA) synthesis 400 ng RNA and 25 µM random hexamers (Life Technology™) were mixed in a 5 µl reaction, and incubated at 65°C for 5 minutes, followed by incubation on ice for 2 minutes. Hundred units Maxima Reverse Transcriptase (Thermo Scientific™), 4 µl of 5X RT buffer [250 mM Tris-HCl (pH 8.3), 375 mM KCl, 15 mM $MgCl_2$, 50 mM DTT] and 1 mM of dNTPs were added, and made up to a total of 20 µl. The mixture was incubated for 60 minutes at 48°C.

3.2.5.3 Standard correlation curve

A 5-fold dilution series containing 100, 20, 4, 0.8 and 0.16 ng cDNA per reaction was prepared to generate the standard correlation curves of the reference genes and the GLRaV-3 ORF 1a gene, in a Qiagen Rotor-Gene Q thermal cycler. Primer conditions of UBC, elongation factor α and α-Tubulin were previously optimized (pers. comm. R. Bester, 2013) and the GLRaV-3 MTH primers were optimized in this study. The following protocol was used for the GLRaV-3 ORF1a, elongation factor α and α-Tubulin genes: A total of 25 µl reaction mixture contained 2.5 µl of 10X KAPA Taq buffer A (+Mg), 0.4 mM forward primer, 0.4 mM reverse primer, 0.2 mM dNTPs, 25 mM of Syto®9 (Invitrogen™) and 1.5 units of KAPA Taq DNA polymerase (KAPA Biosystems). Reaction mixtures used for UBC contained 0.48 mM of each primer. A standard qPCR amplification programme was used. Cycle conditions for UBC, elongation factor α and α-Tubulin included an initial denaturation step at 94°C for 5 minutes, followed by 45 cycles of 94°C for 10 seconds, annealing at 53°C for 10 seconds and elongation at 72°C for 20 seconds. Cycle conditions for the MTH primers included an initial denaturation step at 94°C for 5 minutes, followed by 45 cycles of 94°C for 15 seconds, annealing at 53°C for 15 seconds and elongation at 72°C for 25 seconds. In

addition, melting curve analyses of all PCR amplicons were obtained with a 0.1°C increase in temperature every two seconds, ranging from 65°C to 95°C.

3.2.5.4 Sample screening using RT-qPCR

The cDNA samples were diluted 25 times, correlating to the third dilution point of the standard correlation curve (4 ng RNA per reaction), and screened in triplicate using the Qiagen Rotor-Gene Q thermal cycler. The third dilution of each standard curve was used as a calibrator sample and included in every run to determine the concentration of each sample using the Relative Expression Software Tool (REST). The REST converts the Ct (cycle threshold) value of each sample into a concentration by plotting the Ct values onto the corresponding standard correlation curve. Melting curve analyses of PCR amplicons were obtained with temperatures ranging from 65°C to 95°C with a 0.1°C increase in temperature every two seconds. The Rotor-Gene software version 1.7 was used to perform RT-qPCR curve analysis.

3.2.6 Resistance level analyses

The data obtained using the GLRaV-3 MTH primers was normalized to the data obtained using the reference genes to determine the normalized virus titre (NVT). The following equation was applied to each sample:

$$NVT = \frac{conc_{MTH}}{\sqrt[2]{(conc_{UBC})^2 \times (conc_{Tub})^2}}$$

Subsequently, to measure the effect of the transgene in the shoot, the NVT of the shoot was subtracted from the NVT of the cane and converted into a percentage, which represents the virus resistance level in the shoot. The following equation was used to calculate the resistance levels.

$$\%\ Resistance\ levels = \left(\frac{NVT_{cane} - NVT_{shoot}}{NVT_{cane}}\right) * 100$$

P values were calculated using the Wilcoxon Sum Rank Test (http://elegans.som.vcu.edu/~leon/stats/utest.html) by comparing the resistance percentages of each plant line to the resistance percentages of the non-modified control group. In general, *p* values equal to or lower than 0.05 are considered to be significant, however, the Bonferroni adjustment type I was applied to reduce the chances of obtaining false-positive results. This

eliminates the probability of observing at least one significant result due to chance. Therefore, the results of this study are considered significant when p values are equal or lower than the significance level as determined for each plant line. The following equation was used to adjust the significance levels:

$$Significance\ level = 1 - 0.95^{\frac{1}{k}}$$

k = number of screened plants

3.3 Results and discussion

3.3.1 Ampelographic analyses of transgenic plant lines

Plant line #3 was morphologically different from the other transgenic plant lines (Figure 3.4). Ampelographic analyses showed that the cultivar of this plant line was not a Richter 110 but more likely a Jaque/Black Spanish (Pers. Comm. D. van Schalkwyk). Since a non-modified Jaque/Black Spanish plant was not available for this study to function as a negative control, the results of this plant line cannot be considered reliable. Follow-up studies including a Jaque/Black Spanish non-modified control plant are required to confirm the results from this study.

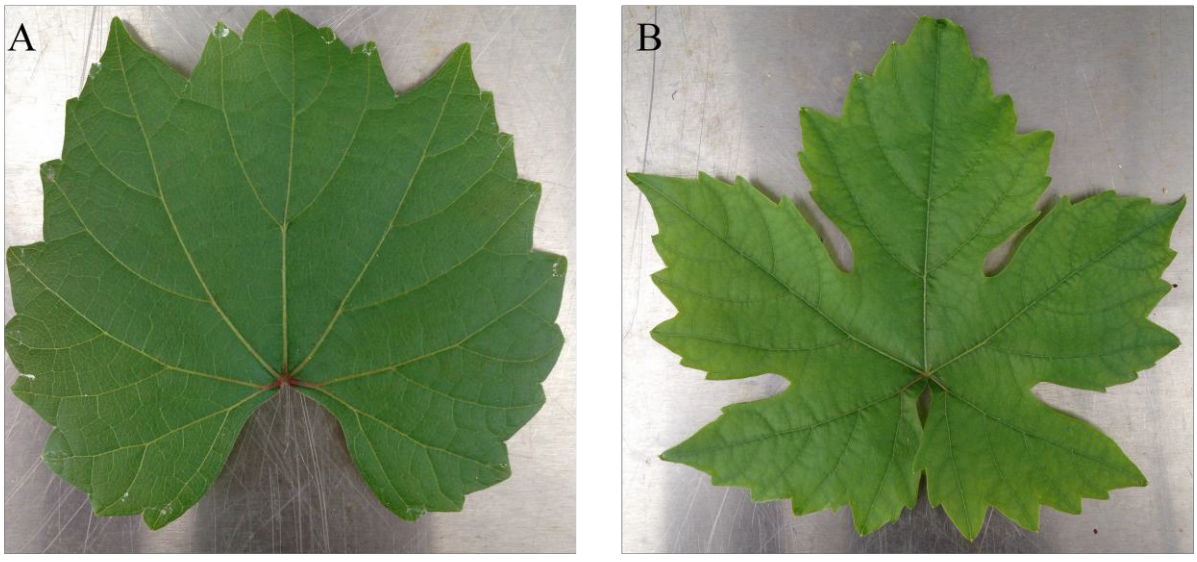

Figure 3.4 Comparison of two grapevine leaves. (A) Leaf of Richter 110 grapevine from plant line #1. (B) Leaf from plant line #3.

3.3.2 Confirmation of the HSP transgene in transgenic plants

To confirm that the dysfunctional HSP transgene was incorporated into the HSP-Mut plants, PCR using Dys-HSP primers was performed on genomic DNA of the plant lines. The expected amplicon size in a positive sample was 470 bp (Figure 3.5).

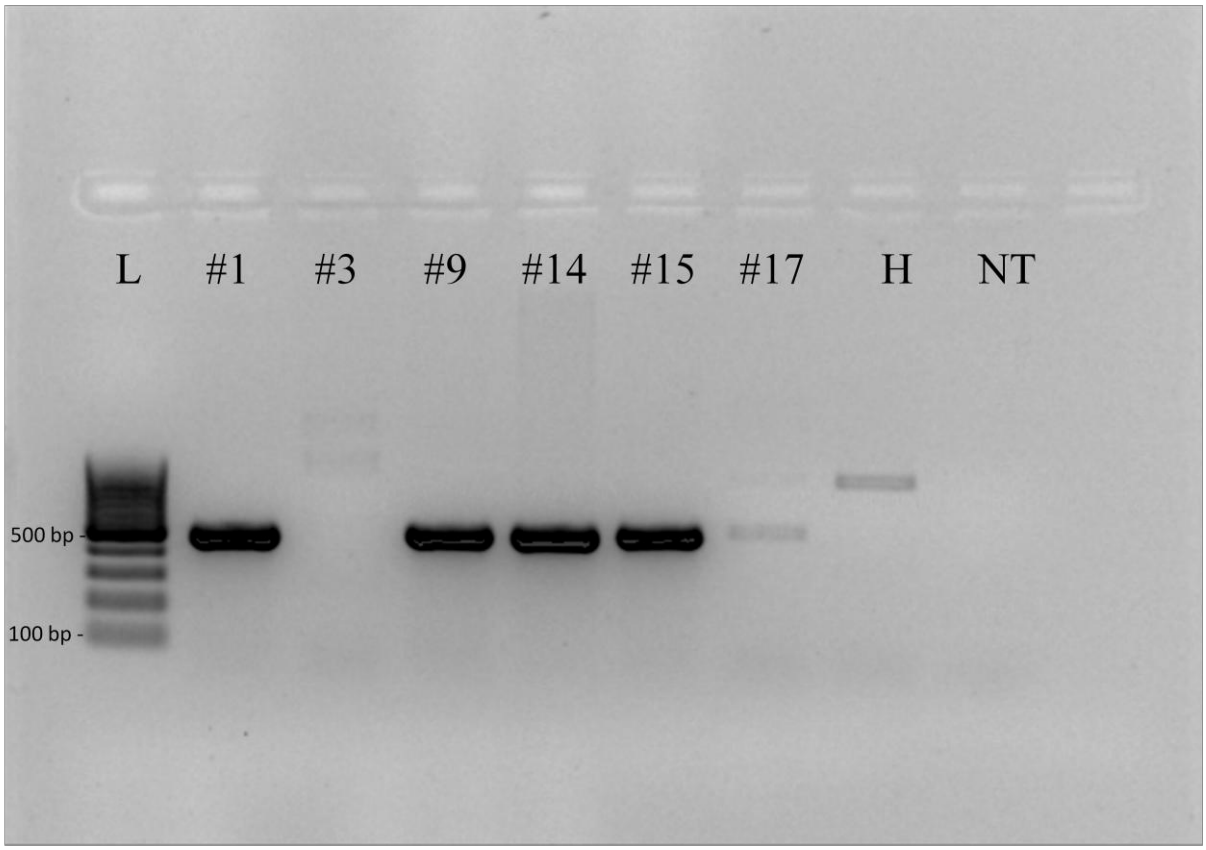

Figure 3.5 A 1% agarose gel showing PCR amplification using Dys-HSP primers. The expected amplicon size in a positive sample was 470 bp. Lane 1: 100 bp ladder; lanes 2-7: DNA samples of plant lines; line 8: DNA sample of non-modified control plant; lane 9 NT: no template control.

Plant lines #1, #9, #14, #15 and #17 showed amplicons with a size of approximately 470 bp, confirming that they contained the transgene. However, plant line #17 shows a less intense amplicon when compared to the other positive plant lines. This can probably be ascribed to spill-over contamination during the electrophoresis. No amplification was observed for plant line #3, indicating that this plant did not contain the transgene. The non-modified control plant line displayed a bigger amplicon than the transgenic plant lines. It is likely that the primers amplified the HSP of *Vitis vinifera* which is homologous to the GLRaV-3 HSP-70h.

To confirm the absence/presence of expression levels of the transgene for plant lines #3 and #17, an RT-PCR amplification was performed on RNA using the Dys-HSP primers. These results can confirm whether the transgene was transcribed. Figure 3.6 shows the results of the RT-PCR amplification using the Dys-HSP primers. Plant line #1 was included as a positive control and a water sample as a no template control.

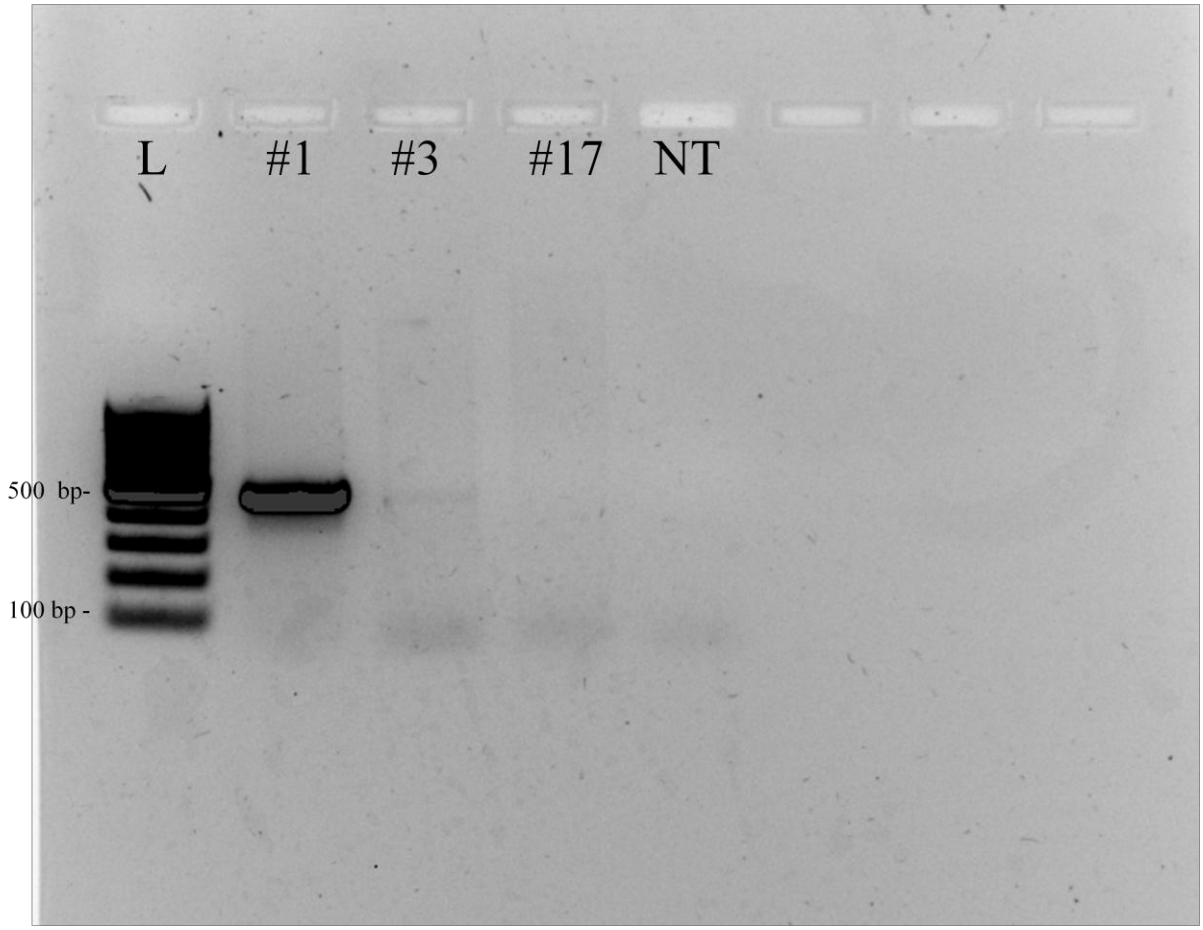

Figure 3.6 A 1% agarose gel showing PCR amplification using Dys-HSP primers. The expected amplicon size in a positive sample was 470 bp. Lane 1: 100 bp ladder; lanes 2-4: DNA samples of plant lines; lane 5: NT: no template control.

Plant line #1 (positive control) displays a clear amplicon of approximately 470 bp, confirming that the PCR reaction was successful. Plant line #3 shows a very faint amplicon indicating that the transgene is expressed, but at very low levels. However, no amplification was observed in the PCR on genomic DNA for plant line #3 (Figure 3.5). Seen the faint amplicon in Figure 3.6, it is likely that the transgene is present, however in very low copy numbers. No expression was observed for plant line #17 which confirms the findings of the study of Malan in 2009 (Table 3.1). These results confirm that plant line #17 can be used as a negative control in this study.

3.3.3 Confirmation of GLRaV-3 status of transgenic plants

To confirm that the transgenic HSP-Mut plants were not infected with GLRaV-3 before graft experiments were performed, RT-PCR amplifications were performed on cDNA samples using the GLRaV-3 MTH primers. The expected amplicon size of a positive sample was 131

bp. Figure 3.7 presents the results of this experiment, confirming that all plant lines were negative for GLRaV-3.

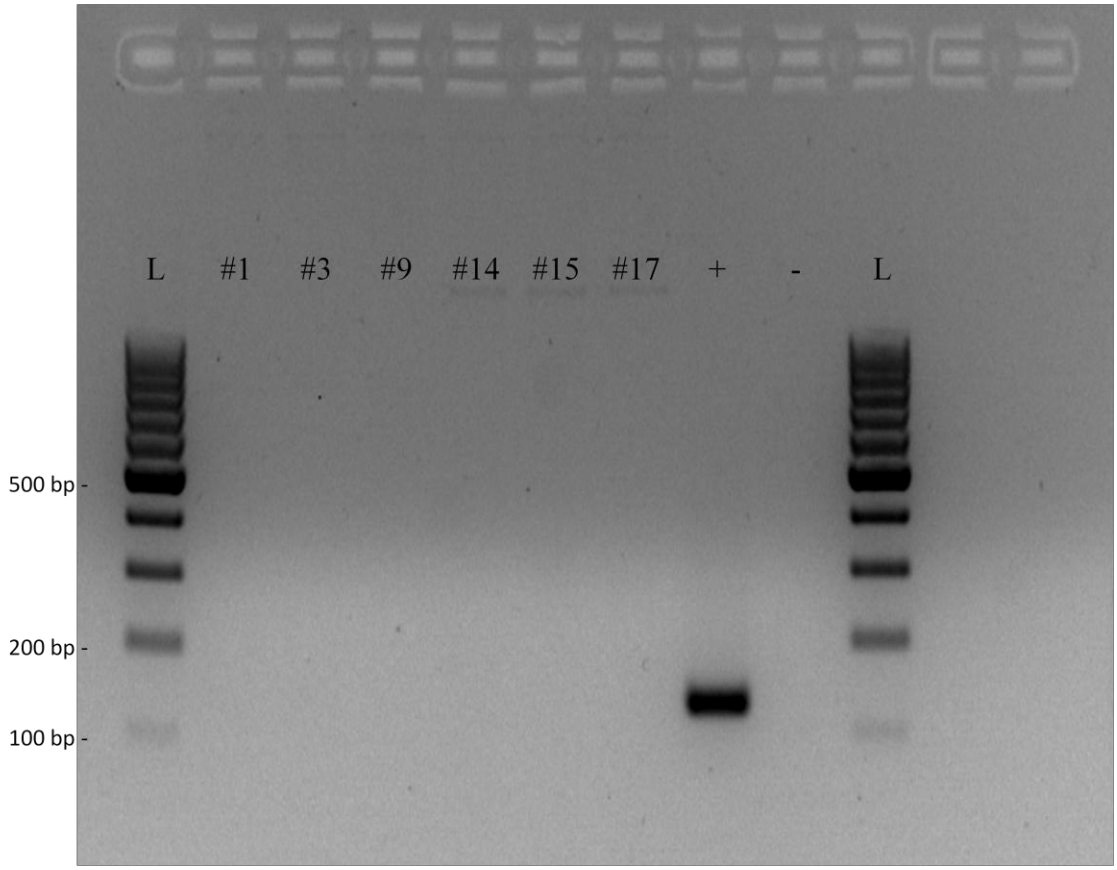

Figure 3.7 A 2% agarose gel confirming all samples were negative for the presence of GLRaV-3. Lane 1 L: 100 bp ladder; lane 2-7: samples of plant lines #1,#3,#9,#14,#15,#17. Line 8 : positive control (GLRaV-3 variant GP18 sample). Lane 9: NT: no template

3.3.4 Grafting HSP-mut buds onto GP18 infected canes

Three batches of plants were generated over a period of 13 months. The plants used for batch 1 were harvested for grafting in May 2013, grafted in June 2013 and sampled for RNA extraction in September 2013. The plants used for the second batch were harvested for grafting in September 2013, grafted in October 2013 and sampled for RNA extraction in March 2014. Plants used for batch 3 were harvested and grafted in January 2014 and sampled for RNA extraction in June 2014. Grafting details are presented in Table 3.3.

Table 3.3 The number of the grafted plants at the time of grafting, the number that took and started growing, sampling for RNA extractions, and RT-qPCR screening presented per batch.

Batch	Grafted	Grown	Sampled	Screened
Batch 1	94	65/94	48/65	24/48
Batch 2	58	2/58	2/2	2/2
Batch 3	84	66/84	39/66	34/39

Batch 1 comprised of 94 grafted plants of which 65 (~70%) took and started growing. Of these 65, material was sampled from 48 (73%). Half of these could be screened using the RT-qPCR. At the time of sampling, the shoots had an approximate size of 2-6 cm. In the last month before sampling, plants stopped growing and leaves turned yellow (Figure 3.8). These plants also yielded RNA of poor quality and low concentrations, thus half of the sampled plants were eliminated from screening. To prevent similar errors in the subsequent batches, the plants used for batches 2 and 3 were transferred to soil after roots appeared and allowed to grow for an additional month. Moreover, the first batch did not contain a non-modified control plant group, therefore plant #17, which did not express the transgene as shown in Figure 3.6, was used as a negative control.

Figure 3.8 Plant from batch 1, containing a small shoot of approximately 2.5 cm. Leaves are yellowish, indicating that the plant has not been actively growing for the last month before sampling.

The second batch comprised of 58 grafted plants, of which only two plants took and started growing. These two plants were both sampled and screened. The low success rate of this batch is probably the result of seasonal influence. The plants used for this batch were grafted in October 2013 and sampled for RNA extraction in March 2014 which covers the hottest part of the year. Although the plants were growing in a controlled greenhouse facility with temperatures below 30°C, the combination of high temperatures and high humanity makes it an ideal environment for fungal growth. In 2012, Frankel *et al.* showed that indoor fungal growth peaked in summer and was influenced by relative high humidity, temperatures and air exchange rates. All but two grafted plants which started growing, developed fungal contamination (Figure 3.9). Furthermore, the plants were positioned closely together which might have contributed to the distribution of the fungal infection.

Figure 3.9 A grafted plant showing white fungal growth on the cane. The fungus also grew under the grafting tape, preventing the bud from forming callus.

The third batch comprised of 84 grafted plants of which 66 (~78%) took and started growing. Of these 66, material was sampled from 39 (~60%), and 34 (~87%) could be screened by RT-qPCR. The adjustment of transferring the plants to soil and allowing the plants to grow for an additional month contributed to the high success rate of batch 3. Several shoots grew to fully lignified mature plants with complex root structures (Figure 3.10).

Figure 3.10 Grafted plant of which the shoot has grown to a fully lignified mature grapevine.

3.3.5 RT-qPCR of standard correlation curves

A standard correlation curve was generated using GLRaV-3 MTH primers (Figure 3.11). The efficiency of the amplification was 1.02, indicating that each cycle was efficient in doubling the PCR product. The R^2 value represents the correlation coefficient between the two axes; when R^2 is 1, the Ct value of the sample can be used to accurately predict the concentration using the correlation curve (Figure 3.11.B). In this case, an R^2 value of 0.99276 is considered to provide a good correlation between the two axes. The melting curve analyses, Figure 3.11.C, shows no non-specific amplification.

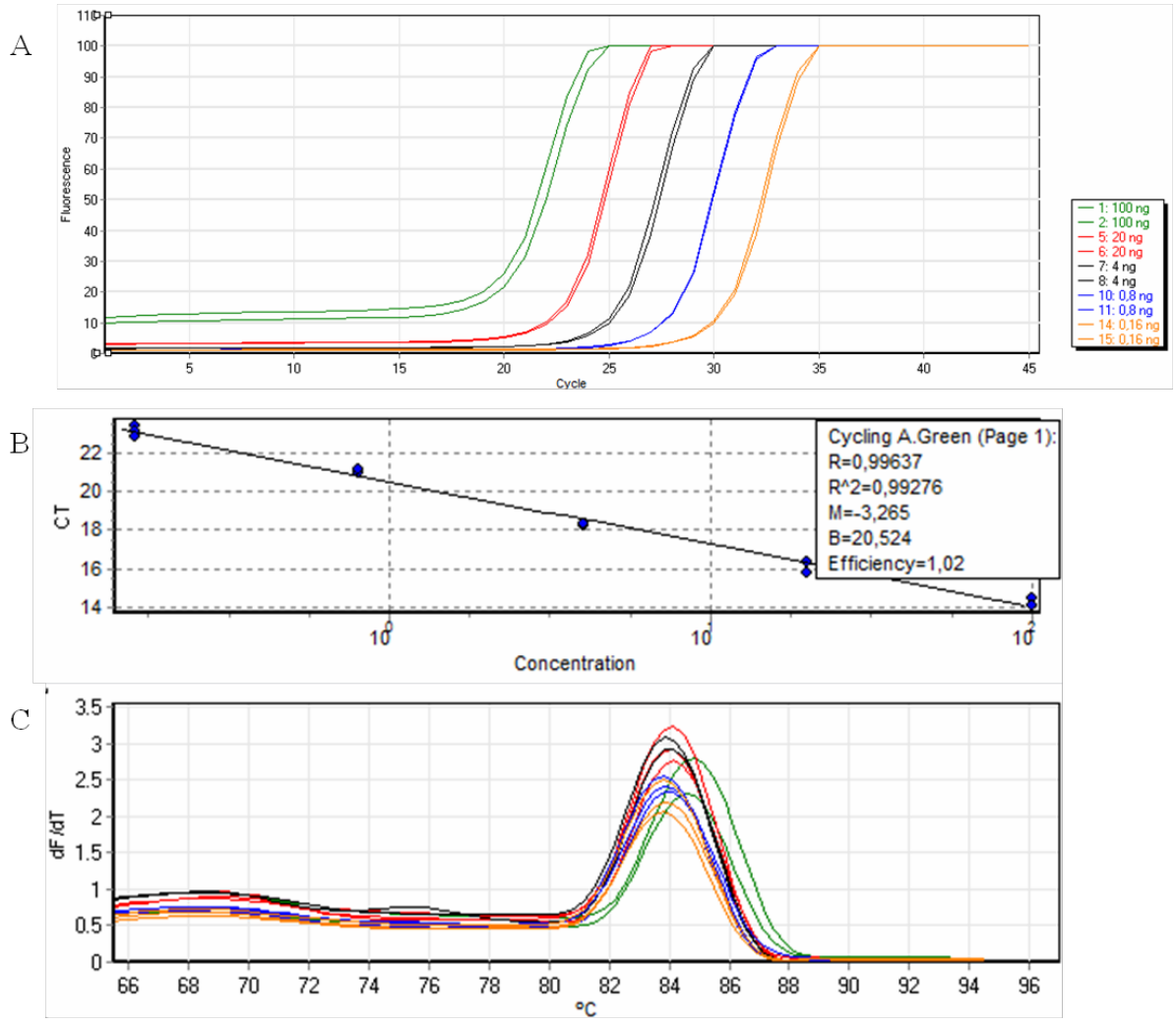

Figure 3.11: (A) Amplification curves of 5-fold dilutions from pooled RNA samples used for this study (dil 1: 100 ng/reaction, dil 2: 20 ng/reaction, dil 3: 4 ng/reaction, dil 4: 0.8 ng/reaction, dil 5: 0.16 ng/reaction. (B) Standard correlation curve using MTH primers. R: square root of correlation coefficient, R^2: correlation coefficient. M: slope of standard curve. Efficiency: doubling of PCR fragments during each cycle. (C) Melting curve analysis confirming amplification of correct PCR product.

The standard correlation curve generated using the UBC primers had an efficiency of 1.03 and an R^2 value of 0.99886 (Figure 3.12). The melting curve analysis does not show non-specific amplification

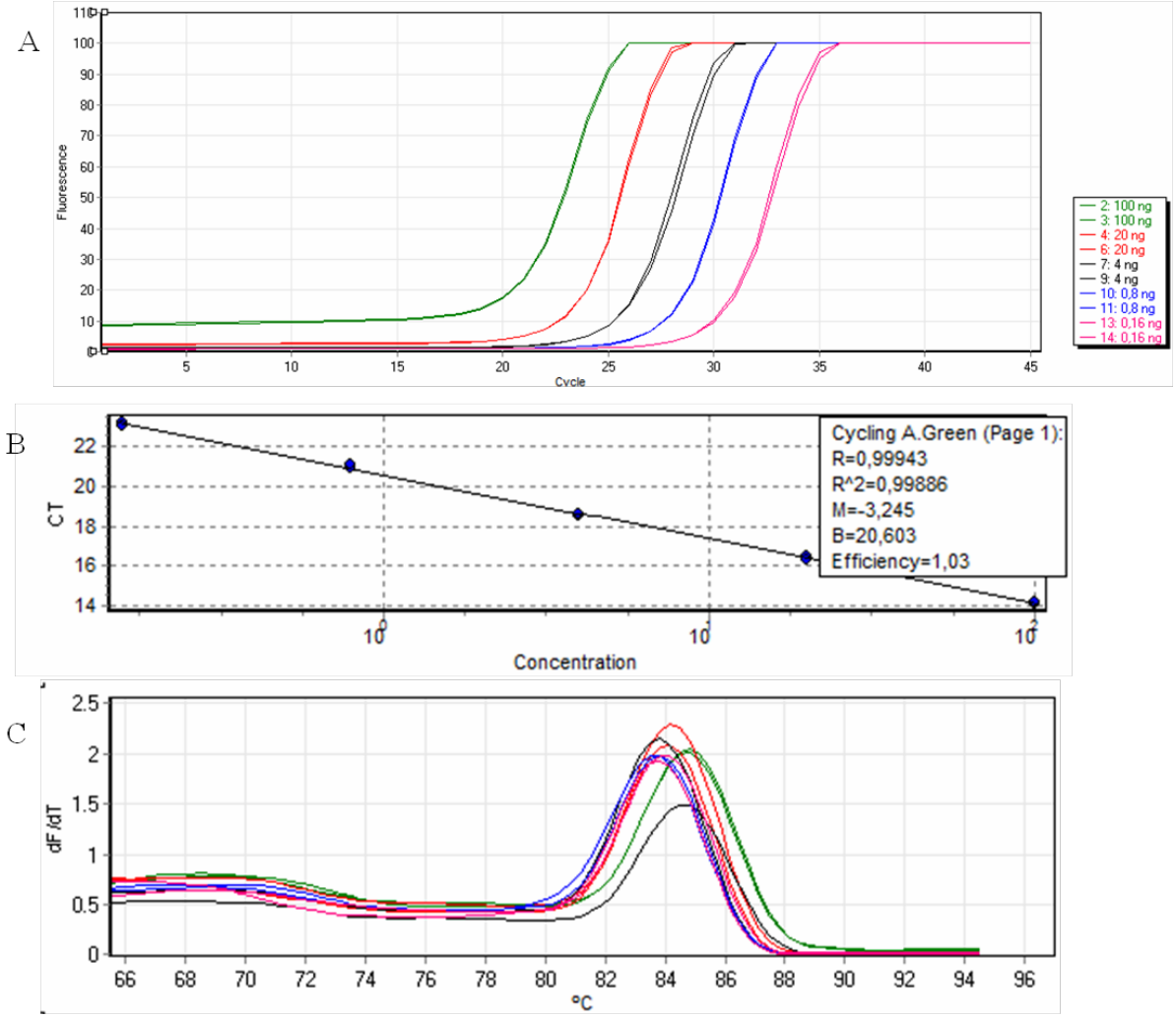

Figure 3.12: (A) Amplification curves of 5-fold dilutions from pooled RNA samples used for this study (dil 1: 100 ng/reaction, dil 2: 20 ng/reaction, dil 3: 4 ng/reaction, dil 4: 0.8 ng/reaction, dil 5: 0.16 ng/reaction. (B) Standard correlation curve using UBC primers. R: square root of correlation coefficient, R^2: correlation coefficient. M: slope of standard curve. Efficiency: doubling of PCR fragments during each cycle. (C) Melting curve analysis confirming amplification of correct PCR product.

Figure 3.13 presents the standard curve generated using the α-Tubulin primers. The efficiency of the amplification was 1.00 and the R^2 value 0.99756. Melting curve analyses indicate that no non-specific products were amplified.

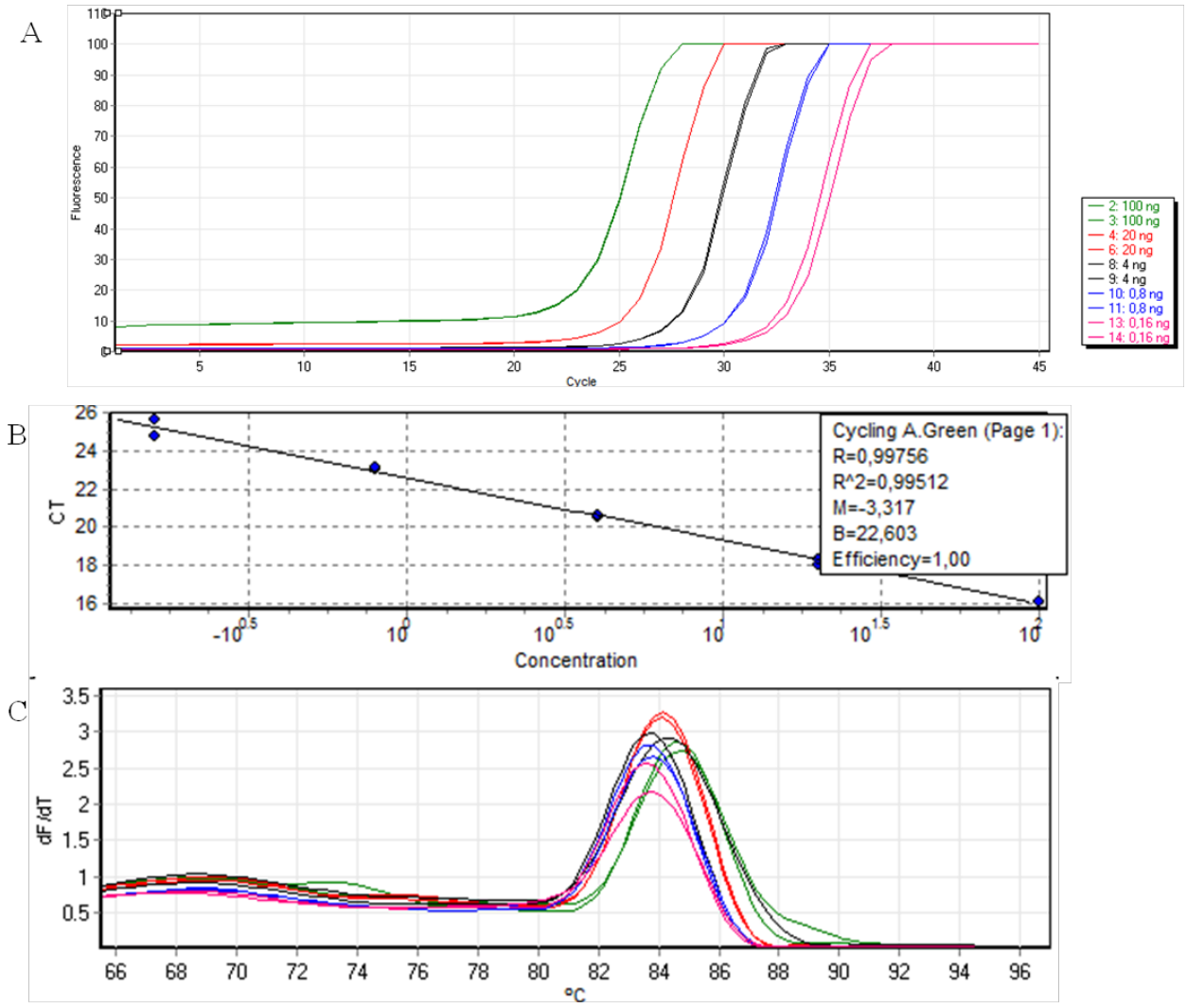

Figure 3.13: (A) Amplification curves of 5-fold dilutions from pooled RNA samples used for this study (dil 1: 100 ng/reaction, dil 2: 20 ng/reaction, dil 3: 4 ng/reaction, dil 4: 0,8 ng/reaction, dil 5: 0,16 ng/reaction. (B) Standard correlation curve using α-Tubulin primers. R: square root of correlation coefficient, R^2: correlation coefficient. M: slope of standard curve. Efficiency: doubling of PCR fragments during each cycle. (C) Melting curve analysis confirming amplification of correct PCR product.

The standard curve generated using the Elongation factor α primers showed an amplification efficiency of 0.71 and an R^2 value of 0.99131(Figure 3.14). The low efficiency indicates that the PCR amplification was not efficient in doubling the PCR product for each cycle. This can probably be ascribed to non-specific amplification since repeated experiments showed similar results (Figure 3.14.C). The non-specific amplifications are likely to be caused by primer dimers. Since the standard correlation curve using the Elongation factor α primers was not successfully optimised, it could not be used and was excluded for quantitation and further analyses.

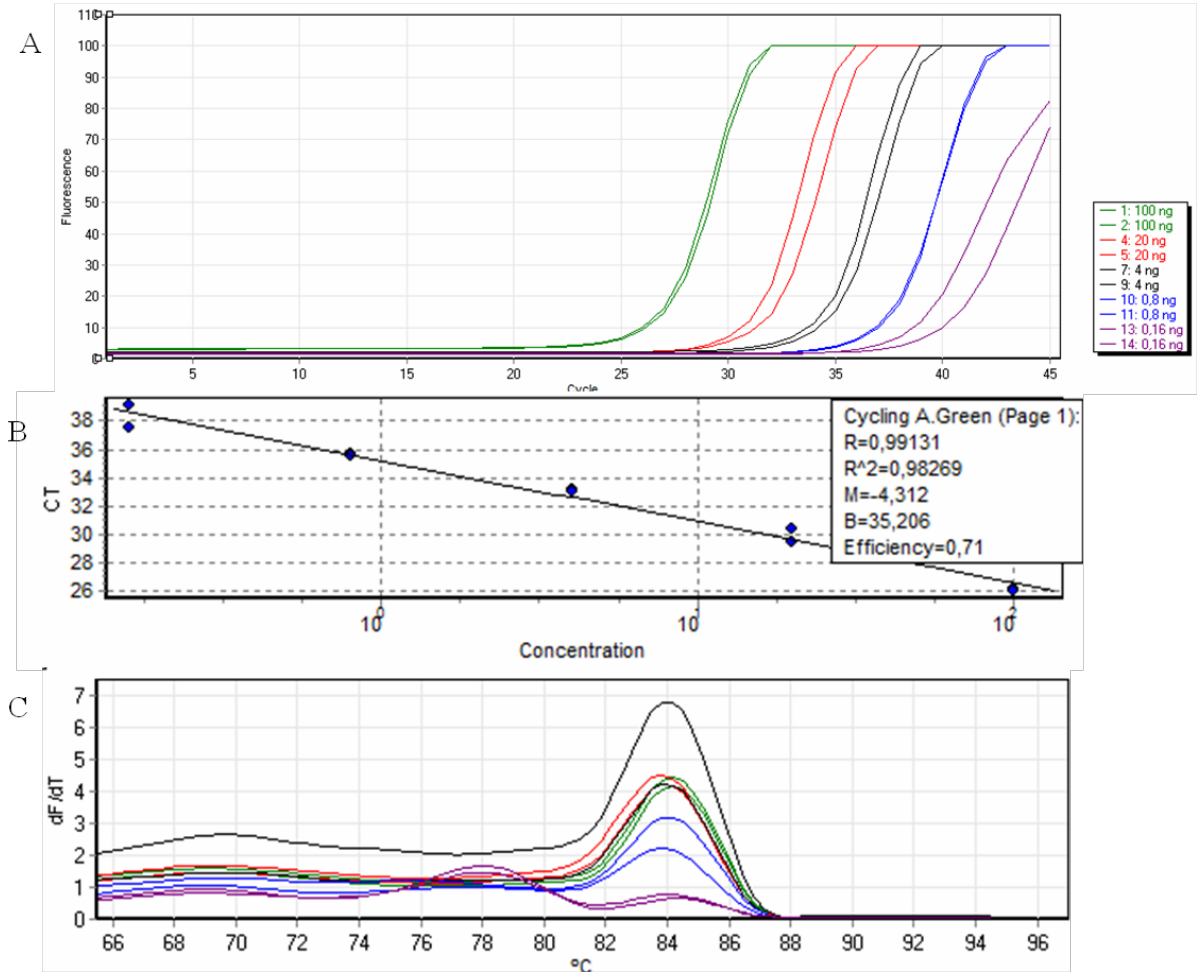

Figure 3.14: (A) Amplification curves of 5-fold dilutions from pooled RNA samples used for this study (dil 1: 100 ng/reaction, dil 2: 20 ng/reaction, dil 3: 4 ng/reaction, dil 4: 0,8 ng/reaction, dil 5: 0,16 ng/reaction. (B) Standard correlation curve using Elongation factor α primers. R: square root of correlation coefficient, R^2: correlation coefficient. M: slope of standard curve. Efficiency: doubling of PCR fragments during each cycle. (C) Melting curve analysis confirming amplification of non-specific PCR product caused by primer dimers.

3.3.6 Resistance levels of transgenic lines

As previously discussed, plants of each batch showed different biological features including the size of the shoot, the development of the roots and the colour of the leaves. These differences represent the state of health of the plants, which might have had an influence on the results. Therefore, the data is presented and discussed per batch (Table 3.4, 3.5 and 3.6).

Table 3.4 Overview of results of batch 1 presented per plant line. The first four columns present the number of the grafts at the time of grafting, the number that took and started growing, sampling for RNA extractions, and RT-qPCR screening. The average resistance levels of each plant are represented as a percentage in column 6, the *p* values in column 7 and the last column represents the significance levels using the Bonferroni adjustment Type I.

Batch 1	Grafted	Grown	Sampled	Screened	%Resistance	*p* value	Significance level
HSP#1	12	8/12	7/8	4/7	100	0.1573	0.0127
HSP#3	25	13/25	8/13	6/8	99.94	0.2453	0.0085
HSP#9	11	7/11	6/7	4/6	99.58	1	0.0127
HSP#14	8	7/8	6/7	3/6	99.62	0.8273	0.0170
HSP#15	23	21/23	11/21	4/11	100	0.1573	0.0127
HSP#17 (- control)	13	9/13	8/9	3/8	99.75		

Table 3.5 Overview of results of batch 2 presented per plant line. The first four columns present the number of the grafts at the time of grafting, the number that took and started growing, sampling for RNA extractions, and RT-qPCR screening. The average resistance levels of each plant are represented as a percentage in column 6, the *p* values in column 7 and the last column represents the significance levels using the Bonferroni adjustment Type I.

Batch 2	Grafted	Grown	Sampled	Screened	%Resistance	*p* value	Significance level
HSP#1	6	-	-	-	-	-	-
HSP#3	13	2/13	2/2	2/2	100	-	-
HSP#9	11	-	-	-	-	-	-
HSP#14	13	-	-	-	-	-	-
HSP#15	8	-	-	-	-	-	-
HSP#17 (- control)	6	-	-	-	-	-	-

Table 3.6 Overview of results of batch 3 presented per plant line. The first four columns present the number of the grafts at the time of grafting, the number that took and started growing, sampling for RNA extractions, and RT-qPCR screening. The average resistance levels of each plant are represented as a percentage in column 6, the *p* values in column 7 and the last column represents the significance levels using the Bonferroni adjustment Type I.

Batch 3	Grafted	Grown	Sampled	Screened	%Resistance	*p* value	Significance level
HSP#1	13	11/13	2/11	2/2	96.71	0.3545	0.0253
HSP#3	17	7/17	6/7	5/6	99.99	0.0143	0.0150
HSP#9	14	14/14	12/14	10/12	88.84	0.3222	0.0051
HSP#14	10	10/10	3/10	3/3	6.46	0.0339	0.0170
HSP#15	6	6/6	4/6	3/4	59	0.7237	0.0170
HSP#17 (- control)	18	14/18	6/14	6/6	59.36		
Non-modified (- control)	6	4/6	4/6	4/6	74.48		

To identify possible trends, the results of batches 1 and 3, as well as all the data combined are presented in graphs as illustrated in Figure 3.15.

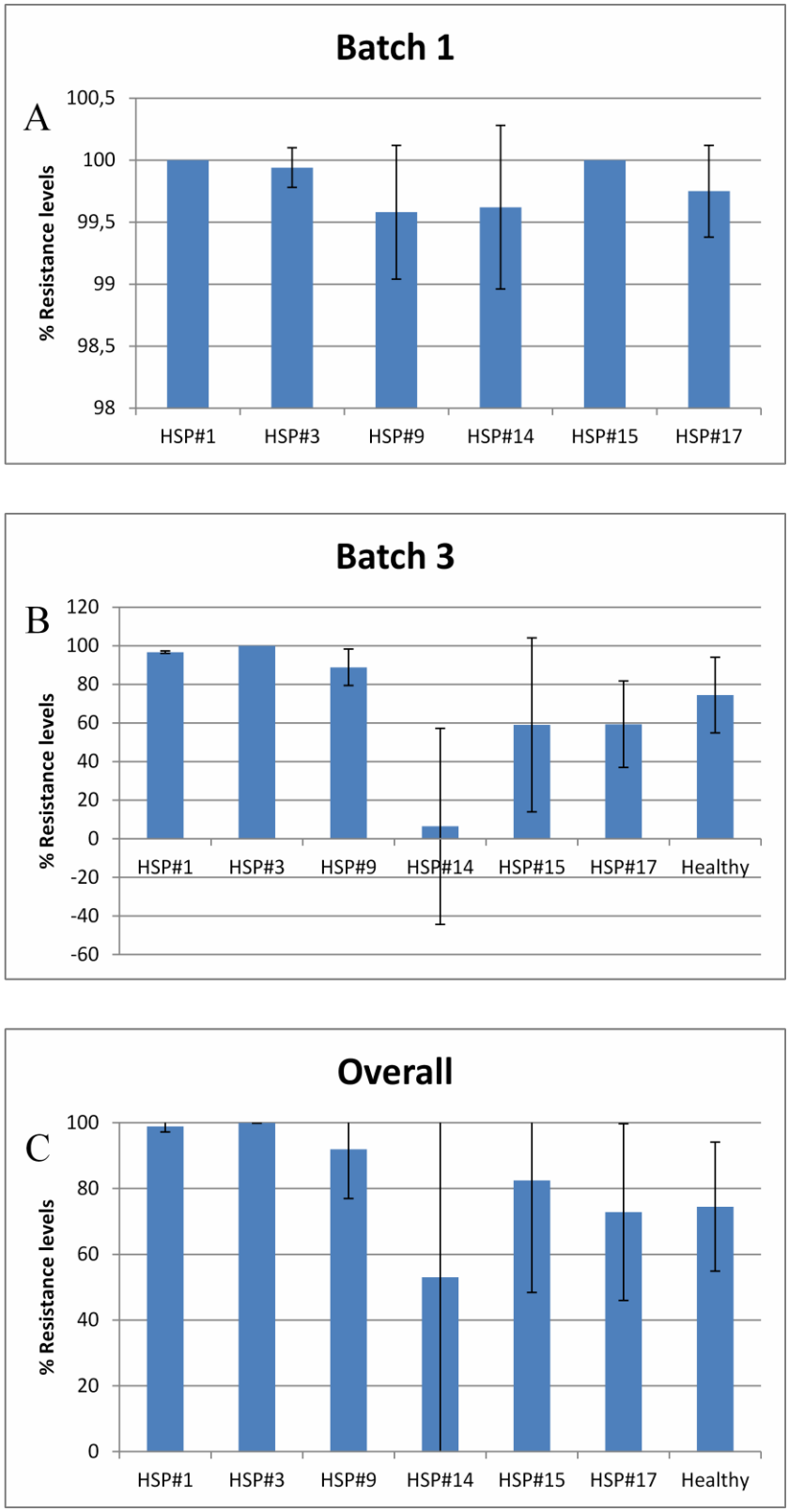

Figure 3.15 Graph representation of resistance level results. (A) graph representation of batch 1, resistance levels presented on the Y-axes (99.3% - 100%) vs plant lines on the X-axes. The black lines represent the error bars (B) graph representation of batch 3, resistance levels presented on the Y-axes (0% - 100%) vs plant lines on the X-axes. The black lines represent the error bars. (C) graph representation of all the batches overall, resistance levels presented on the Y-axes (0% - 100%) vs plant lines on the X-axes. The black lines represent the error bars.

The results of the first batch show that the experimental set-up of this batch was not optimal (Table 3.4). The average resistance levels of all plant lines were in a narrow range, and none of the plant lines showed significant results when compared to the negative control plant line #17. Although the result of the first batch cannot be considered reliable or significant, they did show a similar trend for some plant lines when compared to the results of batch 3 (Figure 3.15). Plant lines #1 and #3 showed enhanced resistance levels in both batches when compared to plant line #17 and unexpectedly, plant line #14 showed a higher susceptibility to the virus.

Batch 2 only represents one plant line and could not be compared to the non-modified control group or plant line #17 (Table 3.5). Therefore, this batch was excluded from further analyses.

Of the three batches, the experimental set-up of batch 3 was the most successful (Table 3.6). Furthermore, an additional non-modified control group was included in this batch. The results of this batch illustrated that plant lines #1, #3 and #9 showed enhanced resistance levels when compared to the control plant lines, however, only the results of plant line #3 were significant (p value ≤ 0.0150). Remarkably, plant line #14 shows a higher susceptibility to the virus when compared to the non-modified plant or negative control plant line #17. Although, the data of plant line #14 was not consistent as reflected by the large standard deviations bars, this trend was also observed in batch 1 (Figure 3.15). Unexpectedly, one grafted plant of plant line #14, contained a higher relative virus titre in the shoot sample than in the cane sample. This was not found in any other plant line, including the negative control plant line #17 or the non- modified control plant line. This suggests that the transgene of this particular plant line possibly contributes to the susceptibility to the virus. Although the data of this plant line cannot be considered reliable considering the low number of replicates and the large standard deviation, the increased susceptibility to the virus when compared to the control plant lines has been observed throughout all the batches (Figure 3.15). An increase in virus susceptibility was also observed in the study of Cooper *et al.* in 1995. Transgenic tobacco plants expressing a functional *Tobacco mosaic virus* (TMV) wild-type movement protein accelerated symptom development. However, the transgenic plants in this study express a dysfunctional mutated movement protein, it is therefore unclear whether the findings of Cooper *et al.* can be related to the findings in this study.

3.3.7 Influence of copy number and/or expression levels of the transgene

As previously discussed, every plant line contained different copy numbers and expression levels of the transgene (Table 3.1). Interestingly, the plant lines showing enhanced resistance levels to GLRaV-3 in this study, plant lines #1 and #3, expressed low levels of the transgene. This phenomenon was also documented in other studies. The first discovery of this occurrence was in 1993 when transgenic plants expressed undetectable and/or low levels of *Tobacco etch virus* (TEV) CP, yet showed high levels of resistance against TEV (Lindbo *et al.,* 1993). It was proposed that the mRNA of the transgene triggers the RNA silencing mechanism resulting in high levels of siRNAs and low levels of mRNA. Therefore, it is more likely that the enhanced resistance levels of the transgenic plants are the result of RNA-mediated resistance rather than protein-mediated resistance. This can be explored in further studies by determining the small RNA levels in the transgenic plants. Moreover, plant line #14 showed higher susceptibility to the virus when compared to the non-modified control plant line and plant line #17, yet expressed high mRNA levels of the transgene (Table 3.1). This correlates with the proposed explanation of the involvement of small RNAs in enhanced resistance plant lines.

It is unclear if the number of copies of the transgene had an influence on the resistance levels of the plants. One of the two plants showing enhanced resistance levels, plant line #3, contained a low copy number whereas the other plant, plant line #1, had a high copy number. However, plant lines #3 and #14, showing very different apparent resistance levels, each contained a single copy of the transgene. Nevertheless, considering the low number of replicates in this study, additional research is required to confirm any correlation between copy number and resistance levels.

3.3.8 Influence of cultivar

Two different cultivars were used as a viral source; Cabernet Sauvignon and Chardonnay. Both plants were infected with GLRaV-3 isolate GP18. Lower quantities of Cabernet Sauvignon plant material was available, resulting in less grafted plants of this cultivar.

Not all batches and/or plant lines contained plants of both cultivars. For example, plant line #1 and the negative control group did not contain Cabernet Sauvignon plants. Since the results are related to plant line and batch line, it is not possible to determine the influence of the cultivar on the resistance levels.

However, since these two cultivars were used as donor plants, the cultivar might have had an influence on the success rate of the number of buds that took and started growing and the growing conditions of the plants (Figure 3.16).

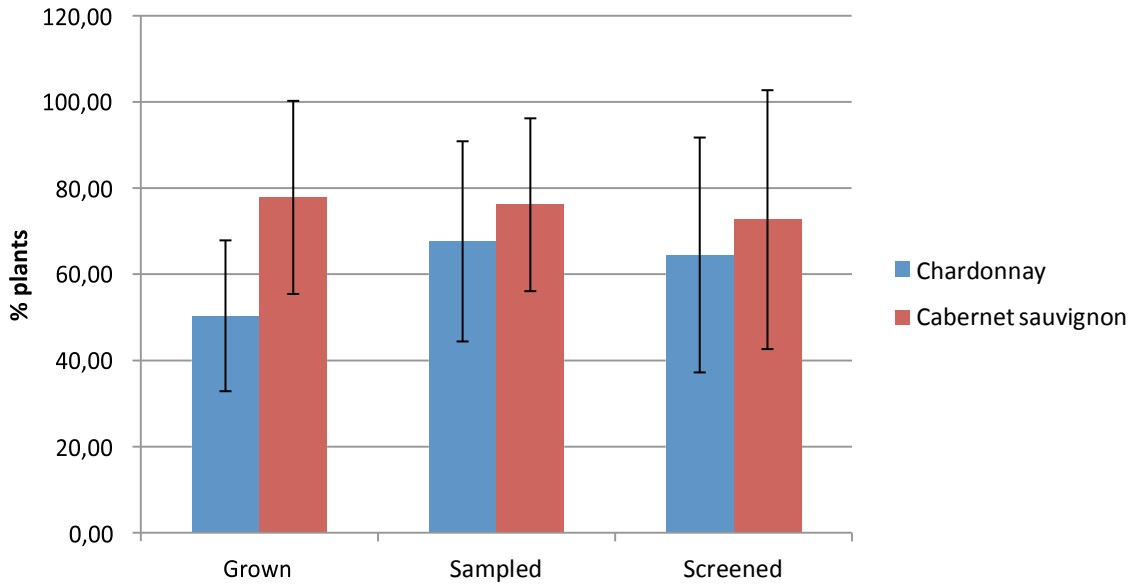

Figure 3.16 Overview of quantity of plants per cultivar. The three groups represent the percentage of plants of which the bud took and started growing, were sampled for RNA extraction and were screened using RT-qPCR. The blue bars represent Chardonnay and the red bars Cabernet Sauvignon. The black error bars represent the standard deviation of the mean.

As presented in Figure 3.16, plants grafted with Cabernet Sauvignon cane material had higher "take" percentages, and thus more could be sampled for RNA extraction and RT-qPCR assays, when compared to Chardonnay plant material. This is probably due to rootstock-scion compatibility.

As discussed previously, plant line #3 was morphologically different when compared to the other transgenic lines and ampelographic observations suggested that this plant line is a different cultivar, likely a Jaque/Black Spanish. It is unknown whether this difference in cultivar has contributed to the significantly enhanced resistance levels of this plant line. It is possible that plants of cultivar Jaque/Black Spanish are naturally more resistant to GLD, however, no research is available confirming a correlation between cultivar and enhanced resistance levels in transgenic plants. Another plausible explanation for the enhanced resistance level of plant line #3, is that the cultivar might have had an influence on the virus

transmissibility through the graft union. Without a non-modified Jaque/Black Spanish plant, it was not possible to determine the significance of the results of plant line #3. Additional studies including a non-modified plant from the same cultivar is required to confirm the results of this study.

3.4 Conclusion

This study suggested that the use of PDR based on transgenic plant lines containing a dysfunctional viral movement protein can be a potential strategy to control GLRaV-3. Plant line #3 showed significantly enhanced resistance levels to GLRaV-3 when compared to the negative control plant lines. However, not all plant lines in this study showed enhanced resistance levels. More specifically, an increased susceptibility to the virus was observed for plant line #14. Further research on these plant lines, with adequate sample numbers, should provide a better understanding of the mechanism behind the resistance/susceptibility levels.

3.5 References

Barrass, I.C., Jerie, P. and Ward, S.A. 1994. Aerial dispersal of first- and second instar longtailed mealybug, *Pseudococcus longispinus* (Targioni Tozzetti) (Pseudococcidae: Hemiptera). *Austr. J. Exp. Agric.* 34: 1205-1208

Carrington, J.C., Kasschau, K.D., Mahaian, S.K. and Schaad, M.C. 1996. Cell-to-cell and long-distance transport of viruses in plants. *Plant Cell.* 8(10): 1669-1681

Citovsky, V. and Zambryski, P. (1991). How do plant virus nucleic acids move through intercellular connections? *Bioessays*. 13: 373-379

Daane, K.M., Almeida, R.P.P., Bell, V.A., Botton, M., Fallahzadeh, M., Mani, M., Miano, J.L., Sforza, R., Walton, V.M. and Zaveizo, T. 2012. Biology and management of mealybugs in vineyards. *Arthropod Management in Vineyards: Pests, Approaches and Future Directions*, eds. N.J. Bostanian, C. Vincent, and R. Isaacs (Springer). 271-307

Engelbrecht, D.J. and Kasdorf, G.G.F. 1990. Field spread and corky bark, fleck, leafroll and Shiraz decline diseases and associated viruses in South African grapevines. *Phytophylactica*. 22(3): 347-354

Frankel, M., Beko, G., Timm, M., Gustavsen, S., Hansen, E.W. and Madsen, A.M. 2012. Seasonal variations of indoor microbial exposures and their relation to temperature, relative humidity, and air exchange rate. *Appl. Environ. Microbio*. 78(23): 8289-8297

Freeborough, M.-J. 2003. A pathogen-derived resistance strategy for the broad-spectrum control of Grapevine leafroll-associated virus infection. *PhD Thesis.* Stellenbosch University

Gölles, R., Moser, R., Pühringer, H., Katinger, H., Laimer da Câmara Machado, M., Minafra, M., Savino, V., Saldarelli, P. and Da Câmara Machado, G.P.M. 1998. Transgenic grapevines expressing coat protein gene sequences of grapevine fanleaf virus, arabis mosaic virus, grapevine virus A and grapevine virus B. *ISHS Acta Horticulturae*. 528

Grant, S.R. 1999. Dissecting the mechanisms of posttranscriptional gene silencing: divide and conquer. *Cell.* 96: 303-306

Habili, N., Fazeli, C.F., Ewart, A., Hamilton, R., Cirami, R., Saldarelli, P., Minafra, A. and Rezaian, M.A. 1995. Natural spread and molecular analysis of grapevine leafroll-associated virus 3 in Australia. *Phytopathology*. 85: 1428-1422

Hodges, A. and Hodges, G. 2006. Pink Hibiscus Mealybug Identification. *Plant Health Progress.*Online:http://www.plantmanagementnetwork.org/pub/php/diagnosticguide/2006/hibiscus/

Kingston, C. 2002. Virus, mealybugs and the search for solutions. *The Australian and New Zealand Grapegrower and Winemaker*. 461: 34-39

Lahogue, F., Boulard, G. and Schneider, C. 1995. Comparison of the viral transmission efficiency of different grafting techniques on grapevines. *Vitis*. 34: 177-183

Le Gall, O., Torregrosa, L., Donglot, Y., Candresse, T. and Bouguet, A. 1994. Agrobacterium-mediated genetic transformation of grapevine somatic embryos and regeneration of transgenic plants expressing the coat protein of grapevine chrome mosaic nepovirus (GCMV). *Plant Science*. 102(2): 161-170

López-Fabuel, I., Wetzel, T., Bertolini, E., Bassler, A., Vidal, E., Torres, L.B., Yuste, A. and Olmos, A. 2013. Real-time multiplex RT-PCR for the simultaneous detection of the five main grapevine viruses. *Journal of Virological Methods. 188(1-2): 21-24*

Malan, S. 2009. Real Time PCR as a versatile tool for virus detection and transgenic plant analysis. *MSc Thesis. Stellenbosch University*

Mauro, M.C., Toutain, A., Walter, B., Pinck, L., Otten, L., Coutos-Thevenot, P., Deloire, A. and Barbier, P. 1995. High efficiency regeneration of grapevine plants transformed with the GFLV coat protein gene. *Plant Science.* 112(1): 97-106

Pathirana, R. and McKenzie, M.J. 2005. A modified green-grafting technique for large-scale virus indexing of grapevine (*Vitis vinifera* L.). *Scientia Horticulturae*. 107(1): 97-102

Petersen, C.L. and Charles, J.G. 1997. Transmission of grapevine leafroll-associated closteroviruses by *Pseodococcus longispinus* and *P. Calceolariae*. *Plant Pathology*. 26: 509-515

Reid, K. E., Olsen, N., Schlosser J., Peng, F. and Lund, S. T. 2006. An optimized RNA isolation procedure and statistical determination of reference genes for real-time RT-PCR during berry development. *BMC Plant Biology*. 6:27-37

Spielmann, A., Krastanova, S., Douet-Orhant, V. and Gugerli, P. 2000. Analysis of transgenic grapevine (*Vitis rupestris*) and *Nicotiana benthamiana* plants expressing an arabis mosaic virus coat protein gene. *Plant Science.* 156(2): 235-244

Stanford, J.C. and Johnson, S.A. 1985. The concept of parasite-derived resistance: deriving resistance genes from the parasite's own genome. *Journal of Theoretical Biology*. 115: 395-405

Van Lent, J., Storm, M., van der Meer, F., Wellink, J. and Goldbach, R. 1991. Tubular strctures involved involvement of cowpea mosaic virus are also formed in infected cowpea protoplasts. *Journal of General Virology*. 72: 2615-2623

Walter, B., Bass, P.,, Legin, R., Martin, C., Vernov, R., Collas, A. and Vesselle, G. 1990. The use of green-grafting technique for the detection of virus-like diseases of grapevine. *Journal Phytopathol.* 128: 137-145

White, E., Venter, M., Hiten, N.F. and Burger, J.T. 2009. Modified cetyltrimethylammonium bromide method improves robustness and versatility: The benchmark for plant RNA extraction. *Biotechnology Journal*. 3:1424-1428

Chapter 4 Development and validation of artificial microRNA constructs to silence specific GLRaV-3 sequences in *Nicotiana benthamiana*

4.1 General introduction

In the 1920s, Wingard discovered that when plants were infected with tobacco ringspot virus, they had become immune to the virus in the upper leaves (Wingard, 1928). It was suggested that the plant had some kind of defence mechanism. Another study in 1990 conducted by Rich Jorgensen *et al.,* tried to over-express the chalcone synthase (CHS) gene in petunias in order to deepen the purple colour of the flower. Surprisingly, many flowers became white and failed to express the transgene. Many years later it was discovered that these findings were the first demonstrations of post-transcriptional gene silencing (PTGS).

In the last decade scientists discovered that small non-coding RNAs (sncRNAs) are responsible for this defence mechanism, better known as RNA silencing or RNA interference (RNAi).

4.1.1 **PTGS applications**

PTGS have been intensively studied, resulting in a better understanding of this silencing mechanism. It has been used for several applications including the generation of transgenic plants based on RNA-mediated virus resistance (RMVR) and the construction of artificial microRNAs (amiRNAs).

RMVR is a form of pathogen-derived resistance (PDR) in which transgenic plants expressing a specific region of the virus such as the coat protein or the movement protein, in order to confer resistance to the virus (Cogoni and Macino, 2000; Finnegan *et al.,* 2001; Lindbo *et al.,* 2001). RMVR has become an important tool for therapeutics, gene function analysis and bio-engineering in conferring resistance against plant pathogens.

Artificial microRNAs, also known amiRNAs, are another tool to confer virus resistance. AmiRNAs are single stranded 21 nt RNA fragments which are not naturally found in plants but are designed to target a mRNA of interest. These mature 21 nucleotide (nt) amiRNAs are incorporated into a plant's own miRNA precursor (pre-miRNA) to retain its secondary structure. Three criteria are required to resemble a natural miRNA; 1) the first nt should be a 'U', 2) the 5' shows instability to its amiRNA* (this is the complementary strand which is not loaded into the RISC) and 3) the 10th nt is preferably an 'A' or otherwise a 'U' (Reynolds *et al.,* 2004; Mallory *et al.,* 2004). Other selection criteria are; no mismatches between positions 2 and 12, one or two mismatches at the 3' end (positions 18-21), absolute hybridization energy between -35 and -38 kcal/mole and the selection of the target position (WMD3 – Web MicroRNA designer).

The selection of the target position for an amiRNA is crucial in order to effectively cleave the mRNA. It should preferably be a conserved region in order to target the specific virus as well as all related variants. Furthermore, mRNAs do not have a single stable structure, they contain secondary local structures which influences the efficiency of RNA silencing. Some targets are more accessible than others (Duan *et al.,* 2008).

4.1.2 Validation of amiRNAs

The validation of amiRNAs can be difficult due to their small size. Several techniques were developed and optimized for miRNA detection including RT-qPCR using stem-loop primers followed by TaqMan PCR analyses (Varkonyi-Gasic *et al.,* 2007). These stem-loop primers extend the miRNA cDNA in order to make detection more sensitive and accurate. However, although this validation system detects the expression of the amiRNA, it does not validate the cleavage efficiency of the mRNA. A validation system which validates both aspects was reported in 2012. Jelly *et al.* (2012) performed a co-transformation assay using pre-amiRNA constructs and a modified GUS-sensor construct, in which the target sequences of the amiRNAs were incorporated in the 3' terminus of the GUS gene. The resulting 21 nt target sequence of GUS-sensors was successfully cleaved by the corresponding amiRNA (Jelly *et al.,* 2012).

In this study, a similar amiRNA validation system using a green fluorescence gene (GFP) was designed, constructed and validated.

4.2 Materials and Methods

4.2.1 Design of an amiRNA-mediated silencing validation system

Two amiRNAs and two target constructs were designed, constructed and validated in this study. The amiRNA targets were incorporated into the 3' terminal of GFP. Once infiltrated into *Nicotiana benthamiana,* this 21 nt insert did not influence the intensity of the GFP expression. However, once co-infiltrated with a corresponding amiRNA, the 21 nt target sequence was cleaved, the GFP gene disrupted and consequently silenced (Figure 4.1). The GFP expression intensity determines the silencing efficiency of the amiRNA.

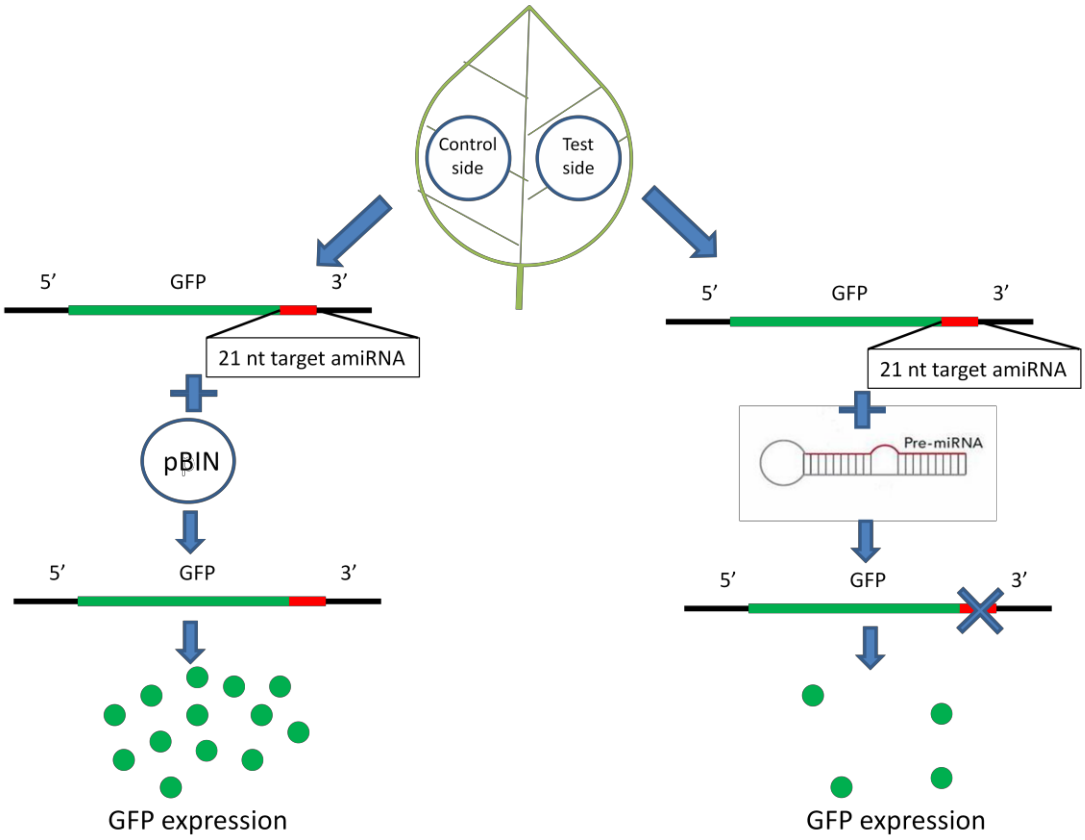

Figure 4.1 Overview of co-infiltrations of modified constructs into *Nicotiana benthamiana*. The 21 nt target sequence, presented in red, can be cleaved when co-infiltrated with a corresponding amiRNA. Consequently, the GFP gene will be disrupted and silenced.

4.2.2 Existing grapevine amiRNAs

In a previous study, several amiRNAs were constructed to target GFP using four different *V. vinifera* amiRNA precursors in order to determine the most efficient precursor for grapevines (M. Snyman, unpublished data). The 21 nt amiRNA sequence was selected based on the study of Liu *et al* in 2010 and was incorporated in each pre-amiRNA. Pre-amiRNA vvi167b was

determined to be the most efficient precursor in silencing GFP (Pers. Comm. M. Snyman, 2014). This amiRNA-167b-GFP (AG) construct targets the GFP gene and was used for this study to function as a positive control. Furthermore, the precursor vvi167b was used as a backbone to construct amiRNAs in this study.

4.2.3 **amiRNA targets**

The target positions of the artificial miRNAs were selected based on multiple factors including accessibility, GC-content and conservation of the potential target region. The online software for Statistical Folding of Nucleic Acids and Studies of regulatory RNAs (Sfold) was used to select a target based on the accessibility of the mRNA target region (http://sfold.wadsworth.org/cgi-bin/index.pl). According to Sfold, regions predicted to be single stranded are likely to be more accessible for miRNA binding. Figure 4.2 shows the selected 21 nt mRNA target region predicted to be accessible, indicated with a green rectangle. This target is located around nt 1800 of the GLRaV-3 variant GP18 genome, located in ORF 1a, which codes for methyltransferase and helicase. This amiRNA is named amiRNA-Access (AA) in further descriptions.

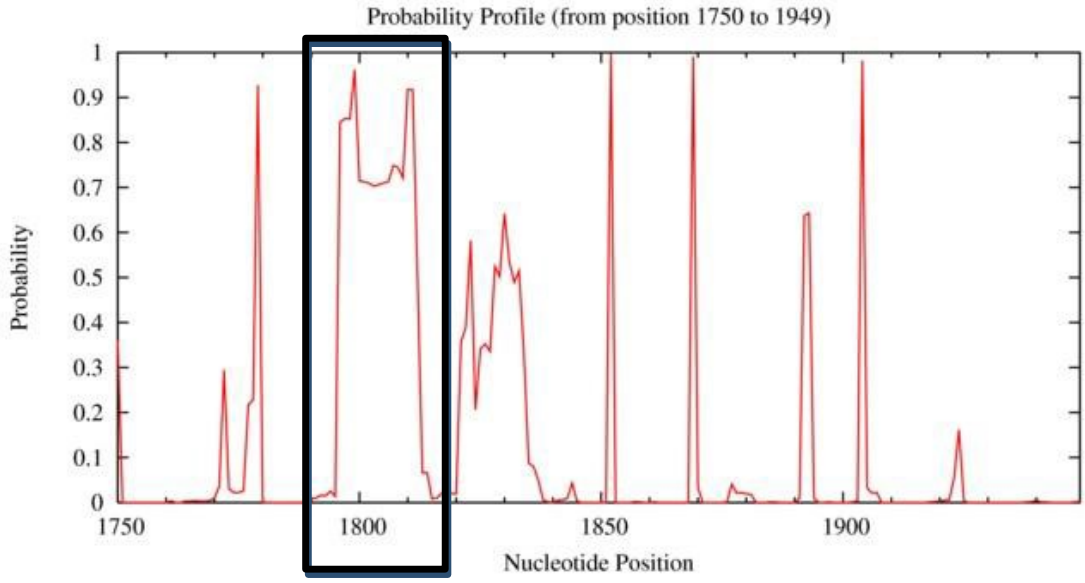

Figure 4.2 Accessibility prediction of mRNA by Sfold. The Y-axes indicates the probability of being single stranded. The position of the target is indicated by the green rectangle. Nt 1795-1815 nt of the grapevine leafroll associated virus 3 isolate GP18 [Genbank: EU259806.1] genome is the selected target for amiRNA-Access.

The target of the second amiRNA was selected based on a conserved region of GLRaV-3. A multiple sequence alignment was generated in CLC Main Workbench including isolates GP18

[Genbank: EU259806.1], 621 [GenBank: GQ352631.1], WA-MR [GenBank: GU983863.1], LN [GenBank: JQ423939.1], PL-20 [GenBank: GQ352633.1], GH24 [unpublished data] and GH30 [GenBank: JQ655296.1] (Figure 4.3). The selected region is 100% conserved for all isolates and located in ORF1a. This amiRNA was named amiRNA-Conser (AC) in further descriptions.

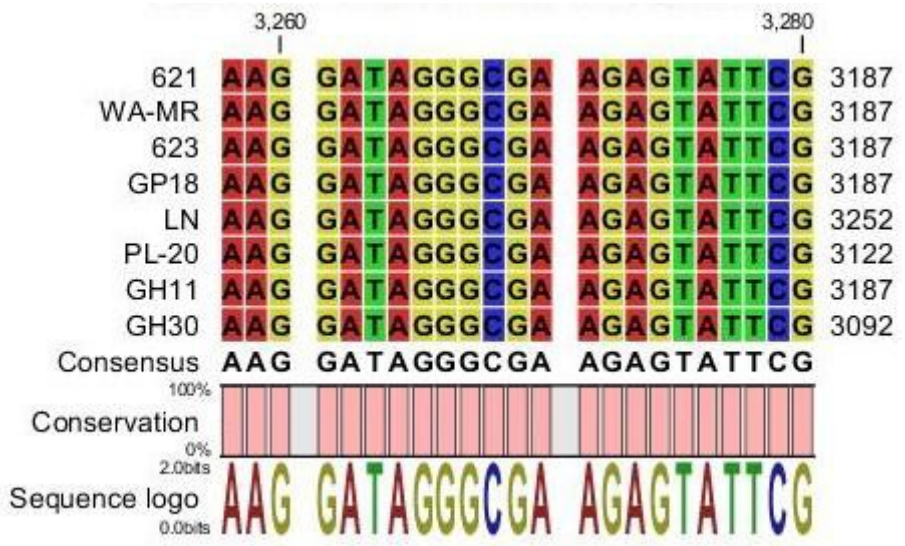

Figure 4.3 Multiple sequence alignment of GLRaV3 isolates 621, WA-MR, 623, GP18, LN, PL-20, GH11 and GH30 generated using CLC Genomic Main Work Bench. The selected 21 nt target sequence is 100% conserved between all isolates.

4.2.4 **amiRNA design**

Vitis vinifera pre-miRNA 167b was used as a backbone for the amiRNAs constructs (Pers. Comm. M. Snyman, 2014). Both amiRNA constructs were designed according to the selection criteria of Weigel World Web MicroRNA Designer (WMD3). Figures 4.4 and 4.5 show the secondary structures of the constructed pre-amiRNAs in this study. Cleavage sites of restriction enzymes *SacI* and *SdaI* were incorporated on the ends of the pre-amiRNAs for further cloning purposes. Both pre-amiRNA constructs had an absolute hybridization energy of 38.7 kcal/mole.

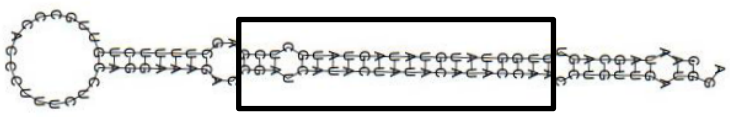

Figure 4.4 Secondary structure of precursor pre-AA. The main sequence of AA is indicated in the black rectangle.

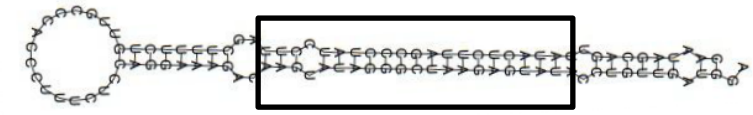

Figure 4.5 Secondary structure of precursor pre-AC. The main sequence of AC is indicated in the black rectangle.

4.2.5 **Construction of pre-amiRNA vectors**

The pre-amiRNA fragments were constructed using a previously optimised overlapping extension PCR protocol (Pers. Comm. M. Snyman, 2014). Primers used for this amplification are shown in Table 4.1, the underlined sequences indicate the overlapping regions. A 25 µl reaction contained: 0.2 mM dNTPs, 1X Kapa Buffer B + Mg, 1 unit of KapaTaq DNA polymerase, 0.8 mM of primer F1, 0.8 mM of primer F2 and 0.8 mM of reverse primer. A modified PCR amplification programme was used. DNA fragments were initially annealed at 38°C for 4 seconds, followed by an elongation step of 72°C for 30 seconds. Subsequently, 20 cycles of 94°C for 20 seconds, annealing at 40°C for 30 seconds and elongation at 72°C for 20 seconds was performed, followed by 20 cycles of 94°C for 20 seconds, annealing at 60°C for 30 seconds and elongation at 72°C for 20 seconds. A final elongation step was performed for 5 minutes at 72°C.

Table 4.1 Primers used for overlapping extension PCR. Underlined sequences indicate overlapping regions.

Primer	Sequence (5' – 3')	Lenght (nt)	Designed
amiRNA-access F2	AAGAGCTCCAATAGCAGTTTGGTATGTATAGTATGCTCGAGCTTTTCTGTTG	52	This study
amiRNA-access F1	AGCTTTTCTGTTGCCCACCCTTTCTCCAGGAAAGAC	36	Snyman,M
amiRNA-access R	TTCCTGCAGGTCCATCAACAGGTTGGTATGTATAGTATGATCGGTCTTTCCTGGAG	56	This study
amiRNA-conser F2	AAGAGCTCCAATAGCAGTTATACTCTTAGCCCTATCCTTAGCTTTTCTGTTG	52	This study
amiRNA-conser F1	AGCTTTTCTGTTGCCCACCCTTTCTCCAGGAAAGAC	36	Snyman, M
amiRNA-conser R	TTCCTGCAGGTCCATCAACAGGTATACTCTTAGCCCTATACTTGTCTTTCCTGGAG	56	This study

The fragments obtained using overlapping extension PCR were separated using agarose gel electrophoresis. The 25 µl reaction mixture was loaded in a 2% Agarose gel [1X TAE buffer (40 mM Tris, 0.114% (v/v) HOAc, 1 mM EDTA pH 8.0)] containing 0.01% v/v ethidium bromide (EtBr) and electrophoresed for 45 minutes at 100 Volts. The gel was visualized under ultraviolet light in a Multi Genius Bio-imaging system (Syngene™).

Pre-amiRNA fragments had a size of 118 bp and were excised from the gel using a clean scalpel blade. A Zymoclean™ Gel DNA Recovery Kit was used to purify the DNA. The DNA fragments were ligated into a pGEM®-T Easy Vector (vector: insert ratio of 1:3). The ligation mixture was transformed into chemical competent *E. coli* JM109 cells. Two microlitres of ligation reaction was mixed with 100 µl *E.coli* JM109 competent cells and incubated on ice for 20 minutes, followed by an incubation step at 42°C for 45 seconds and 2 minutes on ice. A total volume of 700 µl of liquid Luria Bertani (LB) media [Tryptone 10 g/l, Sodium Chloride 10 g/l, Yeast Extract 5 g/l] was added and shaken at 180 rpm for 1h30 at 37°C. Blue-white screening was performed by plating out 100 µl of transformation mixture onto pre-made LB plates containing 12 g/l agar, 100 µg/ml Ampicillin, 80 µg/ml X-Gal (5-bromo-4-chloro-3-indolyl-beta-D-galactoside) and 0.16 mM IPTG (isopropyl-beta-D-thiogalactopyranoside), and grown overnight at 37°C. Colony PCR and Sanger sequencing was performed to confirm that the correct insert was incorporated into the vector.

The pGEM®-T Easy pre-amiRNA constructs were excised with *SacI* and *SdaI* and the fragments were subcloned into the corresponding sites of expression vector pBIN-61S. The pre-amiRNA constructs were transformed and confirmed by colony PCR and Sanger sequencing.

4.2.6 **Construction of target vectors**

Target sequences of the two amiRNAs were incorporated into the 3' terminal of GFP of an pBIN-GFP expression vector (Figure 4.6). Overlapping extension PCR was performed according to a previously optimised protocol using the primers presented in Table 4.2 (Pers. Comm. J. Domingues, 2013). Underlined sequences indicate the amiRNA target sequences.

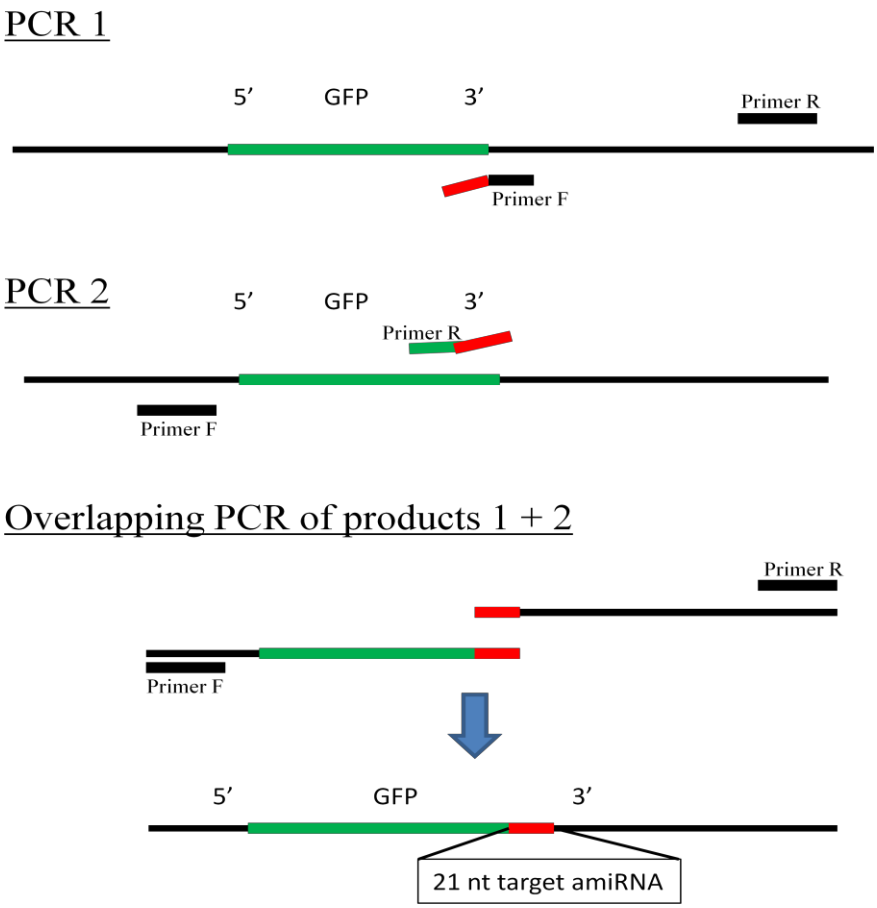

Figure 4.6 Illustration of optimised PCR protocol to incorporate a 21 nt target sequence into 3' of GFP. Black represents the pBIN-GFP expression vector, green the GFP gene and red the 21 nt target sequence.

Table 4.2 Primers designed to incorporate target sequences of the amiRNAs into the 3' UTR of GFP. Underlined sequences indicate target sequence of amiRNA.

Name	Sequence 5'-3'	Lenght (nt)	Designed
pBIN access amiR F	CGAGCATACTACACATACCATGATCGTTCAAACATTTGGC	40	this study
pBIN access amiR R	ATGGTATGTGTAGTATGCTCGGAGCTCTTAAAGCTCATC	39	this study
pBIN conser amiR F	AAGGATAGGGCGAAGAGTATTGATCGTTCAAACATTTGGC	40	this study
PBIN conser amiR R	AATACTCTTCGCCCTATCCTTGAGCTCTTAAAGCTCATC	39	this study
mgfp4_fwd	GGAAGCTTATGAGTAAAGGAGAAGAAC	27	Domingues, J
pBIN35SGFP insert R	CTGTTTGATGGTGGTTCCGAA	21	Domingues, J

Two separate PCR reactions were performed. Each reaction contained a primer with an overlapping target sequence (Figure 4.6). The first 50 µl reaction mixture contained: 1X Phusion HF Buffer, 0.5 mM mGFP4_fwd primer, 0.5 mM amiR reverse primer, 0.2 mM of dNTPs, 1 unit of Phusion High-Fidelity DNA Polymerase (Thermo Scientific™) and 25 ng of pBIN-GFP template. The second reaction contained: 1X Phusion HF Buffer, 0.5 mM amiR

forward primer, 0.5 mM pBIN35SGFP insert reverse primer, 0.2 mM of dNTPs, 1 unit of Phusion High-Fidelity DNA Polymerase (Thermo Scientific™) and 25 ng of pBIN-GFP vector template in a total reaction volume of 50µl. Both reactions were amplified using the same PCR conditions: DNA was initially denatured at 94°C for 5 minutes, followed by 30 cycles of 94°C for 30 seconds, 55°C for 30 seconds and 72°C for 30 seconds. A final extension step was performed for 5 minutes at 72°C. Subsequently, the two PCR products were amplified in an overlapping PCR reaction containing as illustrated in Figure 4.6: 1X Phusion HF Buffer, 0.5 mM mGFP4_fwd primer, 0.5 mM pBIN35SGFP insert reverse primer, 0.2 mM of dNTPs, 1 unit of Phusion High-Fidelity DNA Polymerase (Thermo Scientific™) and 1 µl of each previous PCR reaction mixture in a total volume of 50µl. The same PCR conditions were used as previously described.

The fragments were validated using agarose gel electrophoreses. Positive amplicons with an expected size of 1484 nt were excised and purified from the gel using a Zymoclean™ Gel DNA Recovery Kit.

The target fragments were excised with *DraIII* and *Eco31I* and cloned into the corresponding sites of expression vector pBIN-GFP. The target constructs were transformed and confirmed by colony PCR and Sanger sequencing. The two generated constructs were named Target-Access (TA) and Target-Conser (TC) in further descriptions.

4.2.7 Evaluation of artificial miRNAs

4.2.7.1 Infiltration into Nicotiana benthamiana

Once the insert was confirmed by sequencing, all four constructs were transformed into competent C58C1 Agrobacterium cells using electroporation. The Agrobacterium mixtures were plated onto LB agar plates containing 50 µg/ml of Kanamycin and 50 µg/ml of Rifampicin, and grown for 2 days at 28°C.

Positive colonies were selected and inoculated in 40 ml of liquid LB containing 50 µg/ml Kanamycin and grown overnight at 28°C. The following day, cells were centrifuged at 5000 rpm for 10 minutes at room temperature. The pellet was resuspended in an infiltration buffer containing 10 mM MES [2-(*N*-morpholino) ethanesulfonic acid], 10 mM $MgCl_2$ and 100 µM Acetosyringone [4'-Hydroxy-3',5'-dimethoxyacetophenone]. Mixtures were diluted to OD_{600}

1.0 and incubated at room temperature for 3-4 hours. The bacteria mixtures, containing the modified constructs, were infiltrated into the abaxial surface of *Nicotiana benthamiana* leaves as follows: a modified target construct was co-infiltrated with an empty pBIN vector on the left side of the leaf to function as a control (control side). The right side was co-infiltrated with the same modified target construct and the corresponding amiRNA construct (test side). Furthermore, a control experiment was performed in parallel. The control side was infiltrated with the same constructs as the experimental group, however, the test side was co-infiltrated with a modified target construct and the non-corresponding amiRNA (Figure 4.7). These two experiments (experimental group and control group) were performed for each amiRNA (AA, AC and AG) and was repeated three times.

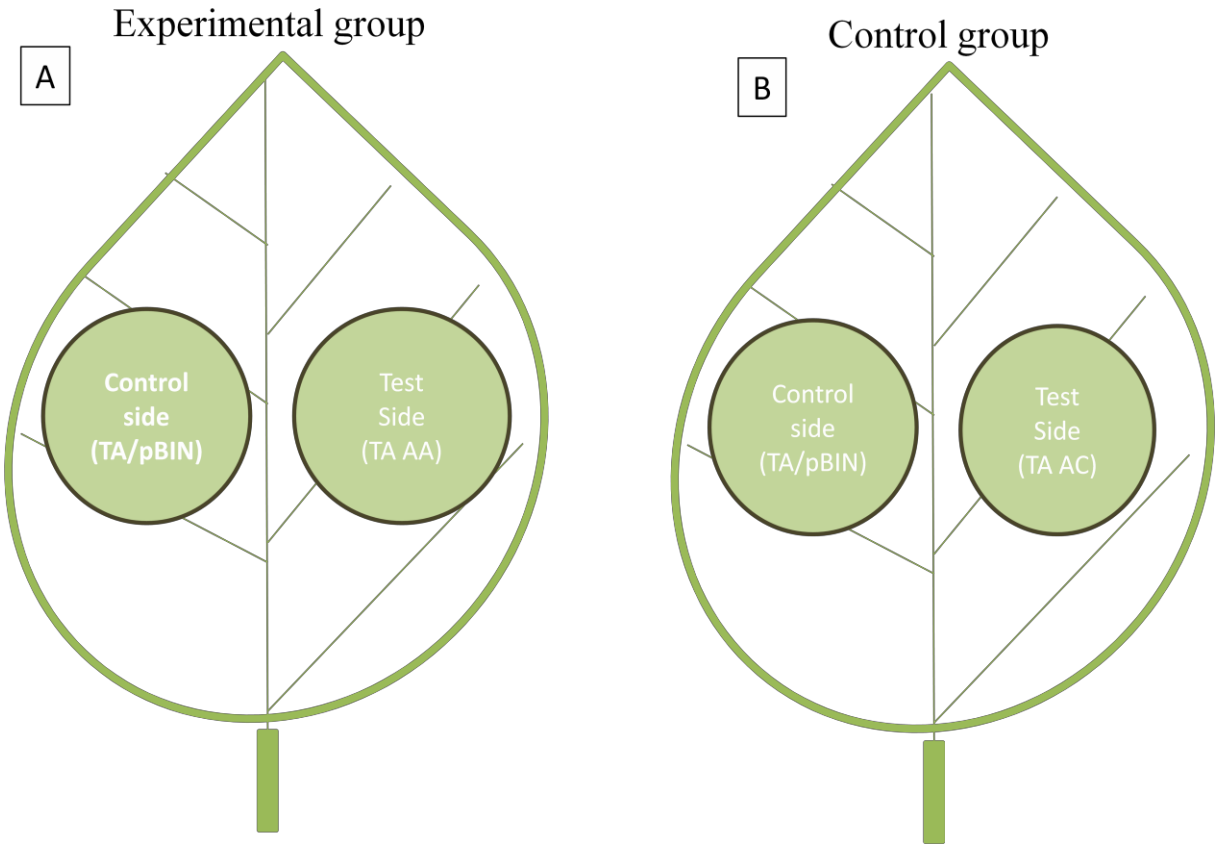

Figure 4.7 Example of infiltration in *Nicotiana benthamiana* using modified constructs. (A) Illustration of leaf co-infiltrations for the experimental group. (B) Illustration of leaf co-infiltrations for the control group.

A total of six plants were infiltrated for each experiment and five leaves, derived from different plants, were sampled from both groups on day 2, 3, 4 and 5 post infiltration. In order to eliminate possible biological differences between the individual plants, infiltration were performed on plants which were in the same growing stage as one another. At this stage the

plants were about to develop flowers, were approximately 20 cm high and the leaves roughly 6 cm wide.

4.2.7.2 GFP expression quantification

GFP expression of the infiltrated *Nicotiana benthamiana* leaves were quantified using the IVIS® Lumina II imaging system and the Living Image software version 3.0 (Caliper Life Science). The system includes three GFP filter sets: excitation filter (445-490 nm), background filter (410-440 nm) and emission filter (515-575 nm). The following parameters were used to set-up the system: GFP filter, exposure time 0.5 seconds, subject height 1.5 cm, f/stop 2, binning medium and field of view 12.5 cm.

Infiltrated areas were separately marked using the 'regions of interest' (ROI) tool of the Living Image software and quantified in photons per second per square centimetre per steradian (p/s/cm^2/sr).

4.2.7.3 In silico analyses

The average p/s/cm2/sr of the test side was subtracted from the average p/s/cm2/sr of the control side to determine differences (ΔD) in GFP expression levels between the two sides. Positive values indicate that the control side contained a higher GFP expression when compared to the test side and negative values, vice versa. These analyses were performed on the five leaves of each day (days 2, 3, 4 and 5 post infiltration) for both experimental and control groups. The following equation was used to determine ΔD between the control and test side:

$$\Delta D_{\text{sides}} = GFP\ expr_{\text{ control side}} - GFP\ expr_{\text{ test side}}$$

The average ΔD sides of all five leaves of the control group was subtracted from that of the experimental group for each day to determine differences (ΔD) in GFP expression levels between the two groups. The following equation was used to determine the ΔD between the experimental and control group:

$$\Delta D_{\text{groups}} = \Delta D_{\text{ experimental group}} - \Delta D_{\text{ control group}}$$

The higher ΔD groups, the greater the difference between the experimental and control group. These differences represent the silencing efficiency of the amiRNA. In a normal distribution, 95% of the data is located within 1.96 times the standard deviation. Results are considered statistically significant when the interval of the mean plus/minus two standard errors does not include the value of zero.

4.2.8 Overview of constructs used in this study

The six constructs used in this study are presented in Table 4.3.

Table 4.3 Overview of amiRNA constructs used in this study, including details of the constructs and their corresponding targets.

Construct	Details	Corresponding	Target details
AA	AmiRNA targeting accessible GLRaV-3 region	TA	Target construct includes 21 nt accessible GLRaV-3 region
AC	AmiRNA targeting conserved GLRaV-3 region	TC	Target construct includes 21 nt conserved GLRaV-3 region
AG	AmiRNA targeting GFP	TG	Target construct includes non-modified GFP gene

4.3. Results and discussion

4.3.1 Construct confirmation

Four vector constructs were generated in this study; AA, AC, TA and TC. The amiRNA constructs each contained an insert of 100 bp (pre-amiRNA), while the two target constructs each contained an insert of 21 bp. Figures 4.8, 4.9, 4.10 and 4.11 show the vector maps of each constructs including restriction sites, primer regions and the insert region.

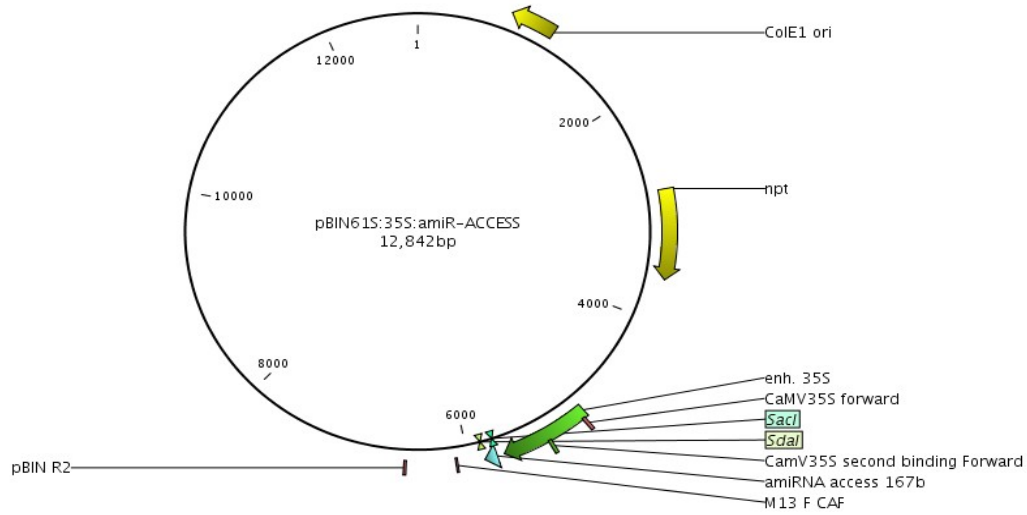

Figure 4.8 Vector map of construct AA including restriction enzyme sites *SacI* and *SdaI*. The inserted pre-AA is presented as a blue triangle and the 35S promoter as a green arrow. Primers used for colony PCR and Sanger sequencing are presented as small rectangles around the insert.

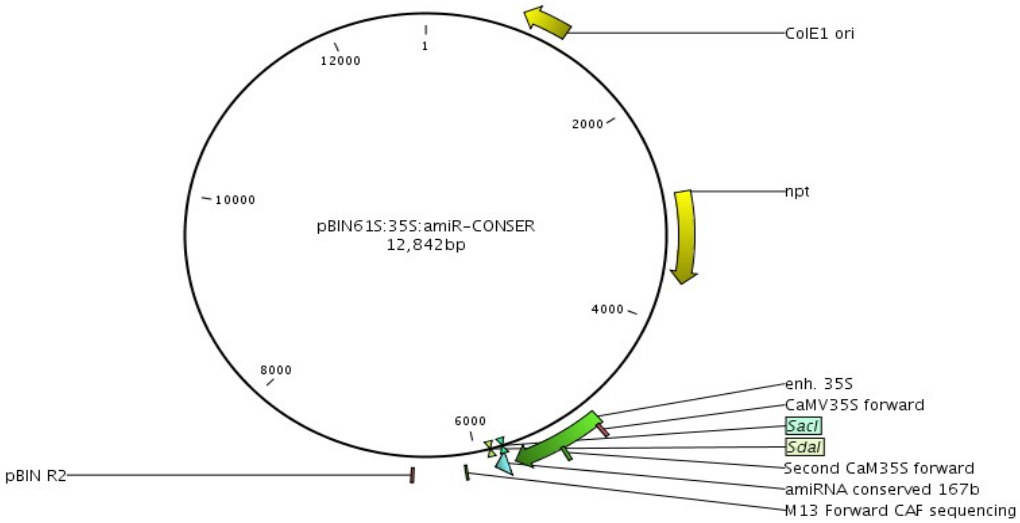

Figure 4.9 Vector map of construct AC including restriction enzyme sites *SacI* and *SdaI*. The inserted pre-AC is presented as a blue triangle and the 35S promoter as a green arrow. Primers used for colony PCR and Sanger sequencing are presented as small rectangles around the insert.

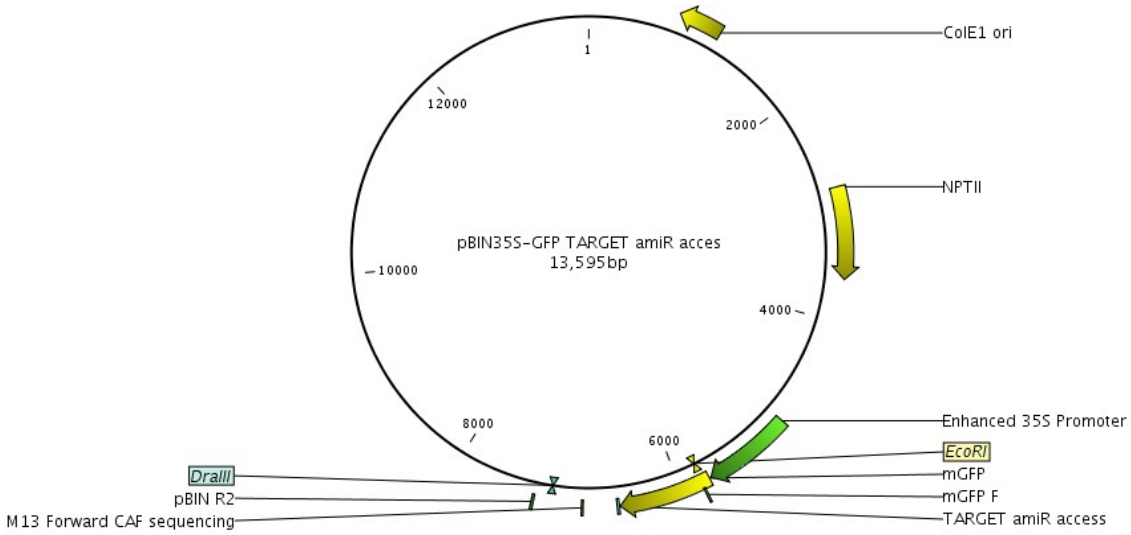

Figure 4.10 Vector map of construct TA including restriction enzyme sites *DraIII* and *EcoRI*. The target region was incorporated just behind the mGFP. The 35S promoter is presented as a green arrow. Primers used for colony PCR and Sanger sequencing are presented as small rectangles around the insert.

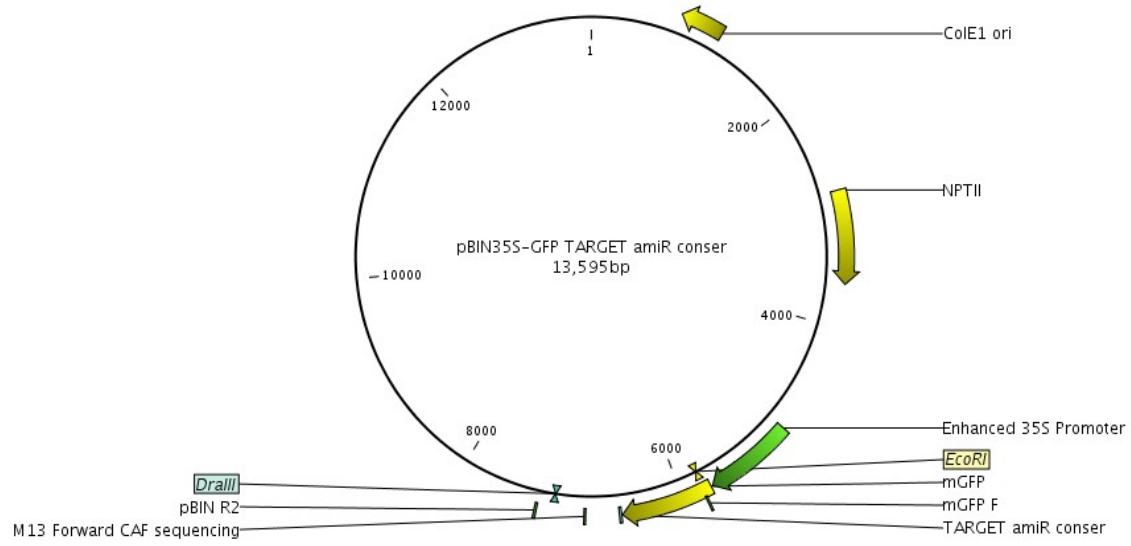

Figure 4.11 Vector map of construct TC including restriction enzyme sites *DraIII* and *EcoRI*. The target region was incorporated just behind mGFP. The 35S promoter is presented as a green arrow. Primers used for colony PCR and Sanger sequencing are presented as small rectangles around the insert.

Colony PCRs were performed on six colonies of each amiRNA construct using the primers CamV35S F and pBIN R2 (Figure 4.8 and 4.9). The forward primer annealed at two places resulting in two amplicons with a size of 1224 bp and 1551 bp when fragments included the insert (Figure 4.12.A). Colony PCRs performed on the target constructs were performed using

the mGFP F and pBIN R2 primers (Figure 4.10 and 4.11). Positive fragments, including the insert, had a product size of 1485 bp (Figure 4.12.B).

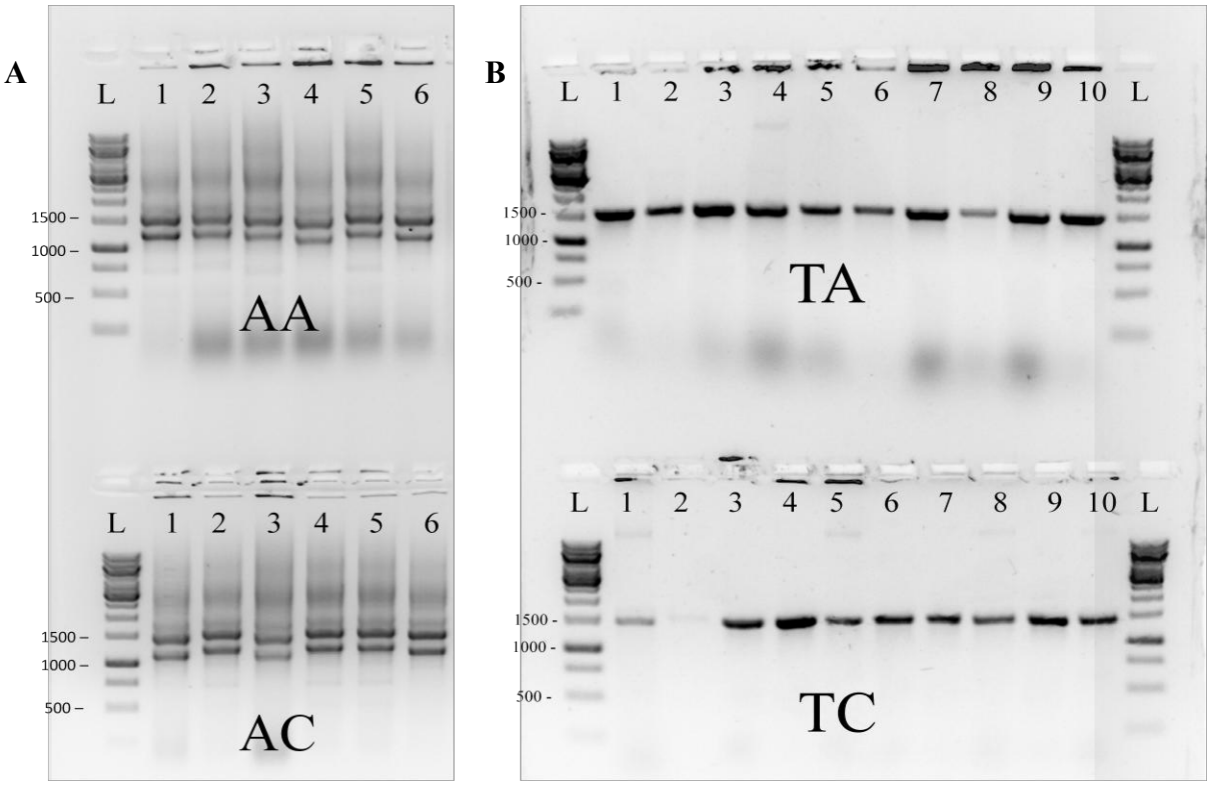

Figure 4.12 Two 1% agarose gels. (A) Colony PCRs performed on six colonies of each amiRNA construct. Numbers 1 – 6 correspond with colony number. L = l kb ladder. (B) Colony PCRs performed on 10 colonies of each target construct. Number 1 – 10 correspond with colony number. L = 1 kb ladder.

As seen on the gel in Figure 4.12.A, amplicon sizes of AA4, AA6, AC1, AC3 and AC6 were slightly lower when compared to the other amplicons. This is an indication that the insert was not incorporated into the construct. Sanger sequencing confirmed the correct insert for colonies AA1 and AC2 and these constructs were used for further experiments (results not shown).

Figure 4.12.B shows the colony PCRs performed on the target constructs. Since the insert is only 21 nt and the colony PCR product is 1485 bp, it is not likely to observe size differences on the gel between a construct with or without an insert. For this reason, plasmids were extracted from multiple colonies and sent for sequencing. The insert of colonies TA8 and TC5 were confirmed by Sanger sequencing and used for further experiments (results not shown).

4.3.2 Infiltration of plants

As previously described, the abaxial surface of each test leaf was infiltrated on two sides (Figure 4.13). The differences between the two sides and between the two groups determined the efficiency of the amiRNAs in silencing GFP.

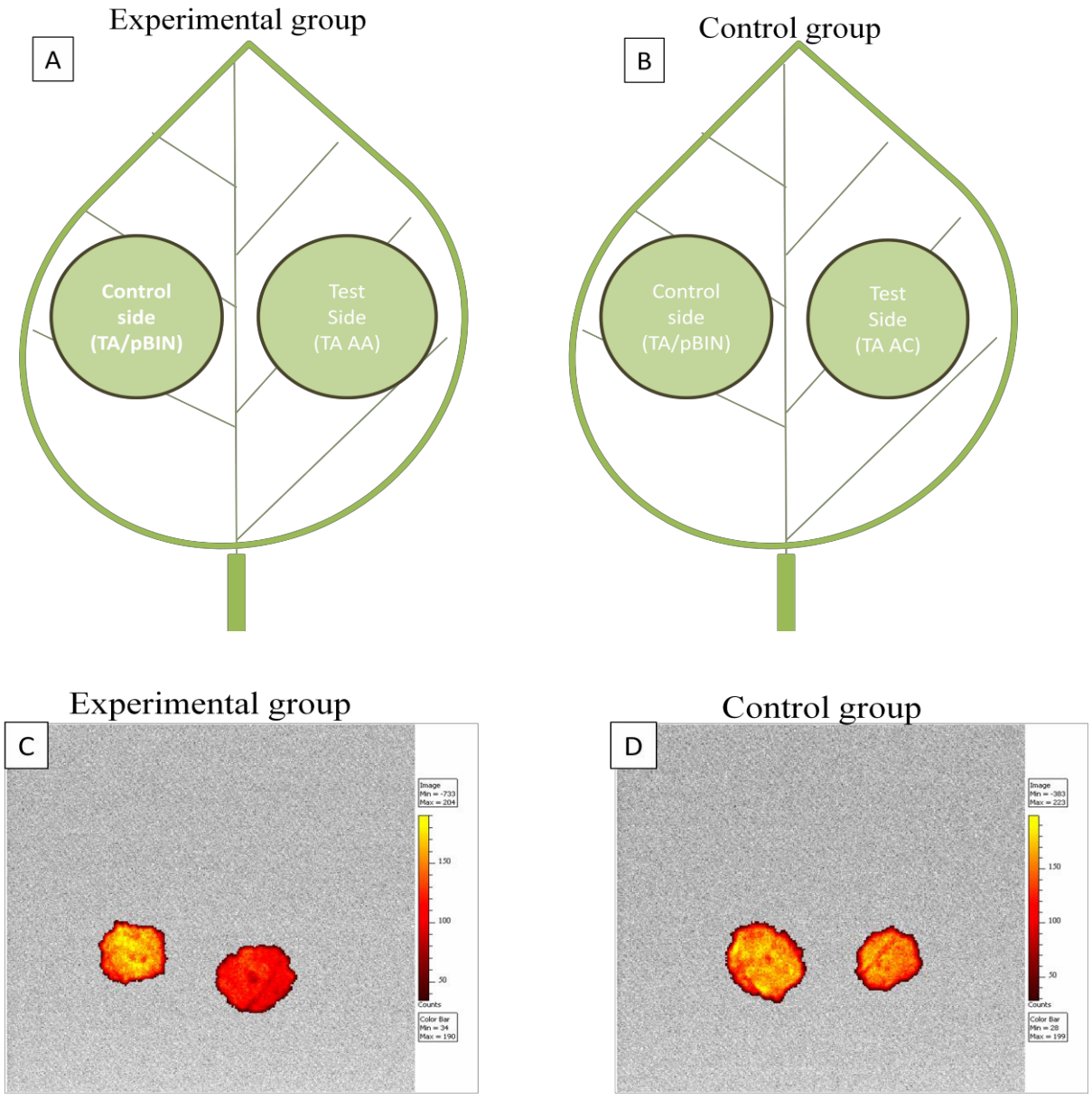

Figure 4.13 Example of infiltration of *Nicotiana benthamiana* using modified constructs. (A) Leaf illustration of co-infiltrated areas on abaxial surface of the experimental group. (B) Leaf illustration of co-infiltrated areas on abaxial surface of the control group. (C) Example of GFP fluorescence photo using the IVIS® Lumina II imaging system. Yellow colours indicate high GFP expression whereas red colours represent lower GFP expression (D) Example of GFP fluorescence photo using the IVIS® Lumina II imaging system. Yellow colours indicate high GFP expression whereas red colours a lower GFP expression

4.3.3 Silencing efficiency of amiRNAs

4.3.3.1 GFP expression differences between the control and test sides of leaves

To determine the silencing efficiency of the amiRNAs, the GFP expression differences (as well as the standard error bars of the mean) between the control and test sides, as measured with the IVIS system, were plotted onto a graph for both the experimental and control groups (Figure 4.14). Values greater than 0.0 p/s/cm^2/sr indicate that the control side had a higher GFP expression than the test side, meaning that the amiRNA did silence GFP. As described previously, results are considered statistically significant when the interval of the mean plus/minus two standard errors does not include the value of zero.

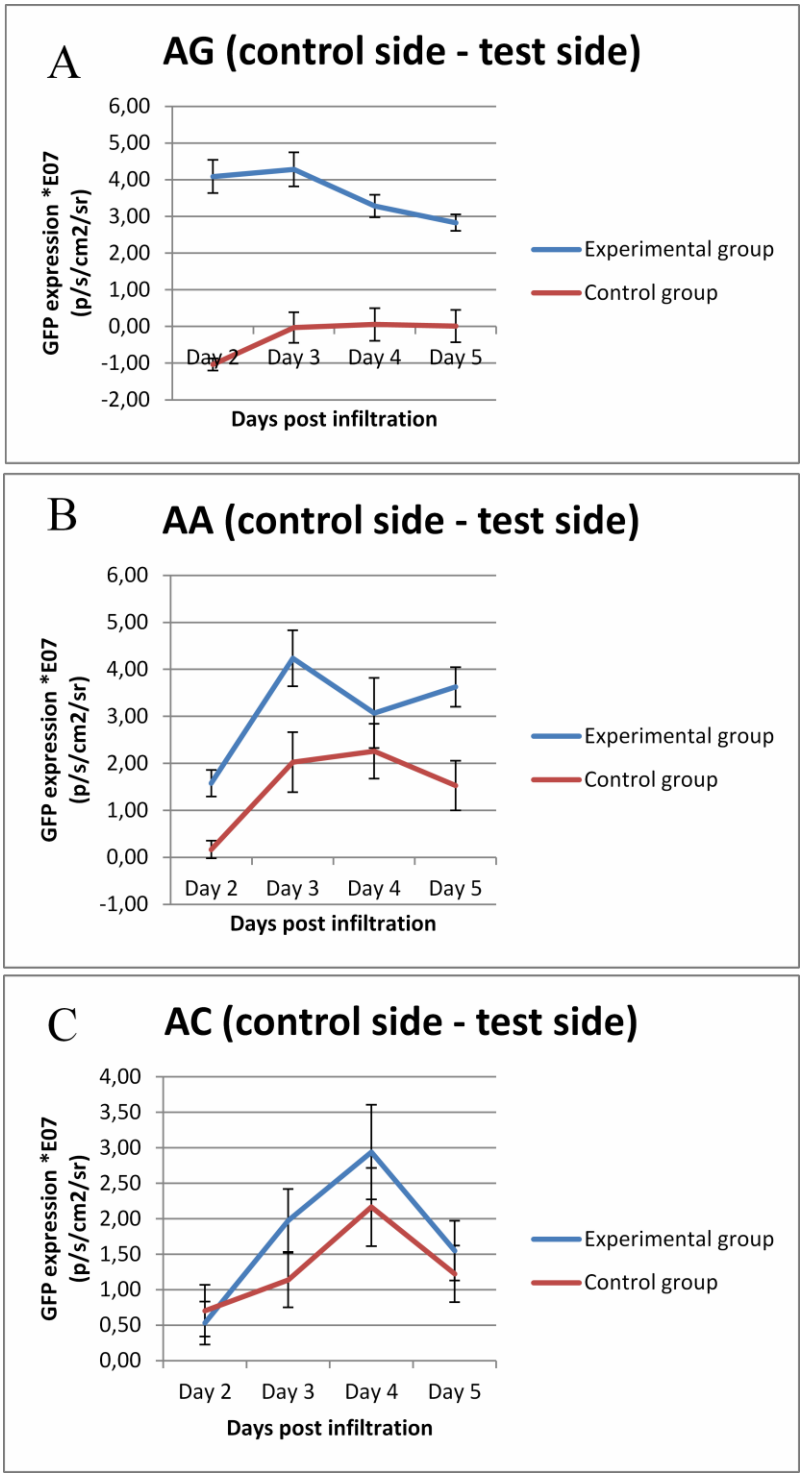

Figure 4.14 Graph representation of GFP expression differences between the control side and the test side of experimental and control groups of three amiRNAs. In each case the blue line represents the difference in GFP expression between the control side and the test side of the experimental group and the red line represents the difference in GFP expression between the control side and the test side of the control group (A) AG (B) AA (C) AC.

Figure 4.14.A shows that the positive control group, AG, was statistically significant efficient in silencing the GFP target construct for all days post infiltration (the interval of the mean minus two standard errors does not include the value of zero). Furthermore, the target construct was specifically cleaved by the corresponding amiRNA and was not silenced using the non-corresponding amiRNA as indicated by ΔD of the control group.

The results of AA and AC (Figure 4.14.B and 4.14.C) showed a different trend. Both amiRNAs were efficient in silencing the target constructs, however, the results were not statistically significant for all days post infiltration. The results of construct AA were statistically significant for days 3, 4 and 5 post infiltration whereas for construct AC, none of the days post infiltration shows statistically significant results. Remarkably, the control group of both AA and AC show ΔD values greater than zero, indicating that the constructs were not specific in silencing their corresponding targets. Nevertheless, both amiRNA constructs were more efficient in silencing their corresponding targets than the non-corresponding targets.

Figure 4.14 shows that the positive control amiRNA, AG, was more efficient in silencing the GFP target construct than the amiRNAs that were constructed in this study. This can probably be ascribed to the location of the silenced target region. AG cleaved the middle of the GFP gene whereas AA and AC targeted sequences in the 3' UTR of GFP. The GFP gene is seemingly more effectively disrupted when cleaved in the middle than in the 3' terminus.

4.3.3.2 GFP expression differences between the experimental and control groups

The GFP expression differences (as well as the standard error bars of the mean) between the experimental and control groups, as measured with the IVIS system, were plotted onto a graph for the three amiRNA experiments (Figure 4.15). Values greater than 0.0 p/s/cm^2/sr indicate that the experimental group had a higher GFP expression difference between the control and test sides than the control group, meaning that the target construct was more efficiently silenced by the corresponding amiRNA than by the non-corresponding amiRNA.

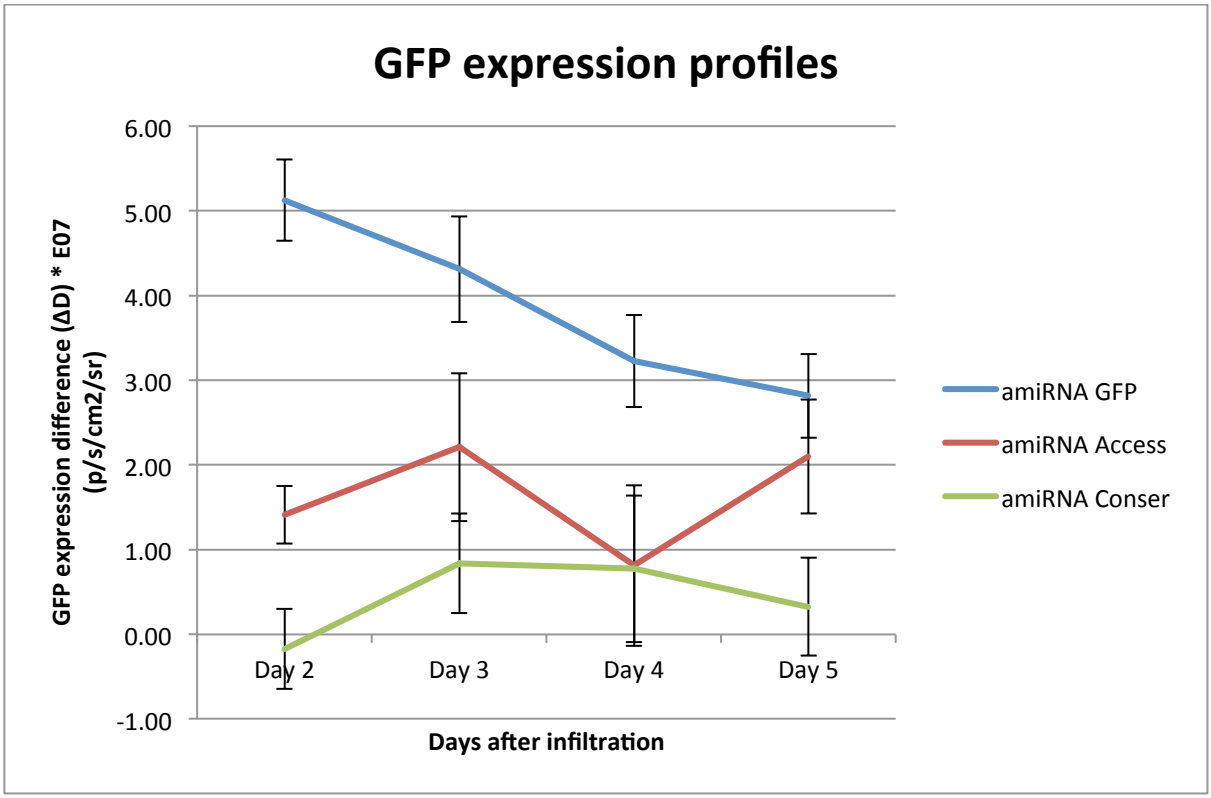

Figure 4.15 Graph representation of GFP expression differences between the experimental and control groups in p/s/cm^2/sr. The blue line represents the results of AG (positive control), the red line represents the results of AA and the green line the results of AC. The black bars represent the standard error of the mean.

The positive control amiRNA, AG, showed statistically significant GFP expression differences between the experimental and control group during the entire experiment (Figure 4.15). The GFP expression differences between the experimental and control groups of AA and AC were not statistically significant. This is most likely the result of the non-specific silencing by the non-corresponding amiRNAs. It is unknown what target region was silenced using the non-corresponding amiRNA since sequence alignment of the targets showed less than 30% similarity. This eliminates the possibility that the amiRNAs recognize both targets.

4.4 Conclusion

This study showed that PDR strategies based on amiRNAs can be a potential tool in order to target specific GLRaV-3 sequences. Furthermore, an amiRNA-mediated silencing validation system was successfully designed, constructed and validated. Two constructed amiRNAs were efficient in silencing their 21 nt target region. However, they were not specific in exclusively silencing only their corresponding target. It is not yet known what target was silenced using the non-corresponding amiRNAs. The positive control amiRNA was

more efficient in silencing the target construct than the two amiRNAs constructed in this study.

4.5. References

Cogoni, C. and Macino, G. 2000. Post-transcriptional gene silencing across kingdoms. *Current Opinion in Genetics and Development.*10: 638-643

Finnegan, E.J., Wang, M.-B. and Waterhouse, P. 2001. Gene silencing: fleshing out the bones. *Current Biology*. 11:R99-R102

Jelly, N.S., Schellenbaum, P., Walter, B. and Maillot, P. 2012. Transient expression of artificial microRNAs targeting Grapevine fanleaf virus and evidence for RNA silencing in grapevine somatic embryos. *Transgenic Research*. 21(6): 1319-1327

Jorgensen, R.A. 2003. Sense cosuppression in plants: past, present, and future, In: *RNAi A Guide To Gene Silencing*, Chapter 1, G.J. Hannon, Cold Spring Harbour Laboratory Press, New York

Lindbo, J.A., Fitzmaurice, W.P. and Della-Cioppa, G. 2001. Virus-mediated programming of gene expression in plants. *Current Opinion in Plant Biology*. 4:181-185

Liu, C., Zhang, L., Sun. J., Luo, Y., Wang, M.-B., Fan, Y.-L. and Wang, L. 2010. A simple artificial micro RNA vector based on ath-miR169d precursor from Arabidopsis. *Mol. Biol Rep*. 37: 903-909

Mallory, A.C., Reinhart, B.J., Jones-Rhoades, M.W., Tang, G., Zamore, P.D., Barton, M.K. and Bartel, D, P. 2004. MicroRNA control of PHABULOSA in leaf development: importance of pairing to the microRNA 5' region. *EMBO J.* 23(16): 3356-3364

Napoli, C., Lemieux, C. and Jorgensen, R. 1990. Introduction of a Chimeric Chalcone Synthase Gene in to Petunia results in reversible co-suppression of homologous genes in trans. *The Plant Cell*. 4(2): 279-289

Reynolds, A., Leake, D., Boese, Q., Scaringe, S., Marshall, W.S. and Khvorova, A. 2004. Rational siRNA design for RNA interference. *Nat Biotechnol.* 22(3): 326-330

Simon-Mateo, C. and Garcia, J.A. 2006. Micro RNA-guided processing impairs *Plum pox virus* replication, but the virus readily evolves to escape this silencing mechanism. *J. Virol.* 80: 2429-2436

Varkonyi-Gasic, E., Wu, R, Wood, M., Walton, E.F. and Hellens, R.P. 2007. Protocol: a highly sensitive RT-PCR method for detection and quantification of microRNAs. *Plant Methods*. 3: 1-12

Wingard, S.A. 1928. Host and symptoms of ring spot, a virus disease of plants. *J. Agric. Res.* 37: 127-153

WMD3 – Web MiRNA Designer http://wmd3.weigelworld.org/

Chapter 5 Conclusion and Future prospects

Grapevine leafroll disease (GLD) is an important viral disease that poses a significant threat to the South African wine industry. Several control strategies, such as vector control and the establishment and maintenance of clean material, are used to prevent crop losses. However, methods based on genetic modification of the grapevine genome can offer alternative control strategies to GLD. One such method is pathogen-derived resistance (PDR) which has become an effective tool in conferring resistance to plant viruses.

The aim of this study was to evaluate pathogen-derived resistance strategies for GLRaV-3 using the following two approaches; 1) evaluation of transgenic plants expressing a dysfunctional GLRaV-3 HSP70h in order to confer resistance against GLRaV-3, and 2) the construction of amiRNAs to use as a tool for silencing specific sequences of GLRaV-3 in the grapevine host and the development of an artificial microRNA-mediated silencing validation system.

5.1 Evaluation of HSP-Mut grapevine

In the first part of this study, six transgenic grapevine lines (plant lines #1, #3, #9, #14, #15 and #17) were evaluated for their ability to confer resistance to GLRaV-3. A virus inoculation protocol using grafting was optimized during this study. The most promising candidate transgenic line was plant line #3, which showed an average resistance level of 99.96%. However, ampelographic observations of plant line #3 suggested that this plant line was a different cultivar than the other plant lines used in this study. It is unknown if the different genotype may have contributed to the enhanced resistance levels of this plant line. Moreover, the transgenic status of this plant is also questionable. PCR analysis failed to confirm the presence of the transgene, yet RT-PCR did show expression of the transgene. A molecular and experimental comparison between plant line #3 and a wild-type plant of the same cultivar is needed to confirm the transgenic status of this plant line as well as the significance of the findings in this study.

Another promising candidate for further studies is plant line #1, which showed an overall average resistance level of 98.9%, and for which the presence of the transgene, as well as its expression was demonstrated. The mechanism behind the enhanced resistance levels are

likely based on RNA-mediated resistance considering the low expression levels of the transgene for this particular plant line. Small RNA profiling, as well as replicating the experiment with a greater number of samples are needed to confirm the findings in this study and to determine whether small RNAs are involved in the mechanisms behind the enhanced resistance levels.

Conversely, plant line #14 showed an increase in susceptibility to GLRaV-3. Although enhanced virus susceptibility has been documented previously for transgenic plants expressing a functional movement protein, it was never observed in plant lines expressing a mutated dysfunctional movement protein. It is not yet known what causes the susceptibility and protein expression in addition to molecular analyses of the transgene are needed to understand this unusual result.

In this study, a previously developed rootstock of grapevine was used. The reasoning was that the transgenic grapevine lines could provide resistance to GLRaV-3 throughout the entire plant, including the scion grafted onto the rootstock. To evaluate these transgenic rootstocks, in this study, we evaluated them by grafting on domesticated grapevine usually used as scion material. Therefore, in future studies, it will be interesting to graft scion material onto the most promising transgenic plant lines and challenge them with viruliferous mealybugs, which would be a more natural simulation of the field. Subsequently, quantitative analyses of the entire plant are needed to determine the resistance levels to GLRaV-3 as well as the spatial distribution of the virus in the plant.

5.2 Development and validation of amiRNA constructs

The second part of this study comprised the construction and validation of two amiRNAs that targeted GLRaV-3 sequences. Two Vitis amiRNAs and their respective target cassettes were constructed, and an amiRNA validation system was optimized in this study. Both amiRNAs were capable of silencing their respective targets, however, neither was specific in exclusively silencing only its corresponding target. It is not yet known what region was cleaved using the non-corresponding targets. Alignments of the target regions showed less than 30% identity, confirming that the amiRNAs could not have been recognizing both targets. Furthermore, the

previously constructed positive control amiRNA, was more effective in silencing the target construct than the two amiRNAs constructed in this study. Since this control amiRNA cleaved a different region (in the middle, as opposed to the 3'-end) of the target construct, amiRNAs targeting that same region needs to be designed, constructed and evaluated in future studies to determine possible silencing efficiency differences between the two target regions. Moreover, the amiRNAs in this study were designed to target GLRaV-3 sequences in order to confer resistance to this virus. It will be of importance to investigate the capability of the amiRNAs to limit the spread of GLRaV-3 in infected grapevine material. This can be determined by infiltrating infected grapevine material with the amiRNAs constructed in this study, and consequently quantify the GLRaV-3 virus titre over time to see whether the amiRNA are successful in targeting the GLRaV-3 genome.